PFG

Photogrammetrie Fernerkundung Geoinformation

Organ der Deutschen Gesellschaft für Photogrammetrie, Fernerkundung und Geoinformation (DGPF) e.V.

Jahrgang 2008, Heft 3

E. Schweizerbart'sche Verlagsbuchhandlung
(Nägele u. Obermiller) Stuttgart 2008

Deutsche Gesellschaft für Photogrammetrie, Fernerkundung
und Geoinformation (DGPF) e.V.
Gegründet 1909

Die *Deutsche Gesellschaft für Photogrammetrie, Fernerkundung und Geoinformation* (DGPF) e.V. unterstützt als Mitglieds- bzw. Trägergesellschaft die folgenden Dachverbände:

International Society for Photogrammetry and Remote Sensing

DAGM
Deutsche Arbeitsgemeinschaft für Mustererkennung e.V.

GeoUnion Alfred-Wegener-Stiftung

Herausgeber:

Präsidentin: Prof. Dr. Cornelia Gläßer, Martin-Luther-Universität Halle-Wittenberg, Institut für Geowissenschaften, Von-Seckendorff-Platz 4, D-06120 Halle, Tel.: +49 (0) 345 55-26020
Geschäftsstelle: Dr. Klaus-Ulrich Komp, c/o EFTAS Fernerkundung Technologietransfer GmbH, Oststraße 2–18, D-48145 Münster, e-mail: klaus.komp@eftas.com

Published by:
E. Schweizerbart'sche Verlagsbuchhandlung (Nägele u. Obermiller), Johannesstraße 3 A, D-70176 Stuttgart. Tel.: 0711 351456-0, Fax: 0711 351456-99, e-mail: mail@schweizerbart.de
Internet: http://www.schweizerbart.de
♾ Gedruckt auf alterungsbeständigem Papier nach ISO 9706-1994

ISSN 1432-8364

Hauptschriftleiter: Prof. Dr.-Ing. Helmut Mayer, Institut für Geoinformatik und Computer Vision, Universität der Bundeswehr München, D-85577 Neubiberg, e-mail: Helmut.Mayer@unibw.de
Schriftleiter: Prof. Dr. rer. nat. Carsten Jürgens, Ruhr-Universität Bochum, Geographisches Institut, Gebäude NA 7/133, D-44780 Bochum, e-mail: carsten.juergens@rub.de, Prof. Dipl.-Ing. Thomas P. Kersten, HafenCity Universität Hamburg, Department Geomatik, Hebebrandstr. 1, D-22297 Hamburg, e-mail: thomas.kersten@hcu-hamburg.de, Prof. Dr. rer. nat. Lutz Plümer, Universität Bonn, Institut für Geodäsie und Geoinformation, Meckenheimer Allee 172, D-53115 Bonn, e-mail: Lutz.Pluemer@ikg.uni-bonn.de und Dr.-Ing. Eckhardt Seyfert, Landesvermessung und Geobasisinformation Brandenburg, Heinrich-Mann-Allee 107, D-14473 Potsdam, e-mail: eckhardt.seyfert@geobasis-bb.de

Erscheinungsweise: 6 Hefte pro Jahrgang.
Bezugspreis im Abonnement: € 126,– pro Jahrgang. Mitglieder der DGPF erhalten die Zeitschrift kostenlos.

Anzeigenverwaltung: Dr. E. Nägele, E. Schweizerbart'sche Verlagsbuchhandlung (Nägele u. Obermiller), Johannesstraße 3A, D-70176 Stuttgart, Tel.: 0711 351456-0; Fax: 0711 351456-99.
e-mail: mail@schweizerbart.de, Internet: http://www.schweizerbart.de
Bernhard Harzer Verlag GmbH, Westmarkstraße 59/59 a, D-76227 Karlsruhe, Tel.: 0721 944020, Fax: 0721 9440230, e-mail: Info@harzer.de, Internet: www.harzer.de

Printed in Germany by Tutte Druckerei GmbH, D-94121 Salzweg bei Passau

PFG – Jahrgang 2008, Heft 3
Inhaltsverzeichnis

Originalbeiträge DFG Bündel ,,Abstraktion von Geoinformation‘‘

Berichtigung

Berichte und Mitteilungen

Zusammenfassungen der „Originalbeiträge“ und der Beiträge „Aus Wissenschaft und Technik“ (deutsch und englisch) sind auch verfügbar unter www.dgpf.de/neu/pfg/ausgaben.htm

Photogrammetrie • Fernerkundung • Geoinformation 3/2008, S. 153–155

Editorial: Abstraktion von Geoinformation bei der multiskaligen Erfassung, Verwaltung, Analyse und Visualisierung

MONIKA SESTER & CHRISTIAN HEIPKE, Hannover; REINHARD KLEIN, Bonn; HANS-PETER BÄHR, Karlsruhe

Unsere Wahrnehmung und unsere Begriffswelt sind durch das Thema Abstraktion bzw. Mehrskaligkeit beherrscht. Sehen, verstehen, kommunizieren – alles geht von unterschiedlichen Abstraktionsstufen aus und kombiniert sie in idealer Weise, wobei eine Grob-zu-Fein-Herangehensweise typisch ist. Für raumbezogene Phänomene unserer Umwelt gilt dies analog: in verschiedenen Skalen oder Maßstabsebenen eröffnen sich dem Betrachter unterschiedliche Aspekte von Objekten und nur in dieser Maßstabsbezogenheit können sie auch ganzheitlich wahrgenommen und verstanden werden. Daher kann man räumliche Phänomene nur dann umfassend interpretieren und nutzen, wenn ihre Skalenabhängigkeit mit in Betracht gezogen wird. In der Geoinformatik werden raumbezogene Objekte typischerweise über ihre geometrischen, thematischen und kontextuellen Eigenschaften beschrieben. Die Einbeziehung des Maßstabes erweitert dies um eine zusätzliche Dimension.

Dieser Tatsache wird in der analogen Darstellung raumbezogener Daten in der traditionellen Kartographie in Form von Kartenserien unterschiedlicher Maßstäbe Rechnung getragen. Diese Funktionalität auch in digitalen Systemen vorzuhalten und zur Verfügung zu stellen, eröffnet gänzlich neue Möglichkeiten der räumlichen Datenverarbeitung. Dies gilt für alle räumlichen Datentypen, d. h. Vektordaten (1D, 2D, 3D-Objekte), Bilddaten und 2.5D-Oberflächen.

In verschiedenen Disziplinen wird an diesen Fragestellungen gearbeitet und geforscht:

- Generalisierung in der Kartographie und in der Geoinformatik.
- Pyramidale und Scale-Space-Ansätze in der Bildverarbeitung und Bildanalyse.
- Vereinfachungsverfahren bei der Oberflächenbeschreibung und -visualisierung in der Computergraphik.
- Abstraktionshierarchien in der Linguistik, der Informatik und den Kognitionswissenschaften.

Hier setzte ein in den letzten vier Jahren von der Deutschen Forschungsgemeinschaft (DFG) geförderter Paketantrag an: die Ansätze, die bislang relativ separat voneinander in den jeweiligen Disziplinen bearbeitet worden waren, sollten gemeinsam betrachtet werden. Es galt zu eruieren, ob und wie die jeweils unterschiedlichen Methoden und Herangehensweisen der verschiedenen Disziplinen einander angenähert werden können bzw. wo Synergien zu finden sind.

Die Idee zu diesem Projekt wurde im Arbeitskreis GIS der Deutschen Geodätischen Kommission (DGK) entwickelt und durch weitere Teilnehmer aus relevanten Arbeitsgebieten erweitert. In diesem Sonderheft der PFG werden die Forschungsprojekte dargestellt, die im Rahmen des Paketantrags bearbeitet wurden.

Die Projekte widmeten sich dem Thema „Maßstab“ in unterschiedlicher Weise und aus der Sicht unterschiedlicher Datentypen:

- Vektordaten:
  - Institut für Kartographie und Geoinformation, Universität Bonn
  - Institut für Kartographie und Geoinformatik, Leibniz Universität Hannover
  - Institut für Geoinformatik und Fernerkundung, Universität Osnabrück

1432-8364/08/2008/153 $ 0.75

- Bild- bzw. Rasterdaten:
  - Institut für Photogrammetrie und Kartographie, Universität der Bundeswehr München
  - Institut für Photogrammetrie und GeoInformation, Leibniz Universität Hannover
  - Institut für Photogrammetrie, Universität Bonn
- 2,5D, 3D-Daten:
  - Institut für Informatik II, AG Computergraphik, Universität Bonn
- Sprache:
  - Institut für Photogrammetrie und Fernerkundung, Universität Karlsruhe

Dirk Dörschlag, *Gerd Gröger* und *Lutz Plümer* widmen sich der Frage der angemessenen Modellbeschreibungen für Gebäude. Sie beschreiben einen Ansatz, der formale attributierte Grammatiken zur Erzeugung komplexer Gebäudemodelle verwendet. Ausgehend von groben Gebäudeteilen können diese in den Daten identifiziert und sukzessive – aufgrund vorgegebener Übergangsregeln – verfeinert werden, wodurch ein Übergang in der Generalisierungsstufe, dem Level of Detail, entsteht.

Jan-Henrik Haunert entwickelte im Rahmen des Projekts eine Methode zur automatischen Ableitung unterschiedlicher Auflösungen von digitalen Landschaftsmodellen. Im Gegensatz zu gängigen Verfahren, die heuristisch und iterativ arbeiten, stellte er einen globalen Ansatz auf Basis von Optimierungverfahren vor. Mit diesem Verfahren ist es möglich, Qualitätsparameter der Generalisierung wie logische Konsistenz und semantische Genauigkeit als so genannte Constraints zu beschreiben und sie als Maß für die Qualität einer Generalisierung zu nutzen. Dies wird im Beitrag von *J.-H. Haunert* und *Monika Sester* vorgestellt. Mit diesem Ansatz wurde ein objektives Maß gefunden, mit dem optimale bzw. exakte Verfahren mit heuristischen Ansätzen verglichen werden können.

Andreas Thomsen, *Martin Breunig* und *Edgar Butwilowski* schlagen vor, ein etabliertes Topologiemodell, die so genannten Generalized Maps, zu erweitern, um die Verwaltung und Analyse multiskaliger Daten zu ermöglichen. Die Anwendung wird für die Verwaltung von aggregierten Landnutzungsdaten in mehreren Maßstäben eingesetzt.

Sergej Reznik und *Helmut Mayer* interpretieren automatisch Gebäudefassaden aus terrestrischen Bildfolgen. Zunächst werden individuelle Fenster mittels so genannter Implicit Shape Models detektiert. Diese werden auf einer höheren Abstraktionsstufe als zu einer speziellen Fassadenstruktur gehörig identifiziert: mögliche Strukturen sind Fensterzeilen, Fensterreihen und Einzelfenster. Anhand eines informationstheoretischen Maßes wird die beste Struktur ausgewählt.

Janet Heuwold untersucht die Frage, wie Modelle für die Interpretation geringer aufgelöster Bilder automatisch aus hoch aufgelösten Modellbeschreibungen abgeleitet werden können, wobei die Modelle als semantische Netze repäsentiert werden. Ihr Untersuchungsgegenstand sind Straßen. Für diese entwickelt sie mit Hilfe eines Analyse-durch-Synthese Ansatzes mögliche Übergänge auf der Basis von Kenntnissen über das Verhalten von Straßenstrukturen im Maßstabsraum. Dies wird im Beitrag von *J. Heuwold*, *Kian Pakzad* und *Christian Heipke* beschrieben.

Roland Wahl widmet sich dem Problem der Handhabung und Visualisierung sehr großer Datenmengen von Stadtlandschaften. Diese lassen sich mit gängigen Verfahren der Computergraphik wie Maschenvereinfachungsverfahren zwar in ihrer Menge reduzieren, jedoch ist dadurch nicht sicher gestellt, dass die Bedeutung der Objekte und ihre charakteristische Form erhalten bleiben. Im Beitrag von *R. Wahl*, *Ruven Schnabel* und *Reinhard Klein* wird ein Verfahren zur Generalisierung präsentiert, welches nicht nur geometriebezogen vereinfacht, sondern die Semantik der Objekte mit einbezieht. Die Semantik wird dabei durch generische Eigenschaften der betrachteten Objekte bestimmt: Gebäude werden durch spezielle Formen wie Ebenen charakterisiert – diese werden durch die Vereinfachungsmethode so weit wie möglich erhalten.

Christian Lucas, *Marina Müller* und *Hans-Peter Bähr* beschreiben das Problem der Verbindung zwischen graphischer und verbaler Beschreibung räumlicher Informationen. Anhand zweier Anwendungsszenarien diskutieren sie die Relevanz und den Bedarf an Transformationen zwischen den beiden Repräsentationsformen. Dies wird besonders deutlich am Beispiel des Katastrophenmanagements, wo textliche Hinweise auf Unfälle automatisch erkannt und schnell mit Geoobjekten in Zusammenhang gebracht werden müssen. Abstraktion zeigt sich in dem Beitrag in den verschiedenen Ebenen der benötigten Detaillierungsgrade.

Im Laufe der vier Jahre fanden regelmäßig ca. alle zwei Monate Treffen der Teilnehmer des Bündels statt. Sie dienten den Fortschrittsberichten sowie der intensiven Diskussion unter Doktoranden und Projektleitern. So wurde erreicht, dass innerhalb der Gruppe neue Ansätze und Methoden vorgestellt und diskutiert wurden, und auf diese Weise eine gemeinsame Sprache in dem interdisziplinären Projekt gefunden wurde. In dieser Form hatte das Bündel die Funktion einer strukturierten Doktorandenausbildung. Die Ergebnisse der Arbeiten wurden weiterhin in Zeitschriften und auf Konferenzen vorgestellt. Ferner beteiligte sich das gesamte Bündel am ISPRS-Workshop Photogrammetric Image Analysis, der im letzen Jahr in München stattfand.

Zum Abschluss des Projekts fand ein Workshop in Gengenbach im Schwarzwald statt, zu dem auch externe Experten aus den Disziplinen Geoinformatik und Kartographie, Bildanalyse sowie Visualisierung eingeladen wurden. Die Ergebnisse der vierjährigen Arbeiten wurden vorgestellt und mit den Experten diskutiert. Diese attestierten dem Projekt eine sehr gute Zusammenarbeit sowie wichtige Fortschritte in der Beantwortung relevanter Fragen im Kontext ,,Maßstab“ bzw. ,,Datenabstraktion“.

Im Projektantrag wurde seinerzeit formuliert: ,,Die Arbeiten aller Projektpartner bilden somit essentielle Puzzleteile, die ineinander greifen, um somit in der Summe das facettenreiche Bild der multiskaligen Geodatenverarbeitung in den nächsten vier Jahren weiter zu komplettieren.“

Bei dem Workshop wurde deutlich, dass dieses Ziel erreicht worden ist – wenngleich sicherlich noch weitere Puzzleteile zu finden und auszufüllen sind. Das bedeutet, dass dieses wichtige Thema noch weiterer intensiver Forschung bedarf, die von den Disziplinen der raumbezogenen Datenverarbeitung in naher Zukunft aufgegriffen werden sollte; dies insbesondere vor dem Hintergrund neuer technischer Herausforderungen, wie der Verfügbarkeit neuer in Raum und Zeit hoch aufgelöster Massendaten, der Anforderungen an das Verständnis der diesen Daten zugrunde liegenden Prozesse, sowie der Formulierung dedizierter Modelle für die Interpretation von Geodaten, zu deren Aufstellung speziell automatische Lernverfahren geeignet scheinen.

Wir danken der Deutschen Forschungsgemeinschaft für die Förderung dieser Arbeiten. Ferner danken wir der Schriftleitung der PFG für die Gelegenheit, ein Sonderheft zu dieser Thematik zu gestalten. Wir hoffen, dass die Artikel bei der Leserschaft Interesse für die Themen ,,Maßstab“ und ,,Datenabstraktion“ wecken und beim Lesen die eine oder andere Anregung für eigene darauf aufbauende Arbeiten entsteht.

Prof. Dr.-Ing. Monika Sester, Prof. Dr.-Ing. Christian Heipke, Prof. Dr. Reinhard Klein, Prof. Dr.-Ing. Hans-Peter Bähr, e-mail:
monika.sester@ikg.uni-hannover.de,
heipke@ipi.uni-hannover.de,
rk@cs.uni-bonn.de,
hans-peter.baehr@ipf.uni-karlsruhe.de.

Photogrammetrie • Fernerkundung • Geoinformation 3/2008, S. 157–164, 3 Abb.

Über die schrittweise Erstellung und Verfeinerung von Modellhypothesen für Gebäude

DIRK DÖRSCHLAG, GERHARD GRÖGER & LUTZ PLÜMER, Bonn

Keywords: Formale Grammatiken, Gebäuderekonstruktion, Modellselektion, Skalen

Summary: *About the Stepwise Generation and Refinement of Model Assumptions for Buildings*. This paper focuses on the stepwise generation and refinement of model hypotheses for the reconstruction of 3d buildings, based on image or laserscan data. An approach is presented, which uses attributed formal grammars. It starts with the largest components and proceeds stepwise from one scale to the next finer scale allowing a generic generation of a wide variety of highly detailed building hypotheses. This also allows a sequential validation of extension or refinement steps by model selection. The grammar presented in this paper is intended to produce models build up from aggregated cuboids and with a complex floor plan. In the future, the level of detail of the resulting model will be controlled by model selection.

Zusammenfassung: Dieser Artikel fokussiert auf die schrittweise Erstellung und Verfeinerung von Modellhypothesen für einen auf Bild- oder Laserdaten aufsetzenden Rekonstruktionsprozess für dreidimensionale Gebäudemodelle. Hierzu wird eine formale attributierte Grammatik verwendet. Das Erzeugen der Modellhypothese beginnt mit den gröbsten Bestandteilen, den Geschosskörpern, die definierte Übergänge zu feineren Bestandteilen wie Dachgauben oder Schornsteinen aufweisen. Dieses Vorgehen ermöglicht generisch die Erzeugung vielfältiger detaillierter Modellhypothesen, die sequentiell durch Modellselektion gesteuert wird. Die mit der hier präsentierten Grammatik produzierbaren Modelle eignen sich trotz der einfachen Basiskörper zur Erzeugung von Gebäudemodellen mit sehr komplexen und nicht rechtwinkligen Grundrissen. Insbesondere durch die Einbindung in Modellselektionsverfahren wird in Zukunft der Detaillierungsgrad der entstehenden Modelle gesteuert.

1 Einleitung

Die Rekonstruktion von Gebäudemodellen aus Massendaten wie Luftbildern und LIDAR-Daten ist ein wichtiges, relevantes wissenschaftliches Problem, das bisher nicht zufrieden stellend gelöst ist. Im Allgemeinen beinhalten Verfahren für die Rekonstruktion folgende Schritte:

1. Erfassung der Rohdaten
2. gegenseitige Registrierung von Rohdaten aus unterschiedlichen Quellen (z. B. Luftbild und Laserscan)
3. Gruppierung der Rohdaten zu größeren klassifizierbaren Einheiten (z. B. Punkte zu Ebenen)
4. Klassifikation

Bei der Erfassung der Ausgangsdaten ist heutzutage eine gute Basis erreicht, was Verfügbarkeit, Auflösung und Qualität der Daten anbelangt. Laserdaten aus Befliegungen sind oft flächendeckend vorhanden, etwa in Nordrhein-Westfalen. Zusätzlich sind teilweise auch terrestrisch erfasste Daten verfügbar. Viele Systeme ermöglichen zudem eine gleichzeitige Erfassung von Geometrie und zugehörigen Farbinformationen (ABMAYR et al. 2004). Auch im Bereich der gegenseitigen Registrierung der Rohdaten gab es sowohl in der Photogrammetrie als auch im Bereich Computer Grafik große Fortschritte (siehe auch (BORNAZ et al. 2003) oder (KAHLEZ et al. 2007)), so dass eine qualitativ hinreichende Registrie-

1432-8364/08/2008/157 $ 2.00

rung der Eingangsdaten kein Problem darstellt.

Für die Gruppierung der Rohdaten gibt es ebenfalls bereits eine Reihe verfügbarer Verfahren, die z. B. alle zu einer Ebene gehörigen Punkte in einer Punktmenge gruppieren können. Beispiele für leistungsfähige, etablierte Verfahren sind *Clustering* (Mierswa et al. 2006) und *RANSAC* (Fischler & Bolles 1981).

Für die spätere Nutzung der Daten bei Analysen muss neben der Geometrie auch die Semantik rekonstruiert werden. Diese *Klassifikation* eröffnet die Möglichkeit, Vorwissen über die jeweiligen Objekte in den Prozess einzubringen. Wichtige Vorbedingung für den Klassifikationsprozess ist die Verfügbarkeit von Modellen, welche in der Lage sind, die Daten zu erklären. Unter *Modell* verstehen wir die Einheit aus einem mathematischen Modell, im Folgenden *Modellklasse* genannt, und einem konkreten Parametersatz; dieser wird als *Modellparameter* bezeichnet. Diese Modelle werden im Schritt der Modellselektion mit den Daten verglichen und das am besten zu den Daten passende wird gewählt. An dieser Stelle ist es wichtig, eine Abwägung zwischen Modellkomplexität und Güte der Anpassung zu treffen, um eine Über- oder Unteranpassung zu vermeiden. Dies leisten Informationskriterien wie z. B. das *Akaike Informationskriterium – AIC* (Akaike 1974); hier wird die Güte der Zuordnung durch statistisch begründete Ähnlichkeitsmaße beschrieben.

Die Bereitstellung von geeigneten Gebäudemodellen für die Rekonstruktion von komplexeren Gebäuden ist durch die große Vielfalt und Kombinierbarkeit der elementaren Bestandteile schwierig und durch Aufzählung aller Alternativmodelle aufgrund der kombinatorischen Explosion der Möglichkeiten praktisch nicht durchführbar.

In diesem Artikel wird ein Ansatz vorgestellt, diesem Dilemma zu begegnen. Hierzu werden die für die Modelle notwendigen generischen Primitive und die Aggregationsmechanismen identifiziert. So ist es möglich, die komplexen Modelle nach Bedarf zusammenzubauen bzw. die Modelle schrittweise anzupassen und somit zu verbessern. Dieser Artikel präsentiert ein Verfahren, das – basierend auf dem aus der Informatik stammenden Konzept der *formalen Grammatik* – die notwendigen alternativen Modellklassen aus Modellklassenprimitiven zu erstellen und verfeinern versucht. Gebäude sind Strukturen mit einer unter Umständen sehr hohen Komplexität in ihrer Form und somit auch in deren geometrischer Beschreibung. Eindrucksvolle Beispiele der möglichen Komplexität sind insbesondere in Innenstadtbereichen mit historischer Bebauung, die z. B. aus der Gründerzeit stammen, zu finden. Dennoch eröffnet die Sprache ein generisches Konzept, um Gebäudeformen zu beschreiben. Die komplexe Gesamtstruktur wird hierbei in kombinierbare Komponenten zerlegt. Ähnlich gehen auch CAD-Systeme vor, bei welchen das Gebäude aus vorher spezifizierten parametrisierten Teilen zusammengesetzt wird. Die Komposition dieser Komponenten ist jedoch nicht völlig beliebig, sondern unterliegt Regeln. Diese Regeln ergeben sich aus dem spezifischen Zweck der Komponenten, den diese im Gesamtkontext des Gebäudes erfüllen müssen, und den physikalischen Gesetzen.

Steinhage (1998) erzeugt Modellklassen aus einfachen Komponenten auf Basis der von (Stiny 1982) vorgestellten *Gestaltgrammatiken* (*shape grammars*) für die Rekonstruktion. Das Verfahren setzt Gebäudemodelle aus Gebäudeendstücken (*Terminalen*) und -verbindern (*Konnektoren*) zusammen. Terminale und Konnektoren sind offene Modellkörper mit mindestens einer definierten Anschlussöffnung (*plug face*). Da die Anschlussöffnungen jedoch integraler Bestandteil der Primitive sein und für zwei verbindbare Teile die gleiche Gestalt haben müssen, ist es nicht möglich, eine gewünschte Detailrekonstruktion mit einer handhabbaren Menge von Primitiven zu erreichen. Eine Verfeinerung der erzeugten Modelle ist somit in diesem Ansatz ausgeschlossen.

Eine formale Grammatik, die auf dem Konzept der *set grammar* (Stiny 1982) aufbaut, wird bei (Müller et al. 2006) verwendet. Die Geometrie ist hierbei in impliziter Form an die Bestandteile der Grammatik gebunden. Gleichzeitig werden Bedingungsgleichungen verwendet, um Vorwissen über z. B. Mindest- oder Höchstwerte von Gebäudeparametern in den Produktionsprozess zu integrieren. Zusätzlich wird ein von (Duarte 2002) in seiner Doktorarbeit erstmals verwendetes Konzept der Aufteilung eines bereits existenten räumlichen Objektes in Bestandteile in das System integriert und von (Wonka et al. 2003) in eine *split grammar* überführt. Hierbei wird ein Symbol mit geometrischer Form in eine Menge von Symbolen mit disjunkten, sich nur am Rand berührenden geometrischen Formen gleicher Dimension gespalten. Notwendige Voraussetzung für die Anwendung des Grammatikkonzepts ist der *scope*, der den maximal verfügbaren Raum für ein Gebäude umfasst (Müller et al. 2006). Nachteilig macht sich das scope-Konzept vor allem im Rekonstruktionsverfahren bemerkbar, da die Bestandteile des scope nicht direkt beobachtbar sind, was die Steuerung der Generierung auf Basis der Beobachtungen verhindert. Die Verwendung des Konzeptes der set grammars hat zudem den Nachteil, dass Geometrien und ihre Bedingungen in diesem Formalismus nicht vollständig und explizit repräsentiert sind. Dies ist insbesondere für die Rekonstruktion von Nachteil, da diese vorhandenen Informationen dort dann nicht nutzbar sind.

Dass Teile des in (Müller et al. 2006) vorgestellten Verfahrens sich auch für Rekonstruktionsprozesse eignen, wird am Beispiel der Fassadenrekonstruktion deutlich (Müller et al. 2007). Ein ähnlicher Ansatz wird auch bei (Ripperda & Brenner 2007) verfolgt. Beide Gruppen stützen sich hierbei auf die Rekonstruktion auf Basis von terrestrischen Bildern. Die in diesem Ansatz eingesetzten Grammatiken adressieren jedoch im Unterschied zu den in diesem Artikel vorgestellten ein zweidimensionales Problem und setzten ein hohes Maß an Symmetrien in den zu rekonstruierenden Fassaden voraus. Das Problem der Fassadenrekonstruktion wird hier nicht weiter behandelt; es ist mit dem hier vorgestellten Verfahren kombinierbar.

Dieser Artikel gliedert sich im Weiteren wie folgt: In Abschnitt 2 wird der Weg von einer Ontologie zu einer attributierten Grammatik vorgestellt, sowie ein Verfahren zur Zuordnung zwischen Modellhypothesen und Daten beschrieben. Abschnitt 3 stellt eine attributierte Grammatik zur Erzeugung von Gebäudemodellen grober Auflösung vor. Der Artikel endet mit einem Ausblick auf die Erweiterung der Grammatik für Modellhypothesen mit Dächern und Gauben.

2 Von Ontologien zu attributierten Grammatiken zur Erzeugung von Modellhypothesen für Gebäude

Eine Möglichkeit, Wissen über die Welt zu sammeln, zu analysieren und zu formalisieren sind *Ontologien*. Im Rahmen der Erstellung einer Ontologie werden die zwischen den Objekten und den Objektklassen bestehenden mereologischen (Bestandteilsrelationen), topologischen (Nachbarschaftsrelationen) und taxonomischen Beziehungen herausgearbeitet. Insbesondere die mereologischen und topologischen Beziehungen enthalten Information, die in Regeln für den Aufbau von Gebäuden aus Komponenten abbildbar sind. Ein weiterer Aspekt einer Ontologie sind die Relationen zwischen einem Begriff, dem zugehörigen physischem Körper und seiner geometrischen Repräsentation. Dieser Aspekt führt zu einer Analyse der notwendigen inneren Restriktionen, denen die Geometrie eines Gebäudeteils unterliegt und zur Identifikation von Konfigurationen, anhand welcher Geometrien klassifiziert werden können. Jede Konfiguration besitzt erstens eine geometrische Interpretation. Zweitens besitzt sie eine Menge von Eigenschaften, welche erfüllt sein müssen, z. B. die Geschlossenheit der Gebäudehülle. Drittens besitzt jede Konfiguration einen Bezug zur Ontologie und somit eine Einbettung in die mereologische und topologische Gesamtstruktur des Gebäudes.

Ein Mechanismus, um aus Komponenten und Regeln komplexe Strukturen zu generieren oder diese zu zerlegen, sind *formale kontextfreie Grammatiken*, wie sie z. B. von (Chomsky 1959) beschrieben werden. Zentrale Elemente sind zum einen die Symbole, welche im Kontext dieser Arbeit Komponenten eines Gebäudes repräsentieren, und

Produktionsregeln, die beschreiben wie ein Symbol verändert, ergänzt oder ersetzt werden darf. Zur Repräsentation der oben beschriebenen Konfigurationen ist das Konzept noch um Attribute für die Symbole und semantische Regeln zu einer *attributierten Grammatik* (KNUTH 1968) zu ergänzen. Ein Symbol der Grammatik für Gebäude trägt somit eine Semantik, z. B. Geschoss, und in den Attributen die Parameter der assoziierten Geometrie sowie eine Repräsentation ihrer charakteristischen Eigenschaften. Die semantischen Regeln haben hierbei zwei Aufgaben. Die erste ist die Verknüpfung der Attribute der über eine Produktionsregelanwendung verknüpften Symbole. Die zweite Funktion ist es, Bedingungen für die Anwendbarkeit einer Produktionsregel zu formulieren.

Als Mechanismus zur Repräsentation der charakteristischen Eigenschaften wird ein Graph, der *Constraint-Graph*, gewählt, dessen Knoten für jeweils ein geometrisches Element stehen und dessen Kanten geometrische oder topologische Bedingungen (*Constraints*) repräsentieren, welche zwischen den Knoten oder für die Knoten gelten. Es gibt zwei unterschiedliche Constraint-Graphen. Der erste wird mit der Grammatik generiert und der zweite wird aus den Eingangsdaten, in der Regel Laserscan-Daten, hergeleitet. Die beiden Graphen können über Graphzuordnungsverfahren miteinander verglichen werden. Somit eröffnet die Grammatik eine Möglichkeit, Hypothesen für Gebäudemodelle zu erzeugen, mit deren Hilfe die Eingangsdaten über die Graphzuordnung klassifiziert werden können. Durch die Grammatik können die Modellhypothesen zudem zielgerichtet generiert werden, da eine Entscheidungsfunktion die nächste anzuwendende Produktionsregel auswählt. Hierbei ist es möglich, als Entscheidungsfunktion die in der Einleitung erwähnten Verfahren der Modellselektion in den generativen Prozess zu integrieren.

Im Folgenden wird nun die aus der Ontologie abgeleitete attributierte kontextfreie Grammatik umrissen. *Attributierte Grammatiken* (AG) sind nach KNUTH (1968) definiert als Tupel der Form

$$AG = (N, \Sigma, P, R, A, S) \quad (1)$$

Hierbei repräsentiert N die Menge der Nichtterminale und die Menge Σ der Terminale. $N \cup \Sigma$ ist die Gesamtmenge aller Symbole der Grammatik. Nichtterminale stehen hierbei für Symbole, welche im Gegensatz zu Terminalen durch Produktionsregeln ersetzt werden können. P steht für die Menge der Produktionsregeln der Form

$$N \rightarrow (\Sigma \cup N)^* \quad (2)$$

wobei *, der *Kleene-Sternoperator*, für eine beliebige Aneinanderreihung der Elemente aus $N \cup \Sigma$ steht. Bei einer Regelanwendung wird ein Nichtterminal durch die rechte Seite der Regel ersetzt. R ist die Menge der semantischen Regeln, A die der Attribute und S ist die der Startsymbole, einer Teilmenge der Nichtterminale. Mit ihnen kann eine generative Ableitung von Worten der Grammatik begonnen werden. Die Menge der Symbole umfasst z. B. zwei Gebäudesymbole $\{B, b\}$, zwei Vollgeschosssymbole $\{V, v\}$, jeweils zwei Symbole für Pult-, Sattel- und Walmdachgeschoss $\{PD, pd, SD, sd, WD, wd\}$, sowie zwei Symbole für eine Mischform, die halb Sattel- und halb Walmdachgeschoss ist $\{SWD, swd\}$. Alle aufgezählten Symbole sind sowohl in der Menge der Nichtterminale (Symbolbenennungen in Großbuchstaben) und der Terminale (Symbolbenennungen in Kleinbuchstaben) vertreten. Die Menge der Startsymbole umfasst das Nichtterminalsymbol $\{B\}$ für Gebäude.

Begonnen wird die Produktion mit der einfachsten Form eines Gebäudekörpers, einem Quader, welcher stellvertretend für ein einfaches Flachdachgebäude steht. In der ersten Produktionsphase wird eine Hypothese weiterverfolgt, wenn diese als Teil des zu rekonstruierenden Gebäudes identifiziert werden kann. Diese Weiterentwicklung erfolgt durch das sukzessive Anfügen weiterer Flachdachgebäude an die vorhergehende akzeptierte Modellhypothese. Alle sich ergebenden Modellhypothesen entsprechen in diesem Stadium der Produktion des in *CityGML* (GRÖGER et al. 2005), einem

Format zur Repräsentation von 3D-Stadtmodellen definierten *Detaillierungsgrads* 1 (*Level of Detail 1, LoD1*). Die in diesem Schritt erzeugten Teile der Flachdachgebäude lassen sich in der zweiten Produktionsphase, wenn die Flachdachhypothese nicht zutrifft, durch die Anwendung von Produktionsregeln jeweils durch Hypothesen für Teilgebäude mit anderem Dachtyp (z. B. Satteldach) ersetzen, wobei die bereits erfolgte Zugordnung von Wandgeometrien beibehalten wird. Gleichzeitig erfolgt die Anpassung des Constraint-Graphen durch die Produktionsregel. Dieses Vorgehen ähnlich der von (Brenner 2000) vorgeschlagenen Zerlegung des Grundrisses in Rechtecke zum Finden von Anknüpfungspunkte für Dachhypothesen.

3 Generierung von Gebäudemodellen

Als nächster Schritt hin zur Erzeugung von Hypothesen für komplexe Gebäudemodelle wird zunächst eine Grammatik zur Erzeugung solcher Modelle vorgestellt. Dies ermöglicht eine weitere Nutzung gewonnen Wissens und einen ersten Eindruck von den mit der Grammatik beschreibbaren Gebäudemodellen. Für die Erzeugung typischer Gebäudemodelle werden die Geometrien der Grammatiksymbole durch Primitive der *Constructive Solid Geometry – CSG* (Mäntylä 1988) repräsentiert und ihre freien Parameter mit typischen Maßen und Maßbereichen aus der Ontologie belegt. Darüber hinaus sind Wahrscheinlichkeiten aus Vorwissen abzuleiten. Der Produktionsprozess wird dann nicht mehr durch die Verfahren der Modellselektion bestimmt, sondern durch ein probabilistisches Entscheidungsverfahren z. B. auf Basis einer Gaußverteilung. In diesem Fall lassen sich die Produktionsregeln vereinfachen, da die Fortschreibung des Constraint-Graphen nicht explizit betrachtet werden muss. Die Grammatik hat die folgenden Produktionsregeln:

1. Änderungsproduktion
   $$P_1 : B \rightarrow B \qquad (3)$$
2. Rotationsproduktionen
   $$P_{2\ldots5} : B \xrightarrow{0\cdots3} B \qquad (4)$$
3. Skalierungs- und Instanziierungsproduktion
   $$P_6 : B \rightarrow k, B \qquad (5)$$
4. Terminierungsproduktion
   $$P_7 : B \rightarrow \varepsilon \qquad (6)$$
5. Teilungsproduktion
   $$P_8 : B \rightarrow [B]^n \qquad (7)$$

Neben den Produktionsregeln enthält die attributierte Grammatik auch semantische Regeln, die Attributwerte zwischen den Symbolen einer Produktionsregel übertragen. Da sowohl die Verortung der CSG-Primitive in Form einer Transformationsmatrix T als auch deren Größe durch die Attribute der Symbole bestimmt wird, sind alle bei den Produktionen stattfindenden geometrischen Operationen Teil der semantischen Regeln der jeweiligen Produktionsregel. Im Rahmen der Produktionsregel P_1 wird ein Körper erzeugt und im Raum positioniert. Im Fall der Generierung handelt es sich um ein „typisches“ Geschoss mit dem Ankerpunkt im Ursprung.

Die vier Produktionsregeln (P_3 bis P_6) unterscheiden sich durch den Rotationsursprung, der durch den Index $i \in \{0, 1, 2, 3\}$, der über dem Produktionspfeil notiert ist, angegeben wird. Dies ist in Abb. 1 dargestellt. Bei Anwendung einer solchen Regel wird zuerst das Rotationszentrum auf eine der vier unteren Eckpunkte des Quaders ver-

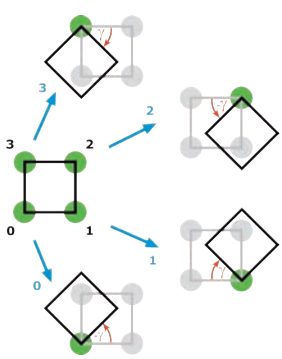

Abb. 1: Graphische Darstellung der Rotationsproduktionen P_2 bis P_5.

lagert (Transformationsmatrix T_i) und dann eine Rotation γ zwischen 0° und 90° (Rotationsmatrix R_γ) zuzüglich einer Basisrotation (Rotationsmatrix R_i) abhängig von der jeweiligen Ecke ausgeführt. T_V ist ein Attribut des linken Nichtterminalsymbols B und T_R vom rechten B. Anwendungen der Regeln sind in Abb. 1 gezeigt; T_R wir dabei durch die folgende semantische Regel berechnet:

$$T_R = T_V \cdot R_\gamma \cdot R_i \cdot T_i \quad (6)$$

Alle nicht explizit aufgeführten semantischen Regeln übertragen die Attributwerte des Symbols auf der linken Seite direkt auf die entsprechenden Attribute der produzierten Symbole.

Eine besondere Art der Produktionsregeln, die erstmals bei (MÜLLER et al. 2006) verwendete Teilungsproduktionsregel (P_8), dient der Aufteilung eines virtuellen Körpers entlang der Längsachse in n gleichlange virtuelle Körper gleicher Dimension. Dieses Vorgehen entspricht semantisch der Aufteilung eines Gebäudes in mehrere Teile auf Basis von Vorwissen. Diese Art der Produktionsregeln wird auch bei der Erzeugung von Gebäuden mit differenzierten Geschossen eine wichtige Rolle spielen, da für diese typische Geschosshöhen vorliegen.

Neben den semantischen Regeln sind die Produktionsregeln auch mit Constraints versehen, die erfüllt sein müssen, damit eine Produktionsregel ausgeführt wird. Die Constraints lassen sich aus der eingangs erwähnten Ontologie für Gebäude ableiten und werden hier nicht explizit wiedergegeben.

Ein Beispiel für die Anwendung der Regeln ist anhand eines Ableitungsbaums in Abb. 2a) gezeigt. Angewendet wurden nacheinander die Regeln P_6, P_8, P_5, P_6, P_8, ... Das Ergebnis der Regelanwendungen ist im Sinne der *constructive solid geometry* (CSG) (MÄNTYLÄ 1988) als CSG-Baum zu interpretieren. Jeder innere Knoten steht für eine Vereinigungsoperation. Die entsprechende Randflächendarstellung (*boundary representation*) kann daraus mit Standardverfahren aus dem Bereich *computer aided design* (*CAD*) abgeleitet werden.

4 Ausblick

Mit der Grammatik steht ein Verfahren zur Verfügung, welches an den Rekonstruktionsprozess angepasst arbeitet. Diese Anpassung ergibt sich aus dem Aufbau des Gesamtmodells aus Modellteilen und zugehörigen Aggregationsmechanismen. Somit ist es möglich, die Daten sequentiell zu erkunden und zu erklären. Durch die Einbringung von Modellwissen ist es dennoch möglich, fehlerhafte Daten zu korrigieren und Lücken in den Daten zu schließen. Durch die Einführung der Rotationsproduktionen ist es gelungen, eine hohe Variabilität der Grundrisse zu erreichen und insbesondere

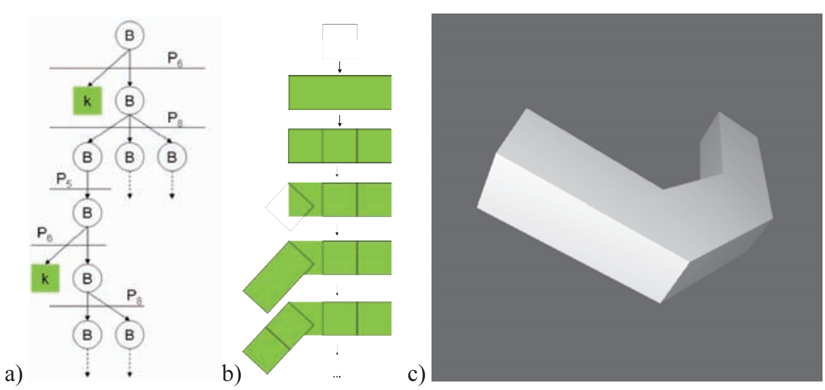

Abb. 2: (a) Auszug des Ableitungsbaums der Grammatik und eine Visualisierung seiner Geometrie (b) für ein Gebäudemodell (c).

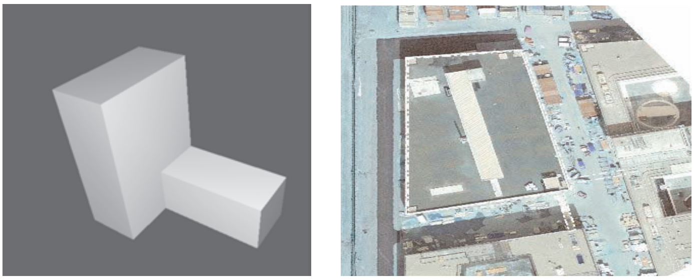

Abb. 3: Eine generierte Gebäudehypothese mit unterschiedlich vielen Stockwerken (links) und ein Gebäudegrundriss mit Eckwinkeln von weniger als 90° (rechts).

das Rekonstruktionsmodell für das in Abb. 2 präsentierte Beispiel mit Hilfe der Grammatik zu erzeugen.

Wie im Abschnitt 2 angedeutet, kann die Grammatik kanonisch erweitert werden, um auch Gebäude mit mehr als einem Geschoss zu erzeugen. Gleiches gilt für die Generierung von Gebäuden mit Gebäudeteilen unterschiedlicher Geschossanzahlen. Ein Beispiel zeigt Abb. 3 links.

Es zeigte sich aber, dass die volle Variabilität im Grundriss aufgrund der gewählten geometrischen Primitivkörper noch nicht in Gänze erreicht ist. So stellen insbesondere Gebäude mit sehr spitzen Ecken, wie in Abb. 3 rechts gezeigt, ein Problem dar, da die Vereinigung von Quadern nur Winkel von mindestens 90° ermöglicht. Diesem Problem kann begegnet werden, indem die in den Primitiven enthaltenen Restriktionen explizit gemacht und somit teilweise deaktiviert oder aufgeweicht werden können. Ein Vorschlag für eine solche Modellierung findet sich in (Brenner 2004); es muss untersucht werden, wie dieser Ansatz in den hier vorgestellten integriert werden kann.

Neben der Aufweichung und Deaktivierung der Constraints sind Erweiterungen der vorgestellten Grammatik in Richtung detailreicherer Modelle erforderlich. Im ersten Schritt muss die Generierung von Dächern ermöglicht werden. Die bislang generierten Modelle sind ausnahmslos Flachdachgebäude und somit nicht geeignet für die Rekonstruktion von typischen Gebäuden unserer Breiten. Hierfür ist es notwendig, auch die Dachlandschaften mit all ihren komplexen Teilstrukturen in die Modelle zu integrieren. Ziel wird es daher sein, die durch den Generierungsprozess entstehende Aufteilung des Grundrisses zu nutzen, um die Dachstruktur der Gebäude abzuleiten bzw. diese zu produzieren. Der nächste Schritt ist die Rekonstruktion der Detailstruktur der Dächer in Form der Dachöffnungen wie Dachgauben, Dachfenster oder Dachbalkonen.

Weiter wird zu untersuchen sein, ob die Kombination des hier vorgestellten Ansatzes mit den in der Einleitung angesprochen Verfahren zur Rekonstruktion der Fassadenstrukturen möglich ist, um ein hoch detailliertes Gesamtmodell für Gebäude zukünftig für die schrittweise Rekonstruktion zur Verfügung stellen zu können.

Danksagung

Besonderer Dank gilt Viktor Stroh, Martin Krückhans und Jan Behmann für Diskussionen und Unterstützung bei der Umsetzung der Konzepte. Diese Arbeit entstand im Kontext des von der Deutschen Forschungsgemeinschaft (DFG) geförderten Bündelprojektes „Abstraktion von Geoinformation bei der multiskaligen Erfassung, Verwaltung, Analyse und Visualisierung“ (FO 180/10-1).

Literatur

Abmayr, T., Härtl, F., Mettenleiter, M., Heinz, I., Hildebrand, A., Neumann, B. & Fröhlich, C., 2004: Realistic 3d-reconstruction – combining laserscan data with rgb-color-information. – International Archives of Photogrammetry, Remote Sensing and Spatial Information Sciences **35:** 198–203.

AKAIKE, H., 1974: A new look at the statistical model identification. – IEEE Transactions on Automatic Control **19** (6): 716–723.

BORNAZ, L., LINGUA, A. & RINAUDO, F., 2003: Multiple scan registration in lidar close range applications. – International Archives of Photogrammetry, Remote Sensing and Spatial Information Sciences **34** (6).

BRENNER, C., 2000: Dreidimensionale Gebäuderekonstruktion aus digitalen Oberflächenmodellen und Grundrissen. – Dissertation, Fakultät für Bauingenieur- und Vermessungswesen der Universität Stuttgart.

BRENNER, C., 2004: Modelling 3d objects using weak csg primitives. – International Archives of Photogrammetry, Remote Sensing and Spatial Information Sciences **35** (3): 1085–1090.

CHOMSKY, N., 1959: On certain formal properties of grammars. – Information and Control **2:** 137–167.

DUARTE, J., 2002: Malagueira Grammar – towards a tool for customizing Alvaro Siza's mass house at Malagueira. – PhD thesis, MIT School of Architecture and Planning.

FISCHLER, M.A. & BOLLES, R. C., 1981: Random sample consensus: A paradigm for model fitting with applications to image analysis and automated cartography. – Communications of the ACM **24** (6): 381–395.

GRÖGER, G., BENNER, J., DÖRSCHLAG, D., DREES, R., GRUBER, U., LEINEMANN, K. & LÖWNER, M.-O., 2005: Das interoperable 3D-Stadtmodell der SIG 3D – Zeitschrift für Vermessungswesen **130** (6): 343–353.

KAHLESZ, F., LILGE, C. & KLEIN, R., 2007: Easy-to-use calibration of multiple-camera setups. – Workshop on Camera Calibration Methods for Computer Vision Systems (CCMVS2007).

KNUTH, D. E., 1968: Semantics of context-free languages. – Theory of Computing Systems **2** (2): 127–145.

MIERSWA, I., WURST, M., KLINKENBERG, R., SCHOLZ, M. & EULER, T., 2006: Yale: Rapid prototyping for complex data mining tasks. Proceedings of the 12th ACM SIGKDD International Conference on Knowledge Discovery and Data Mining.

MÜLLER, P., WONKA, P., HAEGLER, S., ULMER, A. & VAN GOOL, L., 2006: Procedural modeling of buildings. – Proceedings of ACMSIGGRAPH 2006 / ACMTransactions on Graphics (TOG), ACM Press **25** (3): 614–623.

MÜLLER, P., ZENG, G., WONKA, P. & VAN GOOL, L., 2007: Image-based Procedural Modeling of Facades: – Proceedings of ACM SIGGRAPH 2007 / ACM Transactions on Graphics **26** (3).

MÄNTYLÄ, M., 1988: Introduction to Solid Modeling. – W.H. Freeman & Co., New York, NY.

RIPPERDA, N. & BRENNER, C., 2007: Data driven rule proposal for grammar based facade reconstruction. – International Archives of Photogrammetry, Remote Sensing and Spatial Information Sciences **36** (3/W49A): 1–6.

STEINHAGE, V., 1998: Zur automatischen Gebäuderekonstruktion aus Luftbildern. – Habilitation, Faculty of Mathematics and Natural Science of the University of Bonn.

STINY, G., 1982: Spatial relations and grammars. – Environment and Planning B **9**: 313–314.

WONKA, P., WIMMER, M., SILLION, F. & RIBARSKY, W., 2003: Instant architecture. – ACM Transactions on Graphics **22:** 669–677.

Anschrift der Autoren:

Dipl.-Ing. DIRK DÖRSCHLAG, PD Dr. GERHARD GRÖGER, Prof. Dr. LUTZ PLÜMER, Rheinische Friedrich Wilhelm Universität Bonn, Institut für Geodäsie und Geoinformation, D–53115 Bonn, Tel.: +49-228-73-3035 (Dörschlag), 1764 (Gröger), 1750 (Plümer), Fax: +49-228-73-1753, e-mail: doerschlag | groeger | pluemer@uni-bonn.de

Manuskript eingereicht: Dezember 2007
Angenommen: März 2008

Photogrammetrie • Fernerkundung • Geoinformation 3/2008, S. 165–173, 4 figs., 2 tabs.

Assuring Logical Consistency and Semantic Accuracy in Map Generalization

JAN-HENRIK HAUNERT & MONIKA SESTER, Hannover

Keywords: GIS, Data Abstraction, Spatial Data Quality, Aggregation, Optimization

Summary: In recent years national mapping agencies have increasingly integrated automatic map generalization methods in their production lines. This raises the question of how to assess and assure the quality of mapping products such as digital landscape models. Generalization must not only ensure specified standards for an output scale, but also needs to keep semantics as similar as possible under these given requirements. In order to allow for objective comparisons of different generalization results we introduce a semantic distance measure. We present results that optimize this measure subject to constraints reflecting database specifications and show how this measure can be used to compare the results of different methods, including exact and heuristic approaches.

Zusammenfassung: *Gewährleistung logischer Konsistenz und semantischer Genauigkeit in der Generalisierung*. In zunehmendem Maß werden automatische Generalisierungsverfahren für die Produktion amtlicher digitaler Landschaftsmodelle eingesetzt. Dadurch entsteht ein wachsender Bedarf nach Verfahren zur Qualitätskontrolle und Qualitätssicherung. Generalisierung muss nicht nur für den Zielmaßstab definierte Standards realisieren, sondern dabei auch die Semantik repräsentierter Objekte nach Möglichkeit erhalten. Wir definieren ein semantisches Distanzmaß, um einen objektiven Vergleich unterschiedlicher Generalisierungsergebnisse zu ermöglichen, präsentieren Ergebnisse, die unter Nebenbedingungen aus existierenden Spezifikationen hinsichtlich dieses Maßes optimal sind, und zeigen Vergleichsmöglichkeiten von Ergebnissen exakter und heuristischer Verfahren auf.

1 Introduction

According to MORRISON (1995) there are seven elements of spatial data quality: Lineage, positional accuracy, attribute accuracy, completeness, logical consistency, semantic accuracy and temporal information. Most of them are affected by map generalization, for example, when applying displacement or simplification algorithms to lines, their positional accuracy is reduced; selection of objects affects completeness. The assessment and assurance of these quality criteria are important problems, especially, when heuristic generalization methods are applied. In this article we discuss how to assure semantic accuracy and logical consistency, that is, compliance with database specifications.

Following this aim, we have developed a method for area aggregation by optimization, more precisely, mixed-integer programming (HAUNERT & WOLFF 2006). Our method has technically been presented in sufficient depth: we have proven the NP-hardness of the problem, tested multiple optimization criteria (HAUNERT 2007a), and developed specialized heuristics to obtain a better performance (HAUNERT 2007b). This method yields very good results, especially compared with commonly used iterative approaches that locally merge too small objects with their best compatible neighbors (HAUNERT 2007b). However, we have not sufficiently elaborated the usefulness of this method for quality assurance and quality assessment. This article focuses on these

1432-8364/08/2008/165 $ 2.25

issues. In an optimization approach, a global quality measure becomes part of the generalization method: Basically, there should not be any difference between a quality measure for the assessment of the generalization result and the objective function in the optimization approach. Nevertheless, research on the quality assessment of generalization and research on optimization approaches to generalization have seldom been consolidated.

The issue of semantic accuracy is especially relevant, when map objects change their classes. In map generalization this happens in two cases: class abstraction and object aggregation. The latter case leads to class changes, when multiple objects of different classes are replaced by a single composite object. Class abstraction means, for example, to replace all churches and all post offices by objects of type public building. This only needs to be done one time by an expert on a conceptual level and thus it can easily be implemented. In contrast, object aggregation is a labor-intensive problem that needs to be automated. When masses of data are processed, also the quality assessment becomes difficult. Cheng & Li (2006) suggest to measure the semantic accuracy according to the area that changes its class in generalization. Yaolin et al. (2002) introduce a symmetric semantic similarity matrix to compare object types of areas before and after reclassification. Rodríguez & Egenhofer (2004) propose an asymmetric similarity measure. Similarity values are derived from the given data model, taking class hierarchies into account and comparing attribute definitions. Ahlquist (2005) uses a similarity measure based on fuzzy membership functions to assess land cover changes over time.

The quality of map generalization is normally defined by comparison of input and output data sets (Bard 2004 and Frank & Ester 2006). These methods mainly depend on measures that characterize the shapes of objects and their spatial relationships. Basically, observed changes are penalized in the assessment. However, generalization naturally cannot always preserve the original situation: there are driving forces to change the data set, for example, minimal allowed sizes for the target scale. Thus, we compare the results of heuristic generalization methods with results that are optimal under given constraints. These results can be obtained with our mixed-integer program. Though this is only possible for small samples, these offer new possibilities to detect shortcomings of heuristics.

In the sequence of the article, we first explain our conceptions of logical consistency (cf. Section 2) and semantic accuracy (cf. Section 3) and then present our approach to assure and assess these elements of quality (cf. Section 4).

2 Logical Consistency

Kainz (1995) defines logical consistency as follows:

> "A spatial data set is said to be logically consistent when it complies with the structural characteristics of the selected data model and when it is compatible with the attribute constraints defined for the set."

The data model in our work is a planar subdivision, that is, an exhaustive coverage of the plane by areas that must not overlap. This representation is often used for land cover data in topographic databases. The generalization of such data sets is a well known problem (Galanda 2003). Often additional requirements are defined, for example, the shapes of features need to be contiguous. Formally it means that for each two points in a contiguous area, there is a connecting path that is totally contained in the area. These structural requirements are independent of scale and we need to ensure their preservation during generalization. In contrast, requirements on attributes and geometries are often different for the input and output scale, thus we need to change the map. Tab. 1 compares the definitions of forest areas in three different countries. In each example, a minimal size is defined as criterion for selection, which naturally increases for smaller scales. The term "Guaranteed size", which is used in the Canadian specifications, unmistakably states that the defined thresholds must not be violated in any case. This is described accordingly in the other specifications. These strong claims are needed to reduce the influence of subjectivity in map generalization and to provide standardized map products.

Since areas below threshold in the target scale are not allowed, they need to be aggregated with others in order to keep the coverage exhaustive. As all other aims of generalization need to be subordinated, class changes need to be accepted, for example, if there is no neighbor of the same class. Formally, we define the area thresholds for different classes by $\theta\colon \Gamma \rightarrow \mathbb{R}^{+}$, with Γ being the set of all classes. The term constraint fits well for the requirements given by database specifications. However, this must not be mixed up with constraints that allow for a gradual degree of satisfaction. Most researchers in the field of map generalization point out that constraints are often conflicting and compromises need to be found (Weibel & Dutton 1998 and Harrie 1999). As constraints that ensure logical consistency do not allow any compromise, we distinguish hard constraints and soft constraints.

If the input data set is logically consistent, we normally can define simple generalization algorithms that produce logically consistent results. For instance, we can apply merge or collapse procedures to resolve size and proximity conflicts (Bader & Weibel 1997 and Haunert & Sester 2008). However, at this early stage of our discussion we should not commit too much to particular algorithms. Database specifications define the feasibility of solutions, but there remains much freedom in deciding for different options. Thus, we need to formalize additional aims of generalization.

Tab. 1: Selection criteria for forest areas in three different national databases. The Canadian specifications use the term ''Guaranteed size''. In the Australian specifications this is called ''Minimum size for inclusion''.

Germany ATKIS (AdV 2003)		Canada National Topographic Database (Natural Resources Canada 1996)		Australia National Topographic Database (Geoscience Australia 2006)	
Wald, Forst		Wooded Area		Forest or Shrub	
„Fläche, die mit Forstpflanzen (Waldbäume und Waldsträucher) bestockt ist.“		„An area of at least 35 % covered by trees or shrubs having a minimum height of 2 m.“		„An area of land with woody vegetation greater than 10 % foliage cover (includes trees and shrubs).“	
scale	selection criterion	scale	selection criterion	scale	selection criterion
1:25k	area $\geq$ 0,1 ha	1:50k	area $\geq$ 1ha AND width $\geq$ 50m	1:25k	area $\geq$ 0.25ha
1:50k	area $\geq$ 1 ha			1:100k	area $\geq$ 4ha
1:250k	area $\geq$ 40 ha	1:250k	area $\geq$ 25ha AND width $\geq$ 250m	1:250k	area $\geq$ 25ha
1:1000k	area $\geq$ 500 ha				

Tab. 2: Semantic distance matrix. Colors and shades are used in Fig. 1 and Fig. 2.

original class \ new class	Settlement	Farmland	Grassland	Forest
Settlement	0	1	1	1
Farmland	1	0	0.2	0.3
Grassland	1	0.2	0	0.3
Forest	1	0.3	0.3	0

3 Semantic Accuracy

SALGÉ (1995) gives the following definition of semantic accuracy:

> "The purpose of Semantic Accuracy is to describe the semantic distance between geographical objects and the perceived reality."

Formally we express the semantic distance between classes as a function d: $\Gamma^2 \to \mathbb{R}_0^+$. Given a real value s (between 0 and 1) that measures the semantic similarity of two classes, for example, as it can be obtained with the method proposed by YAOLIN et al. (2002), we can define the corresponding value of d simply as 1-s.

Tab. 2 shows a distance matrix that we generated with a less objective approach, that is, we defined the semantic distance values at our own discretion. We considered hierarchies in the data model and textual descriptions (as given in Tab. 1) for this task. For example, since farmland and grassland are classes of cultivated vegetation, we defined a relatively small semantic distance in between. This means that we would rather accept a change of a grassland area into farmland than into settlement. As a global measure of semantic accuracy we introduce the weighted average of the distances that are measured between original classes and classes after generalization. Let V be the set of all areas in the input map, w: $V \to \mathbb{R}^+$ denote the sizes of areas, γ: $V \to \Gamma$ their original classes, γ: $V \to \Gamma$ their new classes, we globally measure the semantic distance by

$$\frac{\sum_{v \in V} w(v) \cdot d(\gamma(v), \gamma'(v))}{\sum_{v \in V} w(v)} \tag{1}$$

In the same way, we can measure the semantic distance for a single area in the input data set, for a single area in the output data set, or for all areas of a certain class.

Though the matrix in Tab. 2 is symmetric, symmetry is not a general requirement for the function d. For example, we can define $d(\gamma_1, \gamma_2) = 0.1$ and $d(\gamma_2, \gamma_1) = 1$, meaning that a class change from γ_1 to γ_2 is more accepted than vice versa. This model is useful, as important classes like, for example, water often should not be lost. Because of this, we do not assume that d meets the formal definition of a metric, which requires symmetry.

In order to measure semantic accuracy, we should not only focus on classes but also consider shapes. Consider two lakes and a long, narrow river that connects both: Aggregating the three objects into a single object of class lake only requires to change the class of the river. Though this will be a good solution in terms of class distances, the shape of the resulting aggregate would be very uncommon for a lake. We therefore penalize shapes that are not geometrically compact. Different measures of compactness have been discussed in an earlier work (HAUNERT 2007a). We ignore this additional criterion in the sequence of this article.

We use the result of the exact optimization approach as a benchmark for quality, as it is able to satisfy our general goal of semantic accuracy in terms of a semantic distance.

4 Optimization Approach

4.1 *Problem formulation*

In terms of optimization, each logically consistent map is a feasible solution. The optimal feasible solution is the one that minimizes the global semantic distance measure from Section 3. We refer to this measure as cost function. The problem is to partition the set V into mutually disjoint subsets $V_1 \cup V_2 \cup \ldots \cup V_k = V$, where k is an unknown integer. Each of these subsets defines a composite area for the target scale. Thus, for each $i = 1 \ldots k$, we define the following hard constraints:

- there is a single class $\gamma_i' \in \Gamma$, such that each area $v \in V_i$ receives class γ_i', that is, $\gamma'(v) = \gamma_i'$
- the composite area has sufficient size, that is, $\Sigma_{v \in V_i} w(v) \geq \theta(\gamma_i')$
- the composite area is contiguous
- there is an area $v \in V_i$ of unchanged class, i. e., $\gamma'(v) = \gamma(v)$. This is referred to as centre

The last requirement simply avoids that classes appear in the generalized map, which have not been present at all. Generally, we do not assume that the set of centers is given in advance.

4.2 *Approach by mixed-integer programming*

Normally, combinatorial optimization problems in map generalization are approached by meta-heuristics such as hill-climbing or simulated annealing (Ware & Jones 1998). Several theoretical achievements have been made, proving asymptotical convergence of simulated annealing under certain conditions. For example, the graph that is defined by the applied neighborhood structure must be strongly connected (Michiels et al. 2007). Though simulated annealing cannot be used in practice to find the exact optimum, it often produces solutions of sufficient quality. We therefore developed a simulated annealing approach for the aggregation problem (Haunert 2007c). However, we needed to relax hard size constraints to reach sufficiently good solutions via feasible paths. In view of database specifications that strictly forbid too small regions, this approach is risky, as we might end up with a result that is not logically consistent. We therefore focused on mixed-integer programming and specialized heuristics, which better allow to consider hard constraints.

Mixed-integer programming is an exact approach to constrained, combinatorial optimization problems (Papadimitriou & Steiglitz 1998). Generally, algorithms for the solution of mixed-integer programs (MIPs) have an exponential time performance. It is unlikely that we can find a polynomial time algorithm, as the aggregation problem is NP-hard. This fact was proven in an earlier publication (Haunert & Wolff 2006). We also presented and tested different MIP formulations. Due to the high complexity we were only able to optimally solve small instances (up to 50 areas) with our exact MIP, but we greatly improved the performance with three heuristics:

1. A strong definition of contiguity according to Zoltners & Zinha (1983) is applied, which excludes certain non-compact composite areas.
2. Large areas are fixed as centers, small areas are excluded from the set of potential centers.
3. Areas with a large distance in between are not merged in the same composite area.

The first heuristic leads to an alternative MIP formulation that can be solved much more efficiently by existing solvers. Both other heuristics are used to eliminate variables in this MIP. A further heuristic has been developed that allows to decompose a dataset of arbitrary size into manageable pieces (Haunert 2007b). The basic idea of this method is to introduce intermediate scales whenever needed to break down the complexity of the problem.

4.3 *Quality assessment*

Without heuristics our optimization approach is too slow for cartographic production. However, as it yields the exact optimum for small problem instances, it can be used to test heuristic methods. For example, applying heuristics 1–3 we usually obtain results not worse than 10% from optimum. Such objective statements about the performance of generalization procedures are very rare in the literature. Often results are only visually assessed by test persons, but this approach is questionable, if the spatial data set is not only to be used for visualization, but also for statistics or other analyses. On the other hand, visualization is still the most important method to assess the quality of spatial data sets. How do 10% affect the understanding of the map content? We can only answer this question when visualizing the results.

Fig. 1 shows a sample from the German ATKIS data set at scale 1:50.000 (DLM50) with two results satisfying specifications for scale 1:250.000 (DLM250): the optimal solution and a solution, which was obtained with our heuristic approach. Some classes were changed, in order to end up with con-

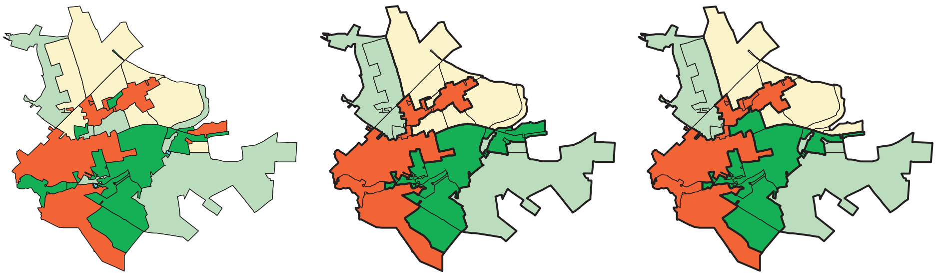

Fig. 1: A sample from the ATKIS DLM 50 (left), an optimal result satisfying specifications for ATKIS DLM 250 (center) and a result with 9 % higher costs obtained with heuristics 1–3 (right). Boundaries of regions are bold, colors correspond to classes as shown in Tab. 2.

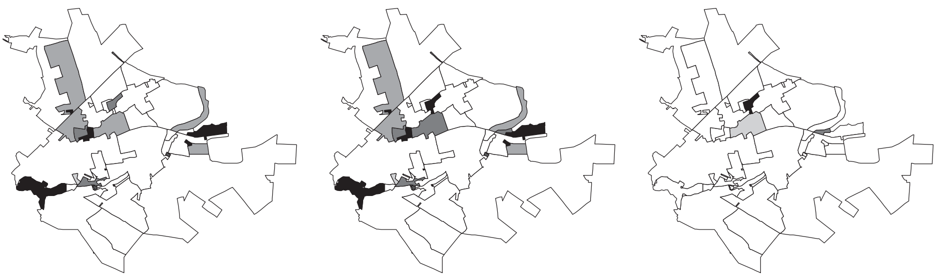

Fig. 2: Semantic distances for classes of single areas before and after generalization. Left: Optimum. Center: Result obtained with heuristics. Right: Difference of both (center-left). Grey shades correspond to values as given in Tab. 2.

tiguous regions of sufficient size. In both cases, this was done in an apparently intelligent way: In order to keep the settlement area in the lower left part of the sample, a small forest area was sacrificed; this results in a connecting bridge to the large settlement. The first solution has an average semantic distance of 0.0519 from the input map. For the second solution this cost is 0.0564, which is approx. 9 % higher. In fact, we observe some differences between both solutions, for example, on the rightmost settlement in the input: in the optimal result it changes to forest, but in the second solution it changes to farmland. If we check the distance matrix (Tab. 2), which was applied here, we see that the same distance of 1 unit is defined for both changes. It turns out that it is relatively difficult to visually detect those areas that were not optimally aggregated by the heuristic method.

In order to identify the reason for the difference in costs, we need to visualize the differences of semantic distances for single areas. Fig. 2 displays distances of class changes as grey shades of areas, dark grey corresponds to expensive changes. In Fig. 2 (right) we see the difference of both solutions: Only for four small areas the reclassification done by the heuristic approach is suboptimal.

Normally, we do not have the optimal solution to compute the differences as shown in Fig. 2 (right). There would not be any reason to apply heuristics, if we generally could exactly solve the problem. However, similar to comparisons with optimal solutions for small samples, we can visually compare results of different heuristics. Fig. 3 shows a sample that was processed with our heuristic approach based on intermediate scales (Haunert 2007b) and with the common iterative merging procedure, which, for example, is explaind by Cheng & Li (2006). Both objectives were considered: class similarity and compactness. In each iteration of the merging procedure, the smallest area was assigned to one of its neighbours. Each time, this neighbour was selected to minimize the cost function; of course, this does not lead to the global optimum. Considering compactness, both procedures performed similarly. Using our optimization method, we only obtained an improvement by 2% of costs for non-compact shapes. However, we obtained 20% less costs for class changes. In Fig. 3 we observe that several settlement areas are lost with the simple iterative procedure. This is due to the fact that the algorithm does not foresee consequences of merge actions for further processing steps. Thus it is not able to sacrifice small areas in order to safe bigger ones.

In Fig. 2 we investigated the quality measure for the original areas; these are minimal mapping units in the aggregation problem. We can do the same analysis on a less detailed level, that is, for each area of the target scale; this is shown in Fig. 4 (left) and (center). A comparison of both results is only

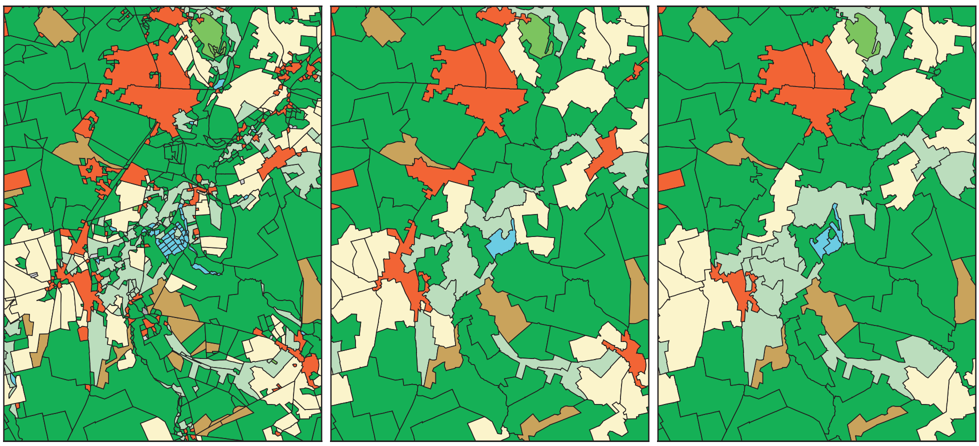

Fig. 3: A sample from the ATKIS DLM 50 (left), a result of the heuristic developed by HAUNERT (2007b), and a result of a simple iterative merging procedure (right). Both results satisfy the specification for the ATKIS DLM 250.

Fig. 4: Semantic distances for regions in Fig. 3. Left: Result from Fig. 3 (center). Center: Result from Fig. 3 (right). Right: Difference of both for areas of input scale (center-left).

possible on the highest level of detail, as the regions in both solutions are different. Fig. 4 (right) reveals those areas whose semantics were kept more similar with the optimization approach (red) and those that were kept more similar with the iterative approach (green). We clearly observe the dominance of red areas. Also we can see that red and green areas are often in vicinity. This confirms our assumption that, in contrast to the simple iterative procedure, the optimization approach can sacrifice unimportant areas, in order to safe more important ones.

5 Conclusions

The definition of semantic similarity or distance measures is considered as the key to quality assessment in map generalization. We have shown that, with given semantic distance values for classes, we can optimally solve the area aggregation problem in map generalization for small instances. With such theoretically proven optima, we have found the "absolute zero" for the degree of badness. This allows to make objective, quantitative statements about the performance of heuristic methods. Additionally, we can compare the performance of heuristics relative to each other. In both cases we have seen that shortcomings of heuristic methods can be detected by visualization. In particular, we have seen that our heuristic based on intermediate scales results in 20% less costs for class change than the simple iterative method. We observed that its relatively good performance is due to its capabilty of sacrificing smaller areas, such that bigger ones can be safed. Future research should focus on better semantic distance measure, not only considering the class memberships of objects. Semantics can also be carried by shapes and patterns of objects. This becomes relevant for other generalization operators, such as typification. In fact, pattern recognition techniques are often applied in map generalization. However, metrics are missing that measure the semantic distance between patterns. Additional research is needed to test the effect of asymmetric class distances. Concerning local search methods for optimization such as simulated annealing we see the need to improve techniques to handle hard constraints, which are needed for logical consistency in map generalization. Future research is also needed to consider additional elements of quality, for example, positional accuracy and completeness. So far we have interpreted the size thresholds in the specifications as prohibition to keep too small areas in the target scale, but there might be size thresholds or other criteria that define which areas must be kept in the generalized map to ensure completeness. In fact classes of areas can be fixed in our optimization approach (Haunert & Wolff 2006), thus the method can ensure completeness, if we define which areas to keep.

References

AdV, 2003: ATKIS-Objektartenkatalog. – www.atkis.de (accessed November 9, 2007).

Ahlquist, O., 2005: Using semantic similarity metrics to uncover category and land cover change. – GeoSpatial Semantics: First international conference, GeoS 2005. Lecture Notes in Computer Science **3799**. Springer, Berlin, Germany.

Bader, M. & Weibel, R., 1997: Detecting and resolving size and proximity conflicts in the generalization of polygonal maps. – 18th International Cartographic Conference: **1525–1532**.

Bard, S., 2004: Quality Assessment of Cartographic Generalization. – Transactions in GIS **8** (1): 63–81.

Cheng, T. & Li, Z., 2006: Toward Quantitative Measures for the Semantic Quality of Polygon Generalization. – Cartographica **41** (2): 487–499.

Frank, R. & Ester, M., 2006: A Quantitative Similarity Measure for Maps. – Progress in Spatial Data Handling. Springer, Berlin, Germany.

Galanda, M., 2003: Automated Polygon Generalization in a Multi Agent System. – PhD thesis, Department of Geography. University of Zürich, Switzerland.

Geoscience Australia, 2006: Topographic data and map specifications. – www.ga.gov.au/map specs/250k100k/ (accessed November 9, 2007).

Harrie, L. E., 1999: The Constraint Method for Solving Spatial Conflicts in Cartographic Generalization. – Cartography and Geographic Information Science **26** (1): 55–69.

Haunert, J.-H. & Wolff, A., 2006: Generalization of land cover maps by mixed integer programming. – GIS '06: 14th annual ACM international symposium on advances in geographic information systems: 75–82.

Haunert, J.-H., 2007a: A formal model and mixed-integer program for area aggregation in map generalization. – International Archives of Photogrammetry, Remote Sensing and Spatial Information Sciences **36** (3/W49A): 161–166.

Haunert, J.-H., 2007b: Efficient area aggregation by combination of different techniques. – 10th ICA Workshop on Generalisation and Multiple Representation.

Haunert, J.-H., 2007c: Optimization methods for area aggregation in land cover maps. – 23rd International Cartographic Conference.

Haunert, J.-H. & Sester, M., 2008: Area collapse and road centerlines based on straight skeletons. – GeoInformatica 12 (2): 169–191.

Kainz, W., 1995: Logical consistency. – Elements of spatial data quality **6**, Elsevier, Oxford, UK: 109–137.

Michiels, W., Aarts, E. & Korst, J., 2007: Theoretical Aspects of Local Search. – Monographs in Theoretical Computer Science. Springer, Berlin, Germany.

Morrison, J. L., 1995: Spatial data quality. Elements of spatial data quality **1**, Elsevier, Oxford, UK: 1–12.

Natural Resources Canada, 1996: National topographic data base: data dictionary. – ftp2.cits.rncan.gc.ca/pub/bndt/doc/dictntd3—en.pdf (accessed November 9, 2007).

Papadimitriou, C.H. & Steiglitz K., 1998: Combinatorial Optimization. – Dover Publications, Inc., Mineola, NY, USA.

Rodríguez, M.A. & Egenhofer, M.J., 2004: Comparing geospatial entity classes: an asymmetric and context dependent similarity measure. – International Journal of Geographical Information Science **18** (3): 229–256.

Salgé, F., 1995: Semantic accuracy. – Elements of spatial data quality **7**, Elsevier, Oxford, UK: 139–151.

Ware, J.M. & Jones, C. B., 1998: Conflict reduction in map generalization using iterative improvement. – GeoInformatica **2** (4): 383–407.

Weibel, R. & Dutton, G., 1998: Constraint-based automated map generalization. – 8th International Symposium on Spatial Data Handling: 214–224.

Yaolin, L., Molenaar, M. & Kraak, M.-J., 2002: Semantic similarity evaluation model in categorical database generalization. – International Archives of Photogrammetry, Remote Sensing and Spatial Information Sciences **34** (4): 279–285.

Zolterns, A.A. & Sinha, P., 1983: Sales territory alignment: A review and model. – Management Science **29** (11): 1237–1256.

Address of the Authors:

Dipl.-Ing. Jan-Henrik Haunert, Prof. Dr.-Ing. habil. Monika Sester, Leibniz Universität Hannover, Institut für Kartographie und Geoinformatik, Appelstraße 9a, D-30167 Hannover, Tel.: +49-511-762-3588, Fax: +49-511-762-2780, e-mail: Jan.Haunert | Monika.Sester@ikg.uni-hannover.de

Manuskript eingereicht: Dezember 2007
Angenommen: März 2008

Photogrammetrie • Fernerkundung • Geoinformation 3/2008, S. 175–186, 9 figs.

Towards a G-Map Based Tool for the Modelling and Management of Topology in Multiple Representation Databases

ANDREAS THOMSEN, MARTIN BREUNIG, EDGAR BUTWILOWSKI, Osnabrück

Keywords: 3D Topology, Multi-Scale Representation, Geo-database, MRDB, LOD, Abstraction of Geoinformation, Generalized Map, Cell-Tuple Structure

Summary: The modelling and management of topology plays an increasing role in Photogrammetry, Remote Sensing and GIS. In new application fields such as 3D city models, 3D navigation systems and early warning of geological events, multi-scale topological data models are needed. In this article a unified model for topology is proposed, based on oriented d-Generalised Maps ($2 \leq d \leq 3$) to represent topology in Multi-Representation Databases (MRDB). Topological data structures and operations are presented in detail. The model can be used as a data integration platform for 2D and 3D topology, as well as for the representation and management of topology in a multi-resolution GIS. An application example, management of topology in a multi-scale land-use map based on aggregation, shows the feasibility of the new approach.

Zusammenfassung: *Auf dem Weg zu einem G-Map-basierten Werkzeug zur einheitlichen Modellierung und Verwaltung der Topologie in Multiple Representation Databases.* Die Modellierung und Verwaltung der Topologie spielt eine größer werdende Rolle in der Photogrammetrie, Fernerkundung und in GIS. In neuen Anwendungsfeldern wie 3D Stadtmodellen, 3D Navigationssystemen und Frühwarnung geologischer Ereignisse werden multiskalige topologische Datenmodelle benötigt. In diesem Artikel wird ein einheitliches Modell für die Topologie vorgeschlagen, das auf orientierten d-Generalisierten Karten ($2 \leq d \leq 3$) basiert, um die Topologie in Multi-Representation Databases (MRDB) zu verwalten. Topologische Datenstrukturen und Operationen werden im Detail vorgestellt. Das Modell kann als Datenintegrationsplattform für 2D und 3D Topologie genutzt werden. Ein Anwendungsbeispiel, die Verwaltung der Topologie in einer multiskaligen durch Aggregation entstandenen Bodennutzungskarte, zeigt die Realisierbarkeit des neuen Ansatzes.

1 Introduction and Related Work

Multiple representation databases are needed in many applications of Photogrammetry, Remote Sensing and GIS (HOPPE 1996, FRADIN et al. 2002, HAUNERT & SESTER 2005 and MEINE & KÖTHE 2005), to model geo-objects in different scales. In new 3D applications, besides geometry the importance of topology is growing, but hitherto this aspect has played a minor role in research and applications.

Exhaustive work on the modeling of topology in GIS has been published (EGENHOFER 1989, EGENHOFER et al. 1989, PIGOT 1992, CLEMENTINI & DI FELICE 1994 and GRÖGER & PLÜMER 2005). General approaches for representing topology in the context of 3D modeling have been examined by different authors. Cellular complexes, and in particular cellular partitions of d-dimensional manifolds (d-CPM) have been described to represent the topology of an extensive class of spatial objects (BRISSON

1432-8364/08/2008/175 $ 3.00

1993). Based on algebraic topology, they provide a general, less rigid framework than more specific topological representations such as simplicial complexes. The topology of d-CPM can be represented by d-dimensional *Cell-Tuple Structures* (Brisson 1993) respectively d-dimensional *Generalized Maps* (d-G-Maps – Lienhardt 1994). Lévy (1999) has shown that 3D-G-Maps have comparable space and time behavior as the well-known Doubly-Connected Edge List (DCEL) and Radial Edge structures, but can be used for a much wider range of applications, allowing for a more concise code. Lévy (1999) also introduces *hierarchical G-Maps* (HG-Maps) for the representation of nested structures. G-Maps have been used to represent the topology of land-use changes (Raza & Kainz 1999) for 3-dimensional spatial data (Mesgari 2000), and are applied, e. g., in the geoscientific 3D-Modelling software GOCAD (Mallet 2002). Fradin et al. (2002) use G-Maps to model and visualize architectural complexes in a hierarchy of multi-partitions, and an interactive graphical G-Map-based 3D-modeller (Moka 2006) has been made available by the group of graphical informatics (SIC) at Poitiers university. Own first approaches to the management of topology in Multiple Representation Databases have been shown in (Shumilov et al. 2002, Thomsen & Breunig 2007, Butwilowski 2007, and Thomsen et al. 2008).

In the remainder of this paper, we investigate how the realisation of oriented Generalized Maps and Cell-Tuple Structures based on an ORDBMS can be used to handle the topology of a digital spatial model in a generic way, supporting 2D manifolds and 3D volume models (Sections 2 and 3). In Section 4, the comparison of the G-Map with other topological models, especially with ISO 19107, is discussed. Section 5 describes some aspects of the implementation based on a object-oriented RDBMS, and Section 6 discusses different methods to handle multi-representation G-Maps and Cell-Tuple Structures. As an ongoing application example, in Section 7 we present the management of topology for a multi-scale land use map. We conclude with an outlook on our future research.

2 Explicit Modelling of d-dimensional Topology

Topological relationships between and within complex spatial objects can be described implicitly, e. g., by attaching some references to neighbours to the items of a geometry model. However, it seems more appropriate to use an explicit mathematical framework for the description and analysis of the transformation of topology during the passage between different representations in a multi-representation database. For this purpose, we use a topological model that consists of the following conceptual layers (Mallet 2002):

- the continuous *d-dimensional manifold*,
- its cellular partition which results in a finite *d-dimensional cellular complex*,
- the representation by a *d-Generalized Map* and its realisation by a *d-Cell-Tuple structure*, and
- the persistent implementation by means of tables, relationships and problem-specific functionality in an *object-relational database*.

Continuous d-manifold. A *d-dimensional manifold M in 3D*, can be roughly described as a continuous part of a space which is *locally homeomorphic* to a *d-dimensional ball in* $\boldsymbol{R}^3$. This means that for any point $p \in$ M, there exists a neighbourhood $U(p) \subseteq M$, a point $q \in \boldsymbol{R}^3$, a d-dimensional ball $B(q) \subseteq \boldsymbol{R}^3$ and a bijection φ_U: $U \leftrightarrow B$, $\varphi_U(p) = q$, continuous in both directions, that maps any point of U to a point of B. Special conditions apply to *bounded manifolds*, which are locally homeomorphic to a *half-space*. By this definition, certain singular configurations (“non-manifold situations”), e. g., “T-shaped” branchings of in 2D-manifolds, are excluded (Lévy 1999).

Cellular partition. Whereas the manifold is a continuous object comprising an infinity of points in space, for a digital representation, a discrete structure is required. This is achieved by the introduction of *cellular partitions* of continuous d-manifolds: the manifold M is decomposed into a number of *cells* c^k of dimension k ranging from *0* to d, the dimension of the manifold. Each cell c^k is homeomorphic to a k-dimensional ball $B^k \subseteq \boldsymbol{R}^k$. Such a *d-dimensional cellular partition* of a d-dimensional manifold M is a *cellular complex* consisting of a finite number of cells c^k of positive dimension $k \leq d$, and verifying the following conditions:

- For each cell c^k, its boundary ∂c^k is composed of cells $c^{k'}$ of lesser dimension $k' < k$.
- For each pair of different cells of dimension k, $c^k{}_i$, $c^k{}_j$, the open interiors $c^k{}_i$, c_j do not intersect.
- For each pair $c^k{}_i$, c_j of different cells of dimension k, the intersection of the boundaries is either void or consists of cells c^l of dimension $l < k$: $c^k \cap c^{k'} = \boldsymbol{U}_{l=0,\ldots,k-1} (\boldsymbol{U}_j \, c^l{}_j)$.

In a d-dimensional cellular complex, multiply connected objects cannot be represented as single d-cells: e. g., a 2D ring, a 3D ring (a "doughnut"), or its surface, a torus. This is different, e. g., from the spatial models provided by Oracle Spatial 11G (Kazar et al. 2008), and ISO19107, which allow, e. g., faces and solids with holes as basic elements. By using partitions of d-dimensional manifolds as discrete model of topology, we ensure that each (d-1)-cell is either part of the common boundary cell of a pair of d-cells, or is part of the outer boundary of the cellular complex. We exclude "non-manifold" configurations like, e. g., T-shaped contacts of d-cells (Lévy 1999). Mesgari (2000) proposes a solution for the modelling of some of these singularities.

Spatial objects in a cellular partition. As illustrated by the above counter-examples, certain spatial objects that occur in practical applications cannot be modelled by single d-cells, but must be represented as sets of d-cells (cf. Fig. 1), consisting of one or more connected components.

D-G-Maps and Cell-Tuple Structures. Cellular Complexes can be interpreted as a generalisation of simplicial complexes, but they lack the geometric and algebraic properties of the latter. However, the *d-dimensional Generalized Map* (Lienhardt 1994) and the *d-dimensional Cell-tuple Structure* (Brisson 1993) provide the cellular partition with the structure of an *abstract simplicial complex*. From a practical point of view, the two models can be regarded as roughly equivalent (Lienhardt 1991). Whereas the d-G-Map focuses on the algebraic structure defined by the transitions between the abstract *darts*, the Cell-Tuple Structure yields a realisation by cell-tuples and the symmetric "switch" relationships between them.

3 Generalized Maps and Cell-Tuple Structures

Following Lienhardt (1994), a *d-dimensional Generalized Map* (*d-G-Map*) consists of a finite set of objects called *darts* and a

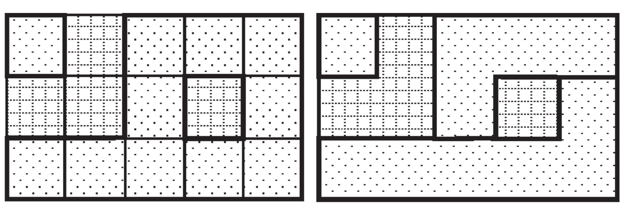

a) b)

Fig. 1: Representation of 2D spatial objects as sets of 2-cells in a 2-G-Map – Objects that are not simply connected require more than one 2-cell for representation (left); Representation by a minimal number of cells (right).

set of bijections α_i, $i = 0, \ldots, d$ linking pairs of darts, that are *involutions*, i. e., that verify the conditions:

$$\alpha_i(\alpha_i(x)) = x \quad (1)$$

$$\text{and for all } i, 0 \leq i < i+2 \leq j \leq d, \quad (2)$$

$\alpha_i\ \alpha_j$ is an involution, i. e., $\alpha_i(\alpha_j(\alpha_i\ (\alpha_j(x)))) = x$, which implies $\alpha_j(\alpha_i(x)) = \alpha_i(\alpha_j(x))$. (3)

The G-Maps are embedded in 2D or 3D space by a mapping that to each dart associates a unique combination of a node, an edge, a face, and in 3D a solid.

In Brisson's (1993) terminology, *Cell-tuple Structures* consist of a set of *cell-tuples (node, edge, face[, solid])* attached to the corresponding spatial objects. The cell-tuples are pairwise linked by "switches" defined by the exchange of exactly one component, and corresponding to Lienhardt's involutions:

$$\alpha_0: (n, e, f, s) \leftrightarrow (n', e, f, s),$$
$$\alpha_1: (n, e, f, s) \leftrightarrow (n, e', f, s),$$
$$\alpha_2: (n, e, f, s) \leftrightarrow (n, e, f', s),$$
$$\alpha_3: (n, e, f, s) \leftrightarrow (n, e, f, s') \quad (4)$$

A d-G-Map can be represented as a graph with cell-tuples as nodes, and edges defined by the involution operations (cf. Fig. 2).

Orientation. We require all d-manifolds to be *orientable*, and the corresponding G-Maps and Cell-Tuple Structures to be *oriented*: the set of darts / cell-tuples can be divided into two parts of equal size carrying opposite sign, and each α_i transition links a pair of items of opposite sign. Whereas Lienhardt's definition permits darts at the boundary of a G-Map, that do not have a counterpart for the α_d transition, such a situation is excluded in our model (Pigot 1992). The G-Maps here are formally considered as *unbounded*, by introducing an outside "universe" that is not a standard cell.

Navigation on G-Maps. The use of the G-Map structure for topological queries and operations, is supported by methods for the *navigation* on the G-Map graph, and for the retrieval of solids, faces, edges and nodes, represented by volume cells, surface patches, curves and points.

a) All navigation on a G-Map relies on the α_i transitions, i. e., the passage from one cell-tuple to its neighbour by the exchange of one cell of dimension i.
b) A sequence of cell-tuples starting with ct_0, finishing with ct_N and linked by α_i transitions with varying index i defines a *path* on the G-Map graph, or a *loop*, if it is closed.

Paths and loops are determined by the sequence of transitions $\alpha_{i_1} \ldots \alpha_{iN}$ or shorter by the indices $i_1 \ldots i_N$, and can be noted $Path_{i1 \ldots iN}(ct_0)$ and $Loop_{i1 \ldots iN}(ct_0)$.

c) The subset of all cell-tuples that can be reached from a given cell-tuple ct_0 by any combination of transitions $\alpha_{i_1} \ldots \alpha_{i_N}$ is called an *orbit* and is noted $Orbit_{i1 \ldots iN}(ct_0)$. To avoid ambiguities, sometimes the dimension of the G-Map is also noted: $Orbit^d_{i1 \ldots iN}(ct0)$.

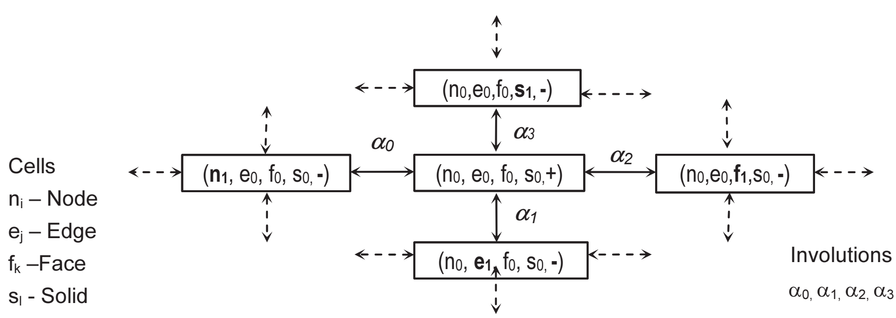

Fig. 2: Graph representation of an oriented 3-G-Map $G\,(D, \alpha_0, \ldots, \alpha_d)$ with cell-tuples as darts and α_i transitions.

Certain orbits describe loops of fixed or variable length, certain loops are defined by orbits, but in some cases the cell-tuples of an orbit may not be arranged in a continuuos loop (Lévy 1999).

Transformations of d-G-Maps. There are two classes of operations: the *Euler operations* (Mäntylä 1988) that preserve the overall topological properties of the cellular complex described by the *Euler characteristic* X *= no. of nodes − no. of edges + no. of faces* [*− no. of solids*], and the *non-Euler* operations. The basic topological operations consist in the division of k-dimensional cells ($k > 0$) by the insertion of $k-1$-dimensional boundary cells, the dual operations – duplication of k-dimensional cells ($k < d$) by insertion of $k+1$-dimensional coboundary cells, and the inverse merging (resp. collapsing) operations by the deletion of a boundary (coboundary) cell (cf. Fig. 3) (Thomsen & Breunig 2007). Note that if the boundary or coboundary cell to be removed is part of the outer boundary of a cellular complex, the deletion operation is not always admissible.

Basic non-Euler Operations like the creation or destruction of an isolated cell or of a connected component, or the "sewing" of two hitherto disconnected components into one, and the inverse operation, affect the overall topological properties of the model. Both the Euler and non-Euler operations are implemented using relational database operations comprised in a transaction. In some of these procedures, paths, loops or orbits are used to identify a sequence of cell-tuples to be updated, e. g., for the splitting of a solid by the introduction of a new face along a closed loop on the inside of the boundary of the solid (cf. Fig. 3).

4 Comparison with Other Topological Models

Ordered topological models. Lienhardt (1991) compares G-Maps with different "ordered topological models": e. g., the winged-edge (Baumgart 1975), the radial-edge (Weiler 1988), the quad-edge (Guibas & Stolfi 1985) and the cell-tuple structures. He concludes that "order models are based on the same ideas, and ... it is possible to show that these models are equivalent (with respect to dimension and orientability)". Cell-tuple structures are equivalent to G-Maps without boundaries. However, some of the other models permit non-manifold configurations, which must be explicitly excluded.

ISO 19107 and GML 3. Quak & de Vries (2005) compare the winged-edge structure to the ISO 19107 model (OPEN GEOSPATIAL CONSORTIUM 2007) and conclude that "it is possible to losslessly map to the ISO19107 model and back", but propose to extend the ISO model to reduce cost.

A detailed comparison of the proposed approach to the modelling of topology and the ISO 19107 and GML 3 model is beyond the scope of this article, therefore we only make some preliminary observations: The ISO 19107 and GML 3 model support oriented 2D and 3D topological models, specifying topological complexes consisting of nodes, edges, faces and topological solids as primitives, and the corresponding directed primitives as building elements for 1D, 2D, and 3D topological complexes, as well as for boundaries, coboundaries, and for "topological collections", i. e., topological curves, surfaces, volumes. In accordance with the object-oriented approach, relation-

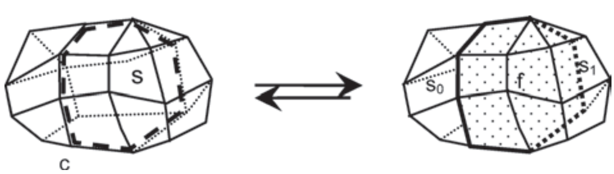

Fig. 3: A 3D Euler operation: splitting a solid *s* into solids s_0 and s_1 by the insertion of a 2D face *f*, and the inverse merge operation. The location of the contact between the face *f* and the boundary of the solid *s* is defined by the loop *c*.

ships between topological, geometrical and other entities are encoded with the topological objects, whereas the G-Map and the Cell-Tuple Structure use a separate system of entities and 1:1 relationships, namely darts/cell-tuples and involutions/switches to represent the topological structure. Thus the incidence, adjacency and order relationships in ISO 19107 have to be translated into sets of darts/cell-tuples, involution transitions and orbits.

The ISO 19107 model is less restrictive than G-Maps and Cell-Tuple Structures, and in consequence, the range of topological configurations that can be represented is larger, admitting, e. g., dangling edges, inner loops, curves that meet the interior of a face etc, which are precluded in G-Maps. On the other hand, topological operations on the ISO 19107 model may be more complicated, as numerous special cases have to be handled or excluded. Provided that the strict requirements of the G-Map are met, we expect no fundamental problems when translating the topological primitives from GML 3 to the corresponding cells in the G-Map model, and of topological complexes into cellular complexes represented by G-Maps and vice versa.

5 Object-relational Database Implementation

Implementation in transient storage. The in-memory-implementation of the graph-representation of a d-G-Map is straightforward (Lévy 1999): for each dart object, the α_j transitions are implemented by d + 1 references to other darts, additional references to geometric objects and to thematic properties realise the geometric representation, and a set of flags is used to mark darts that have been traversed, the next α_i transition to take etc. The α_j references may be extended into objects as well, with methods to check the symmetry of the reference, and for permitting/barring the use of a given transition (Fradin et al. 2002). In order to support the navigation on the G-Map, for each cell of dimension from *0* to *d* a reference to a *starting dart* may serve as an "entry point" into an orbit describing the topological relationships within the cell and outside.

Object-Relational database implementation. For a persistent implementation based on an object- relational DBMS, the cell-tuple structure is more appropriate (cf. Fig. 4). Instead of references to locations, the transitions between cell-tuples are controlled by keyed access using one of three *search patterns* (cf. Fig. 5). In a G-Map without boundary, there is always exactly one corresponding cell-tuple to be retrieved.

Here the tuple (*node, edge, face, cell, solid*) acts as a key, which is augmented by the *sign*, if positive and negative cell-tuples are stored in the same table. For example, the following SQL query, for the cell-tuple $ct(c0, c1, \mathbf{c2}, c3, \sigma, \ldots)$ retrieves the cell-tuple $ct'(c0, c1, \mathbf{c2'}, c3, -\sigma, \ldots)$ corresponding to *ct* by an α_2-transition, i. e., by an exchange of faces:

SELECT * FROM celltuples WHERE node = c0 AND edge = c1 AND solid = c3 AND sign != σ;

Using hierarchical indexing of the cell-tuple relation, we expect the access time for a single transition to grow like $O(\log N)$,

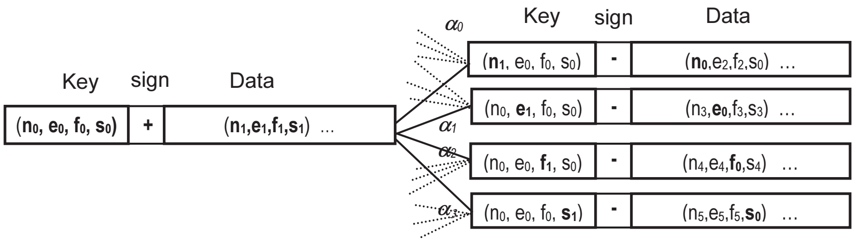

Fig. 4: An oriented 3-G-Map as a pair of relations $(c_0, \ldots, \mathbf{c}_i, \ldots c_d, +) \leftrightarrow (c_0, \ldots, \mathbf{c}_i', \ldots c_d, -)$.

starting cell-tuple ct_0	search pattern	retrieved cell-tuple $\alpha_j(ct_0)$

$$(c_0,\ldots,\boldsymbol{c_j},\ldots,c_d,sign,\ldots) \rightarrow \left\{\begin{array}{l}(1)\ \text{“}c_0,\ldots,*,\ldots,c_d,-sign\text{”}\\ (2)\ \text{“}c_0,\ldots,\neg\boldsymbol{c_j},\ldots,c_d\text{”}\\ (3)\ \text{“}c_0,\ldots,\boldsymbol{c_j'},\ldots,c_d\text{”}\end{array}\right\} \leftrightarrow (c_0,\ldots,\boldsymbol{c_j'},\ldots,c_d,-sign,\ldots)$$

Fig. 5: Search patterns for α_j transitions. The symbols "¬" and "*" denote "not" and "any".

where N is the total number of cell-tuples. Using hash indexes, even better behaviour can be achieved. This access method, at the cost of some overhead, makes the transition between cell-tuples independent from any particular storage or object identifier details and thus can be used transparently both with persistent storage in a client-server configuration, and in transient storage and easily cope with update operations.

Orbits and loops vs. ordered subsets. In a cellular partition of a d-dimensional manifold, spatial objects are represented by collections of cells, i. e., subsets of the underlying sets of k-cells, $k = 0, \ldots, d$. Therefore, we can always deduce corresponding queries on the associated cell-tuples. Information on the connectivity of the resulting subsets of cell-tuples, however, requires methods that systematically explore the adjacency and incidence relationships between cells, represented by the α_i-transitions, in particular orbits and loops.

Whereas the implementation of involutions and orbits in transient storage is simple, it is more intricate in the context of the relational model. In an RDBMS, the retrieval of subsets by conditions imposed on attribute values is well supported, as are basic sorting operations on resulting subsets. Using appropriate indexing, also a small finite number of links between relations by foreign keys or by joins poses no particular problem, even if some overhead is involved. Orbits, paths, and loops, however, may involve an undetermined and potentially large number of links between cell-tuples, possibly defined by a recursive formula. Although recursion is supported by ANSI SQL, it is not yet implemented in all widespread relational DBMS (PostgreSQL .org 2006) – or is not implemented in the same way. Without SQL recursion, the use

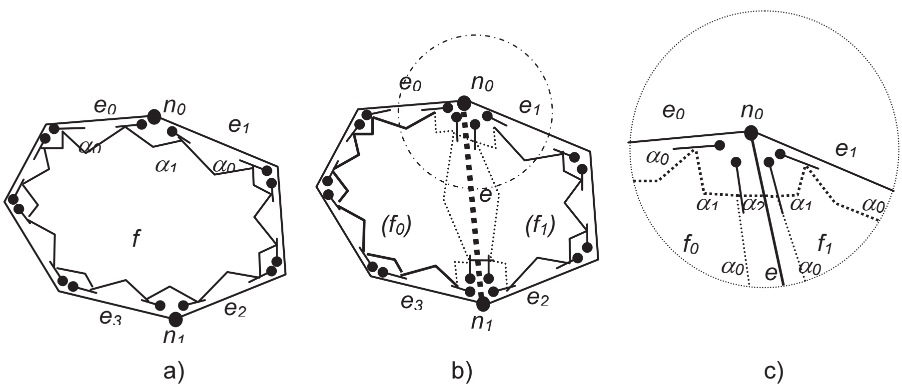

Fig. 6: Controlling the navigation on a 2-G-Map using orbits, loops and switch/stop flags – a) Traversing the boundary of face f by an $orbit^2_{01}(\ )$. b) Separate traversal of the outer boundaries of the two parts of f, stopping at nodes n_0, n_1. c) (Fradin et al. 2002) By blocking or opening α_2 transitions through the edge e, the same structure is used to describe both the common boundary by a loop "$\ldots\alpha_0\,\alpha_1\,\alpha_2\,\alpha_1\,\alpha_0\ldots$" at nodes n_0 and n_1, and the boundaries of the two parts f_0 and f_1 by two $Orbit^2_{01}(\ )$ loops.

of a programming language is required for coding the loop or the recursive procedure, which in turn issues an SQL command for each step. Even if we reduce the overhead incurred using optimisation methods like prepared statements, this remains a clumsy way to solve a simple task. In order to handle this problem, we first have to find out which topological operations can be implemented using simple (ordered) subset retrievals, and for which operations paths, loops or orbits are essential.

Loops and orbits are also necessary for the implementation of division and merge operations (cf. Fig. 6). In order to ensure that the result f of a merging operation on two d-cells f_0 and f_1 is a d-cell, we must ensure that the boundary $e = f_0 \cap f_1$ is connected – otherwise situations like (cf. Fig. 7 c, d) may occur. If e is simply connected, we may first merge it into a single edge e', which then in turn is removed. The inverse procedure, namely the division of a d-cell, also involves the use of an orbit. Within a transaction, we proceed as follows:

1. Mark the two nodes n_0 and n_1 where the dividing edge joins the boundary of c.
2. Insert the dividing edge e into the table of edges.
3. Insert two new faces f_0 and f_1 into the face table.
4. Insert four cell-tuples $(n_0, e, f_0, -s)$, $(n_0, e, \mathrm{f}_1, +s)$, $(n_1, e, f_1, -s)$, $(n_1, e, f_0, +s)$. The sign s being chosen to match the signs of the existing cell-tuples.
5. Update the existing cell-tuples (n_0, e_0, f, s), $(n_0, e_1, f, -s)$, (n_1, e_2, f, s), $(n_1, e_3, f, -s)$ using two new face identifiers, resulting in (n_0, e_0, f_0, s), $(n_0, e_1, f_1, -s)$, (n_1, e_2, f_1, s), $(n_1, e_3, f_0, -s)$.

Note that from step 4 onward until step 7 below, the model is temporarily inconsistent!

6. Update all remaining cell-tuples on the boundary of f_0 such that f is replaced by f_0.
7. Update all remaining cell-tuples on the boundary of f_1 such that f is replaced by f_1.

Steps 6. and 7. require that we determine the two sides of the former boundary of face f before they are explicitly marked by f_0 and f_1. This is not possible by a subset query, but it can be done using two orbits starting, e. g., at cell-tuples $ct_0(n_0, e, f_0, -s)$ and $ct_1(n_0, e, f_1, +s)$, if the alpha-transitions are stored explicitly, or by using two paths starting at ct_0 and ct_1, and stopping, as soon as $ct_2(n_1, e, f_0, +s)$ and $ct_3(n_1, e, f_1, -s)$ are encountered.

Considering the division of a solid s by a newly introduced face f in a 3-GMap (cf. Fig. 3), we note that a closed loop is required to define the *seam* c where the dividing face f meets the boundary of s. For the merging of two neighbouring solids s_1 and s_2, we require their common boundary b to be 2-dimensional and simply connected.

The given examples show that some queries and operations require loops or orbits. Therefore we propose the following 2-step approach to the implementation of topological queries on a RDBMS-based d-GMap: first, retrieve an appropriate subset of the cell-tuples by standard RDBMS methods, and second, generate orbits, loops or paths in transient memory whenever necessary.

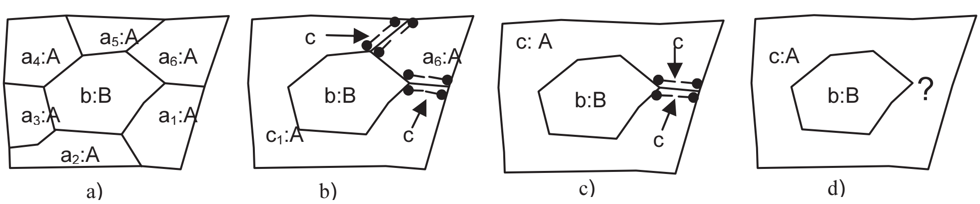

Fig. 7: Problems encountered during aggregation. (a) A face b of class B is completely surrounded by faces a_i of a different class A. (b) Stepwise merging all cells of class A results in a bridge configuration (c) and finally in a ring (d).

6 Aggregation Methods for G-Maps and Cell-Tuple Structures

Hierarchical G-Maps. Levy (1999) proposes to use hierarchical structures for the construction of complex geological subsurface models, both in volume and in boundary representation. These *hierarchical G-Maps* are obtained in the following way: We start with a coarse 3D G-Map. By subdividing its 3D cells (solids), a structure is obtained that consists of *frames* – the coarse cells, and finer G-Maps that fit into the frames. Whereas the darts of the subdivisions possess a geometrical representation in 3D space, the darts of the coarse frame G-Map have no separate embedding. Instead, *embedding by delegation* is used: its darts are associated with a subset of the darts of the fine G-Maps, and use the geometric representation of the subdivision as embedding. Applying a similar approach to the 2D faces of the coarse model, a boundary representation of the coarse model is obtained. Whereas the construction of the topological hierarchy by subdivision proceeds top-down, the delegated geometrical representation is propagated bottom up.

Multiple grouping. For the topological modelling of buildings, Fradin et al. (2002) use *multiple groupings*: for each grouping of cells, $d+1$ flags are associated with the references representing α_i-transitions, that indicate whether the given cell boundary may be ignored during navigation on the G-Map (cf. Fig. 6c). This approach is economic in memory space, as the same fine G-Map, augmented by the space required for the additional flags, is used for several groupings at the same time, and higher-level G-Maps do not require a separate representation. On the other hand, the possibility of reducing processing time for coarser and hence smaller representations is lost. Note that both methods support lower resolution models obtained by aggregation of cells, but not by simplification of boundaries or by displacement.

Classification tables. It is possible to translate hierarchical G-Maps into Cell-Tuple Structures by representing references using foreign keys. Multiple grouping however, is tightly associated with the in-memory implementation of α_i -transitions, orbits and loops using references. The explicit representation of the cells within the cell-tuples leads to a different approach: starting from a high resolution model, successive lower levels of detail are obtained by aggregation as follows. A classification of the d-dimensional cells at high resolution is represented by a N:1-relation that to each cell a associates its class A. In a copy of the original cell-tuples, the d-cells are replaced by their class identifiers. Then all pairs of cell-tuples $(c_0, c_1, \ldots, A, +)$, $(c_0, c_1, \ldots, A, -)$ – the fixed points of the α_d-transitions – are removed, while all pairs $(c_0, c_1, \ldots, A, +)$, $(c_0, c_1, \ldots, B, -)$ with $B \neq A$ are kept.

Separate embeddings at different levels of detail. If generalisation is restricted to aggregation, we can apply embedding by delegation, representing each aggregated cell by a collection of finer cells. As the new Cell-Tuple structure comprises a copy of the old one, however, it is also possible to create a different geometrical embedding, and apply

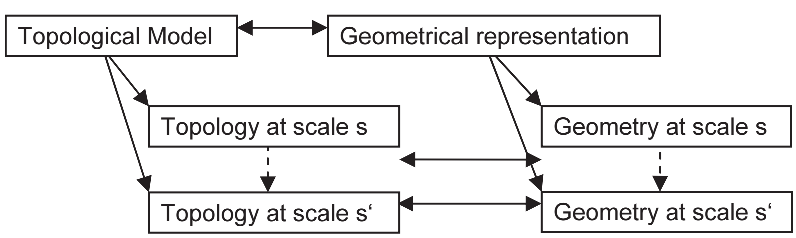

Fig. 8: Topological and geometrical changes must stay consistent during generalisation.

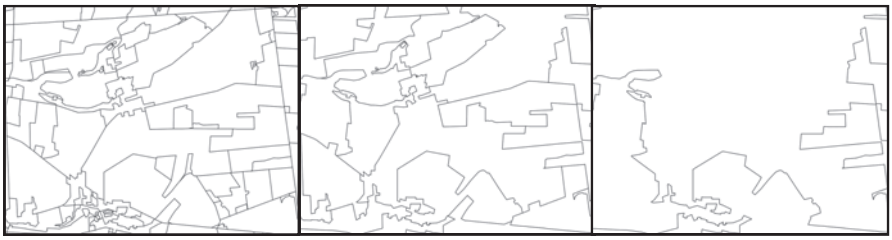

Fig. 9: Application example: a section of ca. 2% of a digital map on land-use at three different scales (by courtesy of J. HAUNERT, IKG Hannover University).

simplification and displacement to it. While this approach is more expensive in storage space, it is more flexible than the previous ones, and navigation on the smaller aggregated representations may be considerably faster. Here, however, a consistency problem arises: if we apply generalisation methods separately to the topological model and its geometrical embedding, then we must take care, that the resulting generalised models are consistent with each other (cf. Fig. 8). This can of course be achieved by having either geometrical operations control the changes in topology or vice versa. However, this depends on the particular application.

7 Applications of the Approach

Topology of a multi-resolution map of land-use. In an ongoing study, the methods presented here are applied to model the topology of a land-use map at three different scales, namely 1:50.000, 1:250.000, and 1:1.000.000. The land use maps were provided by JAN HAUNERT and MONIKA SESTER, IKG, Leibniz University Hannover as Arc GIS shape files. The smaller scale maps were produced by aggregation starting from scale 1:50.000, according to tables defining classes of similar land use. We first construct the topology for the largest scale map and then use the class tables to control the process of aggregation of cells for the 1:250.000 and 1:1.000.000 maps. During this process, the construction of inconsistent cells with holes, or of disconnected entities has to be avoided. Because no displacements occurred during the geometrical generalisation, we can apply the classification table method outlined above, to generate a distinct 2-G-Map at each Level of Detail, and provide links between corresponding cells and cell-tuples using the classification table and the vertex locations.

In another ongoing study, we use the Cell-Tuple structure to study the integration of a 3D city model and building plans with a digital 2D cadastral map (THOMSEN et al. 2008).

8 Conclusions and Outlook

The oriented d-G-Map and the d-Cell-Tuple structure can be employed with an ORDBMS to yield a simple, flexible, and scalable representation of the topology of spatial models based on cellular partitions. After analysis of the topological operations to be used, it can be used for the management of topology in a multi-representation database, in particular for the integration of the topology of models of different dimension and scale. We are currently extending our d-G-Map implementation into a topological access tool for the ORDBMS-based GIS PostGis (POSTGIS.ORG 2006), and for our OODBMS-based spatio-temporal database db3d, and plan to extend the approach to a time-dependent topology model.

Acknowledgements

We thank the Deutsche Forschungsgemeinschaft (DFG) for supporting this work within the DFG joint project "Abstraction of Geoinformation", grant no. BR 2128/6-1.

References

BAUMGART, B., 1975: A polyhedron representation for computer vision. – American Federation of Information Processing Societies (AFIPS) Nat. Conf. **44:** 589–596.

BRISSON, E., 1993: Representing Geometric Structures in d Dimensions: Topology and Order. – Discrete & Computational Geometry **9:** 387–426.

BUTWILOWSKI, E., 2007: Topologische Fragestellungen bei der Kombination von 3D-Stadtmodellen mit 2D-Karten in einer räumlichen Datenbank – Diploma thesis, University of Osnabrück: 116p.

CLEMENTINI, E. & DI FELICE, P., 1994: A comparison of methods for representing topological relationships. – Information Sciences **80:** 1–30.

EGENHOFER, M. J., 1989: A formal definition of binary topological relationships. – Int. Conf. Foundations of Data Organisation and Algorithms (FODO) 1989, Lecture Notes in Computer Science 367, Springer, Berlin: 457–472.

EGENHOFER, M.J., FRANK, A. U. & JACKSON, J. P., 1989: A topological data model for spatial databases. – 1st Symposium on Large Spatial Databases, Lecture Notes in Computer Science 409, Springer: 271–286.

FRADIN, D., MENEVEAUX, D. & LIENHARDT P., 2002: Partition de l'espace et hiérarchie de cartes généralisées. – 15e Journées de l'Association Française d'Informatique Graphique (AFIG): 12p.

GUIBAS, L. & STOLFI, J., 1985: Primitives for the Manipulation of General Subdivisions and the Computation of Voronoi Diagrams. – ACM Transactions on Graphics **4** (2): 74–123.

GRÖGER, G. & PLÜMER, L., 2005: How to Get 3-D for the Price of 2-D-Topology and Consistency of 3-D Urban GIS. – Geoinformatica **9** (2): 139–158.

HAUNERT, J.-H. & SESTER, M., 2005: Propagating updates between linked datasets of different scales. – XXII Int. Cartographic Conference.

HOPPE, H., 1996: Progressive meshes. – 23rd Int. Conf. on Computer Graphics and Interactive Techniques (ACM SIGGRAPH): 99–108.

KAZAR, B.M., KOTHURI, R., VAN OOSTEROM, P. & RIVADA, S., 2008: On Valid and Invalid Three-Dimensional Geometries. – Lecture Notes in Geoinformation and Cartography (LNG&C), Springer: 19–46.

LÉVY, B., 1999: Topologie Algorithmique – Combinatoire et Plongement. – PhD Thesis, Nancy: 202p.

LIENHARDT, P., 1991: Topological models for boundary representation: a comparison with n-dimensional generalized maps. – Computer-Aided Design **23** (1): 59–82.

LIENHARDT, P., 1994: N-dimensional generalized combinatorial maps and cellular quasi-manifolds. – Int. Journal of Computational Geometry and applications **4** (3): 275–324.

MALLET, J. L., 2002: Geomodelling. – Oxford University Press: 599 p.

MÄNTYLÄ M., 1988: An Introduction to Solid Modelling. – Computer Science Press: 401 p.

MESGARI, M. S., 2000: Topological Cell-Tuple Structures for Three-Dimensional Spatial Data. – ITC Dissertation 74, ITC, Enschede: 200 p.

MEINE, H. & KÖTHE, U., 2005: The GeoMap: A Unified Representation for Topology and Geometry. – 5th Int. Workshop on Graph-based Representations in Pattern Recognition 2005. Lecture Notes in Computer Science 3434, Springer, Berlin: 132–141.

MOKA, 2006: Modeleur de Cartes. – www.sic.sp2mi.univ-poitiers.fr/moka/ (accessed 21. 03. 2007).

OPEN GEOSPATIAL CONSORTIUM, 2007: OpenGIS®R Geography Markup Language (GML) Encoding Standard. – OpenGIS®R Standard OGC 07-036, Version: 3.2.1, editor: Clemens Portele. www.opengeospatial.org/standards/gml (accessed: 11. 3. 2008)

QUAK, C.W. & DE VRIES, M. E., 2005: Topological and temporal modelling in GML. – Topology and spatial databases workshop: 1–8.

PIGOT, S., 1992: A topological model for a 3D spatial information system. – 5th Symposium on Spatial Data handling (SDH): 344–360.

POSTGIS.ORG, 2006: PostGIS documentation. – postgis.refractions.net/documentation (accessed 21. 03. 2007).

POSTGRESQL. ORG, 2006: PostgreSQL 8.3.0 Documentation. – www.postgresql.org/docs (accessed 21. 03. 2007).

RAZA A. & KAINZ, W., 1999: An Object-Oriented Approach for Modelling Urban Land-Use Changes. – Urban and Regional Information Systems Association (URISA) Journal **14** N° 1: 37–55.

SHUMILOV, S., THOMSEN, A., CREMERS, A.B. & KOOS B., 2002: Management and visualisation of large, complex and time-dependent 3D objects in distributed GIS. – 10th International Symposium on Advances in Geographic Information Systems (ACM-GIS): 113–118.

THOMSEN, A. & BREUNIG, M., 2007: Some remarks on topological abstraction in multi representation databases. – Int. Workshop on Information Fusion and Geographical Information Systems (IF&GIS'07). Lecture Notes in Geoinformation and Cartography (LNG&C), Springer: 234–251.

THOMSEN, A., BREUNIG, M., BUTWILOWSKI, E. & BROSCHEIT, B., 2008: Modelling and Managing Topology in 3D Geoinformation Systems. – Advances in 3D Geoinformation Systems. Lecture Notes in Geoinformation and Cartography (LNG&C), Springer: 229–246.

WEILER, K., 1988: The radial edge structure: a topological representation for non-manifold geometric boundary modelling. – In: GeometricModeling for CAD Applications, Elsevier: 3–36.

Address of the Authors:

Dipl.-Math. ANDREAS THOMSEN, Prof. Dr. rer. nat. MARTIN BREUNIG, Dipl.-Geogr. EDGAR BUTWILOWSKI, Universität Osnabrück, Institut für Geoinformatik und Fernerkundung, D-49069 Osnabrück, Tel.: +49-541-969-4064, Fax: +49-541-969-4061, e-mail: andthoms | mbreunig | ebut wilo@uos.de

Manuskript eingereicht: Dezember 2007
Angenommen: März 2008

Photogrammetrie • Fernerkundung • Geoinformation 3/2008, S. 187–196, 14 figs.

Implicit Shape Models, Self-Diagnosis, and Model Selection for 3D Facade Interpretation

SERGEJ REZNIK & HELMUT MAYER, Neubiberg

Keywords: Facade Interpretation, Implicit Shape Models, Self-diagnosis, Model Selection, Plane Sweeping, Markov Chain Monte Carlo

Summary: This paper addresses the automatic 3D interpretation of facades from terrestrial image sequences making three novel contributions: First, we employ Implicit Shape Models (LEIBE & SCHIELE 2004) coherently for the detection as well as for the delineation of windows, learning the appearance of windows and their outline from training data. Second, window hypotheses are validated by means of self-diagnosis based on the assumption of a possibly strong similarity of individual windows. Third, we use model selection to choose the most appropriate model for the configuration of windows in terms of rows or columns. These contributions are complemented by plane sweeping for the 3D determination of the windows or the rows / columns made up from them. Results show the potential of the approach.

Zusammenfassung: *Implicit Shape Models, Selbstdiagnose und Modellauswahl für die 3D Interpretation von Fassaden.* Dieser Artikel zielt mit drei neuen Beiträgen auf die automatische Interpretation von Fassaden aus terrestrischen Bildsequenzen: Erstens werden Implicit Shape Models (LEIBE & SCHIELE 2004) kohärent sowohl für die Detektion als auch für die Bestimmung der Umrisse von Fenstern verwendet. Das Aussehen der Fenster und ihre Umrisse werden aus Trainingsdaten gelernt. Zweitens werden Fensterhypothesen mittels Selbst-Diagnose auf Grundlage der Annahme einer z.T. starken Ähnlichkeit individueller Fenster validiert. Drittens wird Modellauswahl genutzt, um das am besten geeignete Modell für die Konfiguration der Fenster in Form von Zeilen oder Spalten auszuwählen. Diese Beiträge werden durch Plane Sweeping für die 3D Bestimmung der Fenster oder der aus ihnen gebildeten Zeilen oder Spalten ergänzt. Die Ergebnisse zeigen das Potential des Ansatzes.

1 Introduction

The inclusion of structured facades extends the modelling of buildings towards highly detailed visualizations suitable for applications ranging from architectural planning to the production of movies. By interpreting the parts constituting facades in terms of their semantics it becomes possible to interact with them, e. g., making it feasible to open windows or doors.

The interpretation of facades from terrestrial images and wide-baseline image sequences has been a focus of research since the seminal work of DICK et al. (2004). They interpret buildings in line with the trend in computer vision towards statistical generative models. Particularly, they employ Reversible Jump Markov Chain Monte Carlo – RJMCMC (GREEN 1995) allowing for the addition and deletion of new parameters and therefore also objects. The results are convincing though restricted to a limited number of objects as the models are complex and generated manually. A more geometric approach is taken by WERNER & ZISSERMAN (2002). They make use of the regular structure of buildings, especially the existence of orthogonal vanishing points. Geometric regularities such as symmetries of dormer

1432-8364/08/2008/187 $ 2.50

windows are used to obtain a high-quality textured model. Becker & Haala (2007) show that by combining laser and image data with rectangular cell decomposition, realistic 3D interpretations of facades can be generated. Müller et al. (2007) and Van Gool et al. (2007) present impressive results for facade interpretation from single images exploiting common repetitions of windows and balconies by means of architectural shape grammars. They particularly show how depth layering can be performed automatically if substantial perspective effects exist in an image.

Our first contribution of this paper lies in employing Implicit Shape Models – ISM (Leibe & Schiele 2004) coherently for the appearance based detection as well as for the delineation of windows. While we used information of corners to delineate windows only on dark facades and employed black rectangles for bright facades in (Mayer & Reznik 2006), we now delineate the outline of whole windows on any kind of facade via ISM.

Our second contribution has been inspired by (Hinz & Wiedemann 2004). The basic idea is to validate weak hypotheses based on self-diagnosis of the generated hypotheses making use of the fact that windows on a facade look often very similar.

The third contribution can be seen as an inversion and at the same time extension of (Alegre & Dallaert 2004, Brenner & Ripperda 2006, and Ripperda & Brenner 2007). We invert, as we do not split the facade, but rather detect and delineate objects and group the constituents into rows and columns. We extend the above work as we employ model selection based on Akaike's Information Criterion (AIC) to compare different groupings. Basically, individual windows always lead to the best likelihood as they can adapt to the individual shapes of windows. Only by taking into account the lower number of parameters for rows, columns, etc., they will prevail. A particular contribution is to show how the likelihood term has to be interpreted in terms of the (minimum) size to be sampled to obtain meaningful results. (Dick et al. 2004) have also used model selection, but to switch between different interpretations for windows, namely with and without arc, etc. In this paper also first results for facades with different distances between windows for different parts of the facade are presented.

We assume, that a wide-baseline image sequence is given, and employ given (approximate) calibration information via the five-point algorithm (Nistér 2004), which makes the reconstruction much more stable. 3D Reconstruction leads to camera parameters and 3D points. From the latter we compute the facade planes via Random Sample Consensus – RANSAC (Fischler & Bolles 1981). We orient the planes using the vertical vanishing points in the images, again employing RANSAC. All images looking at a particular facade are projected on its plane and combined using a consensus-based approach (Mayer 2007) getting rid of partial occlusions. We use a manually defined sampling distance of 1 cm to normalize the further processing. Thus, for the remainder of the article all facade plane images are assumed to be vertically oriented and normalized to a resolution of 1 cm.

We first describe the appearance based detection and delineation of windows on the facade plane images based on ISM in Section 2. Section 3 is devoted to self-diagnosis for the validation of window hypotheses, while Section 4 deals with model selection for the decision between representations based on individual or rows or columns of windows. Plane sweeping leading to the determination of the depth, i. e., the 3D shape of windows, is described in Section 5. The paper ends with conclusions.

2 Detection and Delineation of Windows Based on Implicit Shape Models

We employ Implicit Shape Models – ISM (Leibe & Schiele 2004) for the detection of windows and for the delineation of their outline. For training we cut out image patches containing windows, in our case 120 windows of modern type. We note that none of the windows shown in our results is part

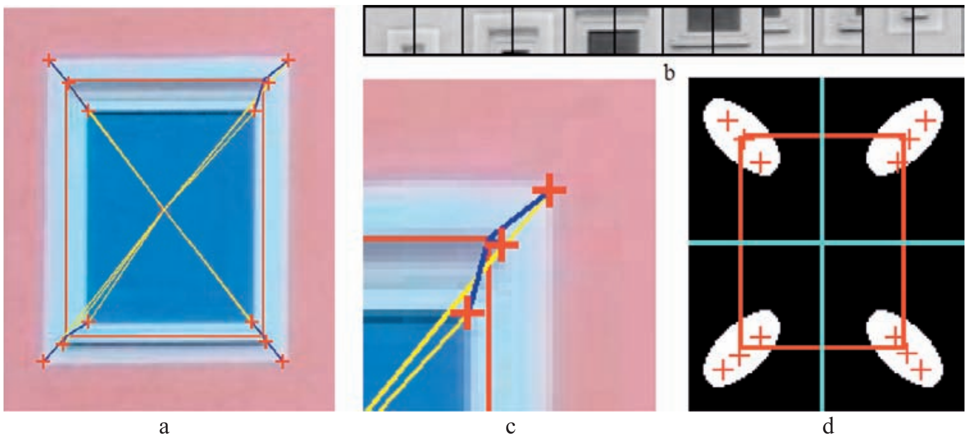

Fig. 1: Training – a – Image patch with manually given outline of window (red rectangle), Förstner points at corners of window outline (red crosses) as well as their vectors to the center of the window (yellow lines) and to their corresponding corner of the outline (blue short lines); b – Image patches around Förstner points; c – Detail of a) focusing on the relation of Förstner points to the corner of the window; d – Elliptical areas around window corners (white) where Förstner points are extracted.

of the training set and that we use the patches as well as their horizontally mirrored versions, making the algorithm more invariant to the viewing direction. The rectangular outlines of the windows are manually delineated (cf. red rectangle in Fig. 1a). Only in elliptical areas around the corners of the outline with radii 20 and 10 pixels / cm for the major and the minor axis (cf. Fig. 1d) Förstner points (Förstner & Gülch 1987) are extracted. The image patches around the Förstner points shown in Fig. 1b are the basis for the appearance based detection of windows together with their arrangement relative to the center of the window computed from the manually delineated outline marked as yellow lines in Fig. 1a.

For the retrieval, i. e., for window detection, Förstner points are extracted with the same parameters as for training, but in the whole image (cf. Fig. 2a). Patches around the points with a size of 35 pixels are matched via cross correlation of the images trans-

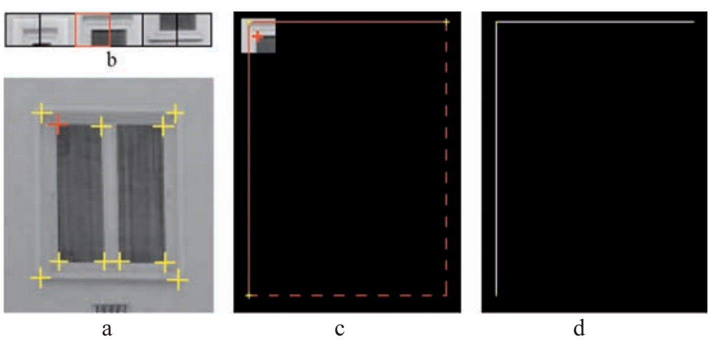

Fig. 2: Retrieval – a – Förstner points; b – Training patches with the patch just left above the "b" being matched to the red cross at the upper left corner of the window pane in a; c – Relation of the center of the patch (red cross) to the window outline in the training data (left cross for position – lengths of sides from training data); d – Hypothesis for parts of the window outline.

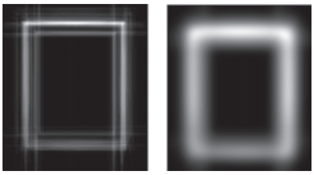

Fig. 3: Distribution for window outline – after accumulation (left) and after smoothing (right).

formed to grayscale to all patches in the training data. If the cross correlation coefficient is above an empirically found threshold of 0.75, the match is accepted and the vector relating the training patch to its center is used to generate a hypothesis for the center of the window in an initially empty accumulation image. The hypotheses are integrated via a Gaussian of the average size of the windows used for training and local maxima of the resulting function are hypotheses for windows. The patches which led to the maxima are employed to delineate the corners of the window outlines.

To precisely delineate the windows, we employ the relation between the centers of the training patches and the given outline of the windows marked as blue lines in Fig. 1a and c. E.g., the point marked in red in the upper left corner of the dark window pane in Fig. 2a has been matched by cross correlation to the training patch marked in red just left above the "b" of Fig. 2b. Fig. 2c shows how the center of the patch marked by a thick red cross is related to the corner of the outline of the window marked by a small yellow cross. From the corner of the outline the two neighboring sides of the rectangle from the training data are drawn (cf. Fig. 2c and d). The result is a hypothesis for parts of the window outline.

The hypotheses for window outlines, as, e. g., Fig. 2d, are accumulated over all points and all training patches that led to the maximum for the window. The result is a distribution for the window outline as in Fig. 3 left which is finally smoothed (cf. Fig. 3 right) and normalized by setting the largest value in the window to 1.

The parameters of the rectangles representing the windows are estimated from the distributions for the window outlines interpreted as likelihood and priors for the window shapes by Markov Chain Monte Carlo – MCMC (Neal 1993) Maximum A Posteriori (MAP) estimation. The employed priors punish too small and too wide or too high windows. The likelihood is the sum over the distribution along the window outline (cf. red lines in Fig. 4b).

3 Self-Diagnosis for the Validation of Window Hypotheses

The proposed algorithm works only well for high quality images and simple facades. If this is not the case, it might detect and delineate false hypotheses, e. g., doors or other rectangular objects. The algorithm also does not deal well with partially occluded windows.

The solution we have devised to cope with the above shortcomings is to use good hypotheses in order to validate weaker hypotheses. The basic assumption is that at least some windows on a facade are of the

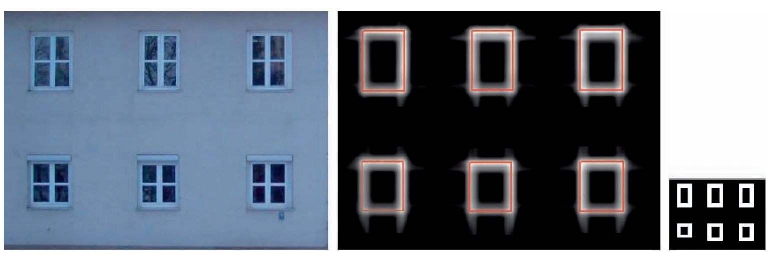

a b c

Fig. 4: a – Facade; b – Determination of the likelihood in the distribution for the window outlines (red); c – Minimal size for model selection according to sampling theorem (cf. Section 4).

same type. The validation of hypotheses works as follows: Image patches containing good hypotheses for windows are cross-correlated with the image function around weak hypotheses, determining the optimal location as the maximum. For describing the quality of the hypotheses we use a grade system empirically evaluating all cases with 1, 2, 3, and 4 recognized corners (cf. Fig. 5) based on the number of corners as well as their relation to the outline. The higher the grade of a hypothesis, the better it is evaluated. Based on the grade system we analyze and validate all hypotheses. Results are given in Figs. 6 and 7.

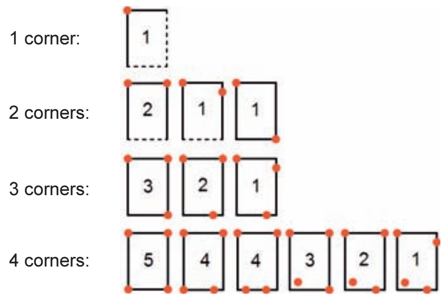

Fig. 5: The grade system for hypotheses – higher grade means better evaluation. Please note that for symmetric configurations only one instance is given.

4 Model Selection: Individual Windows, Rows, and Columns

In the preceding sections we have described how to detect, delineate, and validate individual windows such as in Fig. 8a. Yet, windows are usually not arranged randomly, but in rows, columns, or grids. Rows and columns, in this paper defined to have the same horizontal or vertical distance between windows of the same size, can be built by analyzing the horizontal or vertical arrangement. Yet, it is often not clear if one should

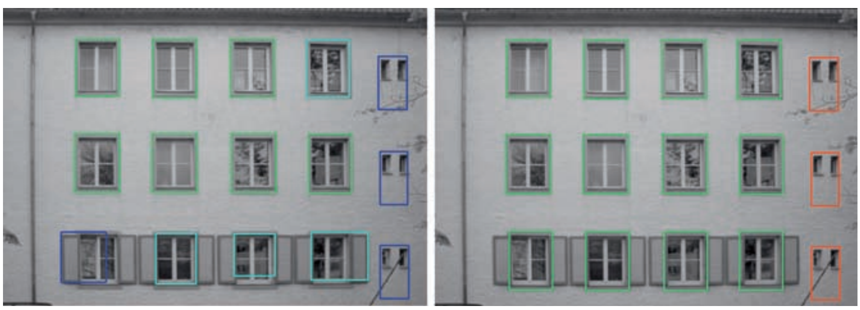

Fig. 6: Validation of hypotheses – left: Before verification. Hypotheses with grade 5 as green, with grade 4 as yellow, with grade 3 as cyan, and with grade 2 as blue rectangles; right: After verification: green – accepted, red – rejected hypotheses.

Fig. 7: Validation of hypotheses – left: Before verification; right: After verification (for colors cf. Fig. 6).

represent a facade by means of individual windows or by rows or columns of windows. E. g., Fig. 8 shows a configuration which can be represented adequately by means of columns, but not rows. Basically, in terms of an optimum fit described in the form of the likelihood always individual windows will be preferred as they can optimally adapt to the data. Thus, one needs a way to reward regular arrangements of objects and one way to do this is to take into account that they can be described by smaller numbers of parameters.

The above problem is thus regarded as a problem of model selection. Numerous means have been devised to balance the complexity of a model, e. g., described by the number of parameters or their accuracy, on one hand and the fit to the data, i. e., the likelihood, on the other hand. Two well known are Minimum Description Length – MDL (Rissanen 1978) and AIC – Akaike's information criterion (Akaike 1973). A very good analysis of the relations of these two means as well as their characteristics, their strengths, and weaknesses can be found in (Schindler & Suter 2006). For its simplicity and as we found it to work well for our application, we employ AIC, though recent work on composition such as (Geman et al. 2002) prefers MDL. Particularly, we use

$$AIC = k - 2n \ln(L) \tag{1}$$

with k the number of the parameters of the model, n the number of observations, and L the likelihood of the outline. The number of parameters is four (width, height and center coordinates) for every individual window and six for a row or column (four parameters for window shape plus – horizontal or vertical – spacing and number of elements). The basic idea is to determine the posterior based on the normalized distribution image by means of MCMC as described in Section 2 above. Fig. 4b shows how the distribution is sampled at one position with the outline given in red. Every boundary point gives one observation of the likelihood which is multiplied leading to the multiplication factor for the log-likelihood.

Yet, a couple of experiments made clear that one cannot just sample the given distribution for windows. We found that one has to reduce the determination of the likelihood to a minimal setup. From the sampling theorem we derived that for a window consisting of parallel lines the minimum size is a length of just above three pixels. We accordingly resample the distribution image to this minimum size (cf. Fig. 4c) for the computation of the likelihood for AIC. (Note: For the delineation the original resolution is used to obtain a higher accuracy.)

Results for this procedure are given in Fig. 9. For all three facades consisting of windows with the same size and a constant horizontal or vertical spacing as well as many other facades we tested our procedure on we selected the correct model. If there is an obvious structure on the facade, it is reflected in significantly different AIC values as shown in Fig. 9.

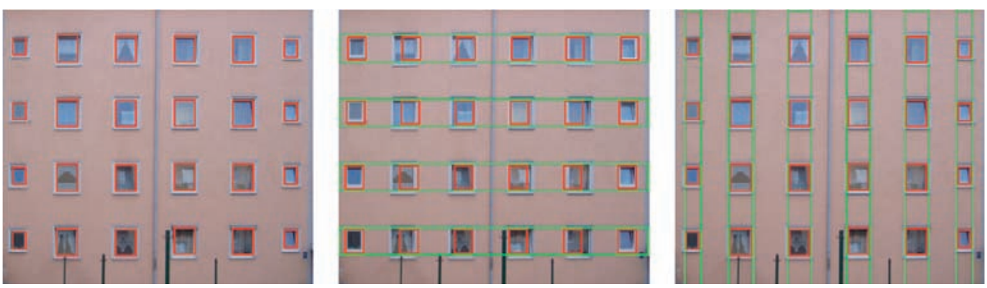

a b c

Fig. 8: Model Selection – Representation of facade by a – individual windows; b – rows; c – columns of windows, the latter two consisting of windows with the same size and a constant horizontal or vertical spacing.

a – **C: 265**, R: 404, W: 359 b – C: 115, **R: 65**, W: 94 c – **C: 76**, R: 83, W: 87

Fig. 9: Results for model selection using AIC values – C: Columns, R: Rows, W: Individual Windows. Selected model in bold.

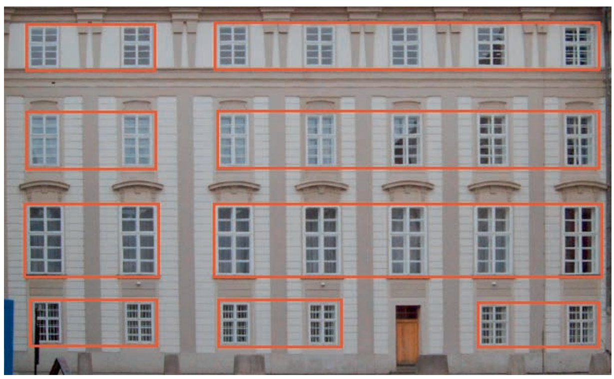

Fig. 10: Results for model selection extending randomly chosen neighbored pairs of windows.

Up to this point we have restricted ourselves to completely evenly spaced rows or columns of windows. To deal with configurations such as in Fig. 10, where the horizontal distances between the windows partly vary, we sample the rows or columns by extending randomly chosen neighbored pairs by other neighboring windows via MCMC until no further window is found anymore which can be linked. Then the next pair is selected, etc. Several start configurations are chosen again randomly and finally the configuration yielding the smallest AIC value is selected. For Fig. 10 it consists of 54 instead of 108 parameters.

5 3D Reconstruction via Plane Sweeping and Results

The results from the above procedure are the outlines of windows on the facade images possibly restricted to form horizontal rows or vertical columns. As we use image sequences as basis, we can determine the 3D extent of the windows. To do so, we follow (Baillard & Zisserman 1999 and Werner & Zisserman 2002) and employ plane sweeping, in this case for planes parallel to their facade plane in the direction of the latter's normal. The determination of the depth for individual windows is based on the sum of the least-squares differences between the projections of the individual images onto the

Fig. 11: Images one, three, five, and seven of sequence Ostbahnhof-1.

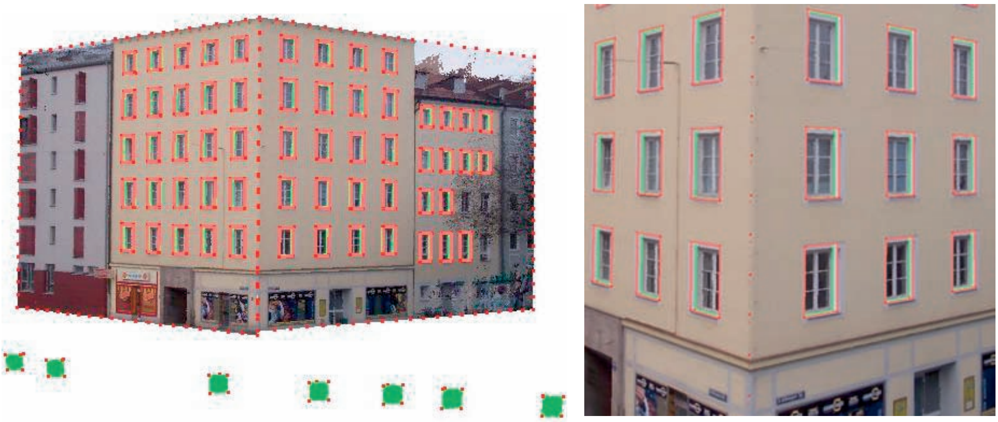

Fig. 12: left: Result for sequence Ostbahnhof-1 (images cf. Fig. 11) – Window outlines for three facades with rows of windows as red rectangles, 3D window positions as green rectangles, and camera positions as green pyramids; right: Detail: part of two walls.

Fig. 13: Result for sequence Bordeaux Square with individual windows constructed from eleven images – explanation cf. Fig. 12.

plane to their average image. This is computed for a meaningful range of depth values for windows and the result is the depth value for the minimum of the sum. For rows or columns we sum up the contributions of all images of a row or column at a particular depth.

Fig 14: Result for sequence Ostbahnhof-2 with columns of windows constructed from ten images – explanation cf. Figure 12.

Fig. 11 shows four images of a sequence with seven images and Fig. 12 the result for three manually coarsely marked facades. Please note that the rows and columns presented in this section consist of windows with the same shape and a constant distance in either horizontal or vertical direction and we do the selection for the whole facade. The 3D reconstruction was done mostly reliably and accurately and led to the windows behind the facade marked by green rectangles which can be seen in Fig. 12, right. Further results are given in Fig. 13 and 14.

6 Conclusions

We have presented three novel contributions for the interpretation of facades consisting of individual windows, i. e., no glass facades, from terrestrial image sequences, namely the coherent use of Implicit Shape Models for the delineation of windows, self-diagnosis to validate hypotheses for windows, and model selection based on Akaike's information criterion (AIC) for selecting between individual windows and rows and columns constructed from them. Combined with plane sweeping we obtain 3D interpretations of facade planes including the windows.

Concerning future work we think into different directions. First, we need to do model selection for individual rows and columns in a more flexible way by using RJMCMC and use a hierarchical model such as the architectural shape grammars of Müller et al. (2007). Then, we want to create more detailed models of the windows including mullions and transoms, the appearance of both possibly learned in an appearance based hierarchy.

On a more global level we want to integrate other objects such as doors on the ground level but also architectural details around windows possibly including their 3D structure as well as balconies. For the latter plane sweeping might be a solution for some shapes of balconies. We consider Composition Systems (Geman et al. 2002) as an important theoretically sound basis for our hierarchical modeling ranging from the window details to grids made up of windows and other architectural objects. Finally, a statistically sound link between discriminative and generative modeling such as in (Tu et al. 2005) could be advantageous.

Acknowledgment

We thank Deutsche Forschungsgemeinschaft for funding Sergej Reznik under grant MA 1651/10.

References

Akaike, H., 1973: Information Theory and an Extension of the Maximum Likelihood Principle. – Second International Symposium on Information Theory: 267–281.

Alegre, F. & Dallaert, F., 2004: A Probabilistic Approach to the Semantic Interpretation of Building facades. – International Workshop on Vision Techniques Applied to the Rehabilitation of City Centres: 1–12.

Baillard, C. & Zisserman, A., 1999: Automatic Reconstruction of Piecewise Planar Models from Multiple Views. – Computer Vision and Pattern Recognition **II:** 559–565.

Becker, S. & Haala, N., 2007: Refinement of Building Facades by Integrated Processing of Lidar and Image Data. – International Archives of Photogrammetry, Remote Sensing and Spatial Information Sciences **36** (3/W49A): 7–12.

Brenner, C. & Ripperda, N., 2006: Extraction of Facades Using RJMCMC and Constraint Equations. – International Archives of the Photogrammetry, Remote Sensing and Spatial Information Sciences **36** (3): 155–160.

Dick, A., Torr, P. & Cipolla, R., 2004: Modelling and Interpretation of Architecture from Several Images. – International Journal of Computer Vision **60** (2): 111–134.

Fischler, M. & Bolles, R., 1981: Random Sample Consensus: A Paradigm for Model Fitting with Applications to Image Analysis and Automated Cartography. – Communications of the ACM **24** (6): 381–395.

Förstner, W. & Gülch, E., 1987: A Fast Operator for Detection and Precise Location of Distinct Points, Corners and Centres of Circular Features. – ISPRS Intercommission Conference on Fast Processing of Photogrammetric Data, Interlaken, Switzerland: 281–305.

Geman, S., Potter, D. & Chi, Z., 2002: Composition Systems. – Quarterly of Applied Mathematics **LX:** 707–736.

Green, P., 1995: Reversible Jump Markov Chain Monte Carlo Computation and Bayesian Model Determination. – Biometrika **82:** 711–732.

Hinz, S. & Wiedemann, C., 2004: Increasing Efficiency of Road Extraction by Self-Diagnosis.

– Photogrammetric Engineering & Remote Sensing **70** (12): 1457–1466.

Leibe, B., Leonardis, A. & Schiele, B., 2004: Combined Object Categorization and Segmentation with an Implicit Shape Model. – ECCV'04 Workshop on Statistical Learning in Computer Vision: 17–32.

Mayer, H., 2007: 3D Reconstruction and Visualization of Urban Scenes from Uncalibrated Wide-Baseline Image Sequences. – Photogrammetrie – Fernerkundung – Geoinformation **3/07:** 167–176.

Mayer, H. & Reznik, S., 2006: MCMC Linked with Implicit Shape Models, and Plane Sweeping for 3D Building Facade Interpretation in Image Sequences. – International Archives of the Photogrammetry, Remote Sensing and Spatial Information Sciences **36** (3): 130–135.

Müller, P., Zeng, G., Wonka, P. & Van Gool, L., 2007: Image Based Procedural Modeling of Facades. – SIGGRAPH / ACM Transactions on Graphics **26** (3): Article 85, 1–9.

Neal, R., 1993: Probabilistic Inference Using Markov Chain Monte Carlo Methods. – Technical Report CRG-TR-93-1, Department of Computer Science, University of Toronto.

Nistér, D., 2004: An Efficient Solution to the Five-Point Relative Pose Problem. – IEEE Transactions on Pattern Analysis and Machine Intelligence **26** (6): 756–770.

Reznik, S. & Mayer, H., 2007: Implicit Shape Models, Model Selection, and Plane Sweeping for 3D Facade Interpretation. – International Archives of Photogrammetry, Remote Sensing and Spatial Information Sciences **36** (3/W49A): 173–178.

Ripperda, N. & Brenner, C., 2007: Data Driven Rule Proposal for Grammar Based Facade Reconstruction. – International Archives of Photogrammetry, Remote Sensing and Spatial Information Sciences **36** (3/W49A): 1–6.

Rissanen, J., 1978: Modeling by Shortest Data Description. – Automatica **14:** 465–471.

Schindler, K. & Suter, D., 2006: Two-View Multibody Structure-and-Motion with Outliers Through Model Selection. – IEEE Transactions on Pattern Analysis and Machine Intelligence **28** (6): 983–995.

Tu, Z., Chen, X., Yuille, A. & Zhu, S.-C., 2005: Image Parsing: Unifying Segmentation Detection and Recognition. – International Journal of Computer Vision **63** (2): 113–140.

Van Gool, L., Zeng, G., Van den Borre, F. & Müller, P., 2007: Towards Mass-Produced Building Models. – International Archives of Photogrammetry, Remote Sensing and Spatial Information Sciences **36** (3/W49A): 209–220.

Werner, T. & Zisserman, A., 2002: New Techniques for Automated Architectural Reconstruction from Photographs. – Seventh European Conference on Computer Vision **II:** 541–555.

Address of the Authors:

Dipl.-Phys. Sergej Reznik, Prof. Dr.-Ing. Helmut Mayer, Universität der Bundeswehr München, Institut für Photogrammetrie und Kartographie, D-85577 Neubiberg, Tel.: +49-89-6004-3429 (Mayer), Fax: +49-89-6004-4090, e-mail: Sergiy.Reznik@unibw.de, Helmut.Mayer@unibw.de.

Manuskript eingereicht: Dezember 2007
Angenommen: März 2008

Photogrammetrie • Fernerkundung • Geoinformation 3/2008, S. 197–206, 6 figs.

Automatic Adaptation of Image Analysis Models for 2D Landscape Objects to a Coarser Image Resolution [1]

JANET HEUWOLD, KIAN PAKZAD & CHRISTIAN HEIPKE, Hannover

Keywords: Multiresolution, Scale Space, Modelling, Image Analysis, Interpretation

Summary: This paper presents a new methodology for the automatic adaptation of image analysis object models for the extraction of 2D landscape objects to a lower image resolution. The object models are represented in form of semantic nets. The developed adaptation method includes a prediction of the object's behaviour in linear scale-space using analysis-by-synthesis. The scale behaviour prediction takes into account all scale events possibly occurring during 2D scale change of area-type object parts with arbitrary orientation. An example for the adaptation of an object model describing a road junction arm with road markings demonstrates the applicability of the methodology. Finally, conclusions point out potential enhancements of the method.

Zusammenfassung: *Automatische Anpassung von Bildanalysemodellen für 2D-Landschaftsobjekte an eine niedrigere Bildauflösung*. Dieser Beitrag beschreibt eine neue Methode für die automatische Anpassung von Bildanalyse-Objektmodellen zur Extraktion von 2D-Landschaftsobjekten an eine niedrigere Bildauflösung. Die Objektmodelle sind als semantische Netze repräsentiert. Die entwickelte Methode zur automatischen Anpassung nutzt Analyse-durch-Synthese zur Prädiktion des Verhaltens des Objektes im linearen Skalenraum. Die Prädiktion des Skalenverhaltens berücksichtigt sämtliche Skalenereignisse, die bei der 2D-Skalenänderung von flächenhaften Objektteilen mit beliebiger Orientierung auftreten können. Die Methode wird an einem Beispiel für die Anpassung eines Objektmodells eines Straßenarmes im Kreuzungsbereich demonstriert. Der Beitrag schließt mit Schlussfolgerungen für potenzielle Verbesserungen der Methode.

1 Introduction

The appearance of landscape objects varies in aerial or satellite images of different resolution. Hence, for knowledge-based object extraction in images of different resolution, different models describing the objects are usually required. The objective of this paper is to introduce a new methodology for the automatic adaptation of image analysis models for object extraction to a lower image resolution. The models for object extraction are represented as semantic nets (TÖNJES et al. 1999). The previously developed method for the automatic adaptation of object models consisting of linear parallel object parts (PAKZAD & HELLER 2004) is only suitable for simple landscape objects such as roads, which can be described exclusively by parallel line-type objects[2]. As a result the pre-

[1] Revised and extended version of (HEUWOLD et al. 2007) presented at the ISPRS conference "Photogrammetric Image Analysis", Munich, Germany, September 19–21, 2007.

[2] In our model *landscape objects* or *objects* are decomposed into *object parts*, which are the smallest entities in our model. In many cases, the extraction of an object is carried out through the extraction of its object parts. Note, however, that we extract the complete objects in cases where no decomposition is foreseen in the model. In the example described later the object is "Road junction arm" and the object parts are the road markings (e. g., "Arrow").

1432-8364/08/2008/197 $ 2.50

diction of scale behaviour is simplified to a 1D problem, since an analysis of the cross-section is in principal sufficient. However, for modelling of a road network, more complex roads (as present in junction and urban areas) or other lansdcape objects an analysis of the scale behaviour of 2D objects is necessary. In the 2D case, the scale behaviour of the objects is more complex. Particularly challenging is the prediction of scale events that may occur during scale change for 2D objects. This paper presents a new adaptation process for image analysis models consisting of a combination of 1D and 2D object parts.

Since the appearance of objects often severely changes between different image resolutions, the extraction model for objects in lower resolution is to be altered by the adaptation method. The central problem is the prediction of the scale behaviour of objects and object parts. The second core issue is the automatic processing of the given and adapted semantic nets.

We use linear scale-space theory for the prediction of the object's scale behaviour. The linear or Gaussian scale-space as defined first by WITKIN (1983) and KOENDERINK (1984) is created by convolution of an image $L(x, y)$ with the Gaussian $g(x, y; t)$ of varying width. Thereby, a family of signals is derived depending only on a single scale parameter t corresponding to the square of the Gaussian standard deviation σ, $t = \sigma^2$, while x, y denote the image coordinates. For details concerning the characteristics of linear scale-space see FLORACK et al. (1994). The analysis of image structure in different scales is also referred to as deep structure (KOENDERINK 1984). LINDEBERG (1993 and 1994) proposed a blob detection algorithm for the automatic scale behaviour prediction of 2D object models, which we use in our methodology.

In the literature some other approaches dealing with scale behaviour analysis of 2D landscape objects from remote sensing data can be found, e. g., scale events for buildings were analysed in morphological scale-space by FORBERG & MAYER (2002); the scale-space primal sketch was used by HAY et al. (2002) for the scale behaviour description of whole landscapes as complex systems. However, the prediction of the scale behaviour of complete 2D object models for image analysis and their adaptation to a lower image resolution is new.

This paper is organised as follows: The next section gives an overview of the adaptation process including strategy and adaptation method developed for object models consisting of line-type parallel (1D) and area-type (2D) object parts. An example for the adaptation of a model for a junction area with road symbol markings is outlined in section 3. The paper finishes with conclusions and an outlook for future work.

2 Adaptation Process

2.1 *Adaptation strategy*

The strategy for the automatic scale-dependent adaptation of object models comprising linear-parallel (1D) and area-type arbitrarily oriented (2D) objects follows a process in three main steps (cf. Fig. 1) – decomposition, scale change analysis, and fusion. Based on the type of object parts in the fine scale a decision is made whether the 1D or 2D scale change analysis method is to be applied. If there are only linear parallel object parts in the object model to be adapted, the 1D scale-dependent adaptation can be used; otherwise the more sophisticated adaptation for 2D objects is to be carried out.

The first stage of the automatic adaptation decomposes the given object model for the fine scale into object parts that can be analysed separately regarding their scale behaviour. The decomposition takes into account the mutual influence of nearby objects when scale changes – denoted as interaction. The possibility of interaction depends on the spatial distances of the object parts to each other. If the distances fall below a particular value, which depends on the quantity of scale change, interaction occurs. In this case, the respective object parts are analysed simultaneously in groups in the following scale change analysis phase.

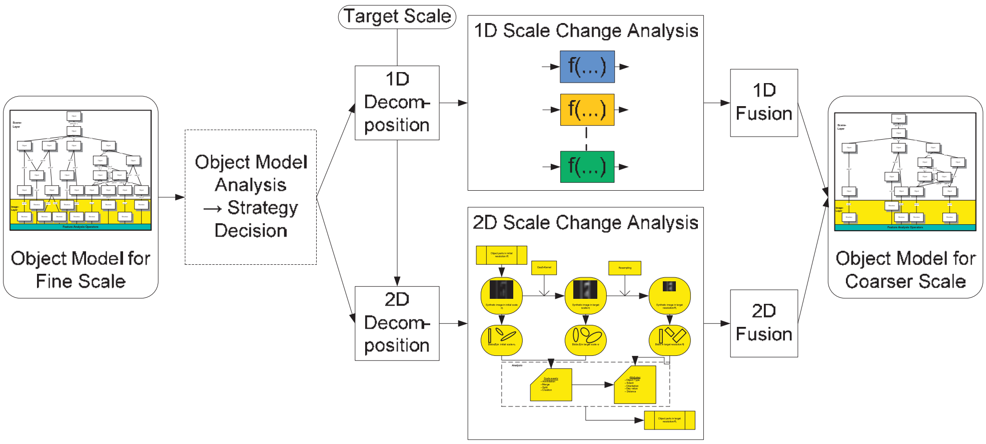

Fig. 1: Strategy for adaptation process (for details see text).

Scale change models predict the appearance and extractability in the target resolution for each interacting group or for single non-interacting object parts resulting from the decomposition. The prediction uses analysis-by-synthesis, simulating the appearance of the object parts in synthetic images of the target resolution.

In the last stage, fusion, all predicted object parts are recomposed back into a complete object model that is suitable for the extraction of the object in the target resolution.

2.2 *Adaptation method*

2.2.1 Decomposition

In order to facilitate the scale behaviour prediction of the object in the scale change models, a separate analysis of the individual parts of the modelled object is desirable. However, during scale change adjacent object parts may influence each other's appearance. This is the case, when they lie close to each other in the target resolution. This condition is checked by looking at their spatial distance in the object model. Object parts, which influence each other, need to be analysed together and form an *interaction group* in the successive scale change analysis stage. All other object parts that are not subject to interaction can be treated as single object parts in the scale behaviour analysis. Depending on the size of the Gaussian kernel associated with the target scale σ_t an *interaction zone* is formed around the object parts. For more details concerning the interaction zone see Heuwold et al. (2007).

2.2.2 Scale change analysis for 2D

Scale change models predict the scale behaviour for single object parts and interaction groups. The prediction is carried out in an analysis-by-synthesis procedure, analysing the objects in synthetic images in original scale, and target resolution (the target resolution includes downsampling, the target scale does not). The result is a description of the appearance of the object parts in the given target resolution in terms of attributes for the nodes and edges of the semantic net. As some simplifications carried out for linear parallel object parts are not applicable to 2D object parts, the previously developed method for linear parallel object parts is no longer appropriate for 2D scale change analysis. Therefore, a new workflow for the analysis-by-synthesis process was developed and is depicted in Fig. 2.

First, from the specifications of the object parts' appearance in the nodes of the given semantic net for the high resolution a synthetic image is created for each object part or interaction group to be analysed. This in-

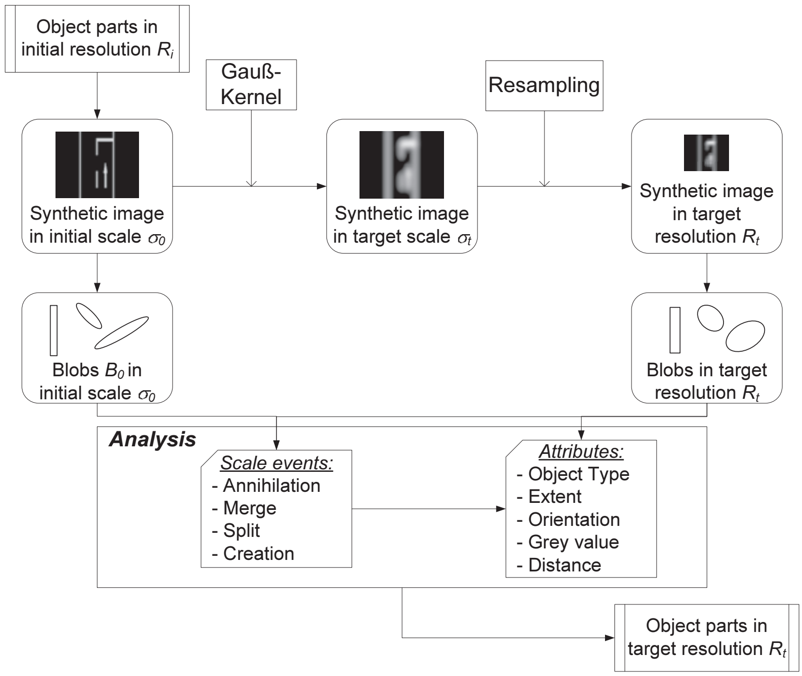

Fig. 2: Analysis-by-synthesis process for 2D adaptation.

itial image L_0 simulates the appearance of the object parts in the original scale σ_0. In a second step, the initial image is transferred to the target scale σ_t by convolution with the respective discrete Gaussian into the target scale image L_t. Since the object's appearance and extractability can vary between the target scale image and the image in the corresponding target resolution, the target scale image L_t is subsequently down-sampled to the corresponding lower resolution R_t. Both the analysis of the possibly occurring scale events and of the attributes describing the appearance of the object parts in the low resolution are carried out in this image. Although the resampling does not result in exactly the same image as a remote sensing sensor of a lower resolution produces, the process proved to be generally sufficient for a simulation of a remote sensing image (Heuwold 2006). In order to obtain an exact simulation, one would have to model the individual sensor characteristics and apply to the target scale image. Considering the amount of different imaging sensors (aerial and satellite), this approach does not seem practicable.

Scale event prediction

During scale change so-called scale events may occur. There are four types to be distinguished: Annihilation, Merging, Split and Creation. In contrast to the one-dimensional case, where only the first two events need to be considered, all four different scale events may occur in 2D images. The prediction of scale events of interacting object parts is thus not as straight forward and requires a more sophisticated approach to scale behaviour prediction than the previously presented method for linear parallel object parts.

The *scale-space primal sketch* was introduced by Lindeberg as an explicit representation of features in scale-space and their relations at different levels of scale (Lindeberg 1993). The sketch was designed as a basis for the extraction of significant image features at stable scales for later processing towards object extraction. Blobs serve as primitives of the scale-space primal sketch. *Grey-level blobs* are smooth image regions that are brighter or darker than the background and thereby stand out from their surrounding. By definition a grey-level blob $B(E)$ is a region of a scale-space image $L(x, y; t)$ associated with a pair of critical points (or regions in discrete scale-space) consisting of one local extremum E and one delimiting saddle S. The grey-level blob is a three-dimensional object with extent both in the spatial and the grey-level domain. The spatial extent of the blob is given by its *support region Supp(B)*.

At first, for the prediction of scale events blob detection is carried out in both the initial image L_0 and the target resolution image L_{Rt} using the sequential blob detection algorithm of Lindeberg (1994). Blob linking between the initial image and the target resolution image is then carried out by matching blobs with intersecting support regions in original and target resolution. We assume that most blobs are not subject to a scale event during the scale change given by the specified target resolution. In the blob linking process we thus first try to establish a so-called *plain link* between the initial and target resolution for all blobs. Based on the set of support regions in initial resolution $Supp_0$ and the set of support regions in target resolution $Supp_{Rt}$ a plain link must fulfil the following condition (with m and n being the number of blobs in initial and target resolution):

Plain Link: One particular blob in initial resolution has one and only one direct correspondence in target resolution. The support region of a blob B_i in initial resolution $Supp_0(B_i)$ intersects the support region of a blob B_q in target resolution $Supp_{RT}(B_q)$. All other blob support regions in target resolution must not intersect $Supp_0(B_i)$.

$$\exists^{=1} q(Supp_0(B_i) \cap Supp_{Rt}(B_q) \neq 0),$$
$$i \in \{1 \ldots m\},\ q \in \{1 \ldots n\} \qquad (1)$$

If a plain link cannot be established for all blobs, scale events must have occurred. The types of scale events must then be resolved automatically. We set up the following postulates for the occurrence of blob events during scale change:

Annihilation: One particular blob in initial resolution has no correspondence in target resolution. The set of support regions in target resolution $Supp_{Rt}$ is empty at the position of a blob support region in initial resolution $Supp_0(B_i)$.

$$\exists\, i(Supp_0(B_i) \cap Supp_{Rt} = 0),\ i \in \{1 \ldots m\} \qquad (2)$$

Merging: Two (or more) initial blobs have one and the same blob as correspondence in target resolution. The support regions of at least two initial blobs $Supp_0(B_i)$ and $Supp_0(B_j)$ intersect the support region of one and the same blob in target resolution $Supp_{Rt}(B_q)$.

$$\exists\, q((Supp_0(B_i) \cap Supp_{Rt}(B_q) \neq 0)$$
$$\wedge\ (Supp_0(B_j) \cap Supp_{Rt}(B_q) \neq 0)),$$
$$i, j \in \{1 \ldots m\}, q \in \{1 \ldots n\},\ i \neq j \qquad (3)$$

Split: One initial blob has two (or more) blobs as correspondence in target resolution. The support region of an initial blob $Supp_0(B_i)$ intersects the support regions $Supp_{Rt}(B_q)$ and $Supp_{Rt}(B_s)$ of at least two blobs in target resolution.

$$\exists\, q\, \exists\, s((Supp_0(B_i) \cap Supp_{Rt}(B_q) \neq 0)$$
$$\wedge\ (Supp_0(B_i) \cap Supp_{Rt}(B_s) \neq 0),$$
$$i \in \{1 \ldots m\},\ q, s \in \{1 \ldots n\},\ q \neq s \qquad (4)$$

Creation: One particular blob in target resolution has no correspondence in initial resolution. The set of support regions in initial resolution $Supp_0$ is empty at the position of a blob support region in target resolution $Supp_{Rt}(B_q)$.

$$\exists\, q(Supp_0 \cap Supp_{Rt}(B_q) = 0),\ q \in \{1 \ldots n\} \qquad (5)$$

Based on these conditions the scale events that have occurred during scale change are inferred. The procedure is described more detailed in Heuwold et al. (2007).

It should be noted that blobs can be composed of several individual object parts that are adjacent to each other. Hence, the number of blobs in initial or target resolution does not necessarily equal the number of nodes in the semantic net for the respective resolution. However, as we know the composition of blobs in initial scale from the synthesis process, we can separate the individual object parts that compose the same blob in target resolution, if no scale events have occurred.

Attribute prediction

The attributes in the nodes specify the appearance of an object part in the image. The values of the attributes in the nodes of the adapted semantic net for the lower resolution are therefore analysed in the synthetic target resolution image L_{Rt}. Blobs are assumed to correspond to the individual object parts. Hence, the number of blobs in the target resolution equals the number of nodes in the semantic net for the target resolution. For each blob in the target resolution the following attributes are derived: *object type* (e. g., line or pattern), *spatial extent* (width and length), *grey value*, and *orientation*.

2.2.3 Fusion

The fusion is the last stage of the automatic adaptation process. All nodes remaining after scale change including their attributes representing the object parts in the given target resolution are compiled to a complete semantic net.

The hierarchical relations between the nodes remain unchanged as long as no scale event occurred. In case of Annihilation, the respective node is simply omitted. For merged blobs only a single *part-of* relation remains. For the Split and Creation events new *part-of* relations are introduced into the respective hierarchy level.

The type of the spatial relation (parallel or perpendicular distance) stays unaffected. However, the distances between the object parts are to be adapted. The adapted distance values are derived from the position of the borders of the blob support regions $Supp_{Rt}$ in target resolution.

3 Adaptation Example

In order to demonstrate the applicability of the adaptation methodology, this section gives an example for the automatic adaptation of a high-resolution object model to a coarser image resolution. A semantic net for the extraction of a road junction arm with 2D symbols (arrows and stop lines) serves as given model for high image resolution (3–5 cm per pixel). We chose $\sigma_t = 8$ as target scale – corresponding to an approximate target resolution of $R_t \approx 0.8$ m. This junction model can be seen as a part of an object model for a road network consisting of roads and junction arms (cf. Fig. 3). The node for an adjacent *Road*, for instance, can be represented by the model given in Heuwold (2006), which consists of linear parallel objects and can be adapted with the 1D adaptation strategy.

The road junction in our example consists of a number of road junction arms with a dashed central line. These arms meet in the junction area. They contain lane markings and additional traffic markings (in our example direction arrows and stop lines).

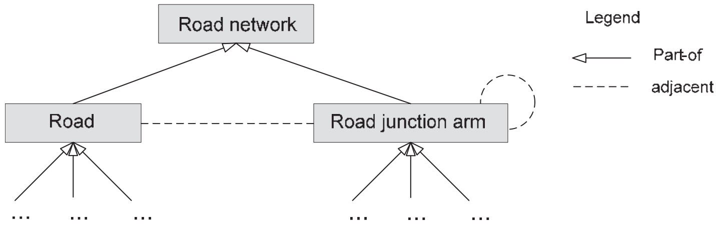

Fig. 3: Object model for road network.

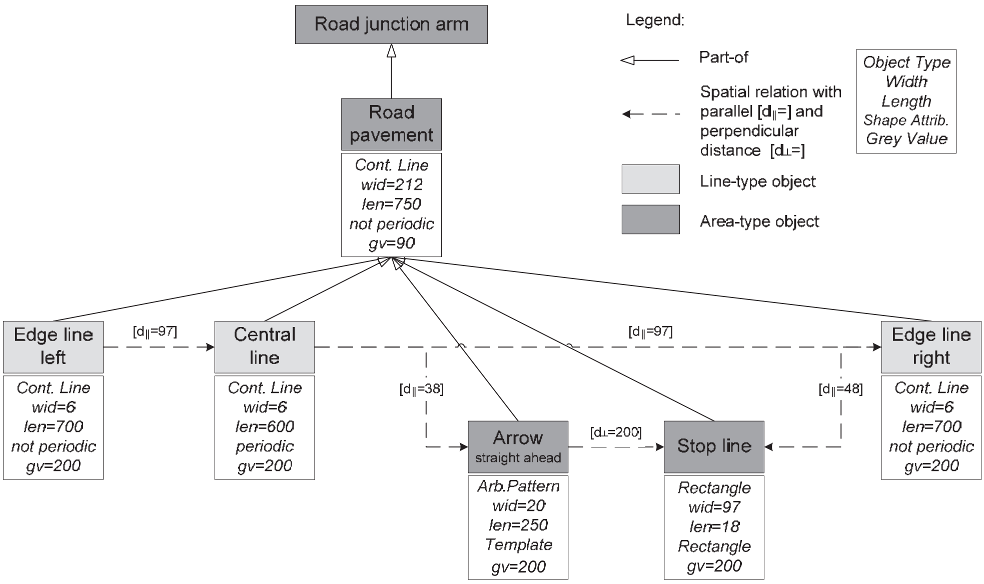

Fig. 4: Object model for junction arm in a resolution of 0.03–0.05 m/pixel.

This means the road junction arms represent the part close to the roads before the junction centre, where the roads contain additional road markings. The width of the road junction arm is modelled to be constant. The 2D position of the object parts is given by distances (in number of pixel in the respective resolution) between them in two perpendicular directions. The model also contains information concerning the extent of the object parts. The model for road junction arms for the high resolution is depicted in Fig. 4.

An essential part of an object model for image analysis is also a set of image analysis operators. They represent the procedural knowledge needed to extract particular object parts from images. The image analysis operators search for the particular parts in the image, which are represented as nodes in the object model. Therefore, the nodes of the semantic net are connected to the corresponding image analysis operators. Different image analysis operators are assigned to different types of object parts. Two object types were defined for area-type objects: *Geometric Shape* (e. g., *Rectangle*) for simple object parts and *Arbitrary Pattern* for more complex ones. The shape of the latter kind of object part is defined by templates. The operators for *Arbitrary Pattern* use cross-correlation matching with provided templates, whereas the line-type objects and the *Rectangle* use the road marking operators based on differential geometry developed in Heuwold (2006).

As mentioned before, the scale behaviour prediction of the junction example is carried out in the scale change analysis stage by analysis-by-synthesis. Due to the width of the discrete Gaussian used for the creation of the target scale image L_t, all object parts of the bottom level except *edge line left* form an interaction group. Hence, the scale behaviour of these object parts is analysed jointly. Fig. 5a) depicts all simulated object parts in a synthetic image, while Fig. 5b) shows the down-sampled filtered image in target resolution L_{Rt}. The number of blobs in initial resolution (5) differs from the number of blobs in target resolution R_t (4), suggesting the occurrence of a scale event: a Merging event is detected for a part of the central line and the direction arrow. Here, the corresponding blobs have merged. The results of the blob detection in the synthetic images of the initial and target resolu-

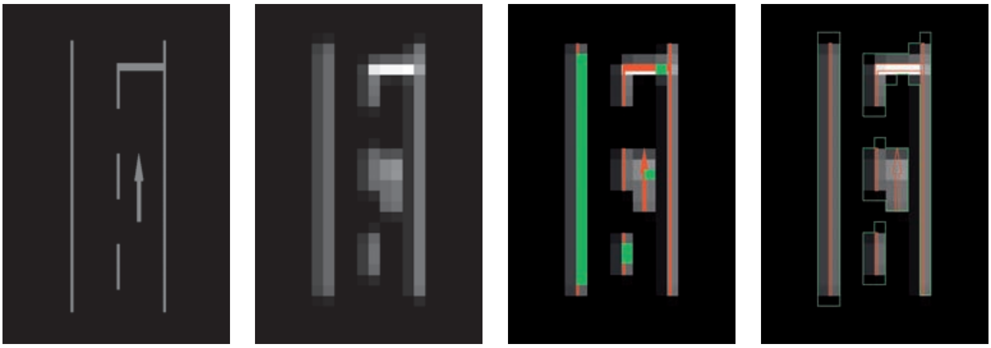
a) b) c) d)

Fig. 5: Blob detection results: initial blob features and target blob features superimposed on synthetic images; a) initial image L_0, b) target resolution image L_{Rt} (grey-value stretched and enlarged), c) extrema E_0 (red), E_{Rt} (green) on target resolution image L_{Rt}, d) support regions $Supp_0$ (red), $Supp_{Rt}$ (green) on L_{Rt}.

tion, illustrated in Fig. 5 d), reflect the postulated condition for Merging events – the support regions $Supp_{RT}(B_q)$ in target resolution R_t. intersect the two support regions $Supp_0(B_1)$ and $Supp_0(B_2)$ of the merged blobs from initial resolution. Fig. 5c) depicts the position of the blob extrema in initial and target resolution.

Although there are only four blobs in the target resolution image L_{Rt}, the resulting object in the target resolution R_t consists of six individual object parts. Because the upper part of the dashed *central line*, the *stop line* and the *edge line right* touch each other, they form one single blob – not only in target resolution but already in initial resolution. For all resulting six object parts in the target resolution the node attributes are derived from the target resolution image L_{Rt}, as illustrated in Fig. 5d): there are four *Continuous Lines* (*edge line left*, *edge line right* and two parts of the dashed *central line*), one

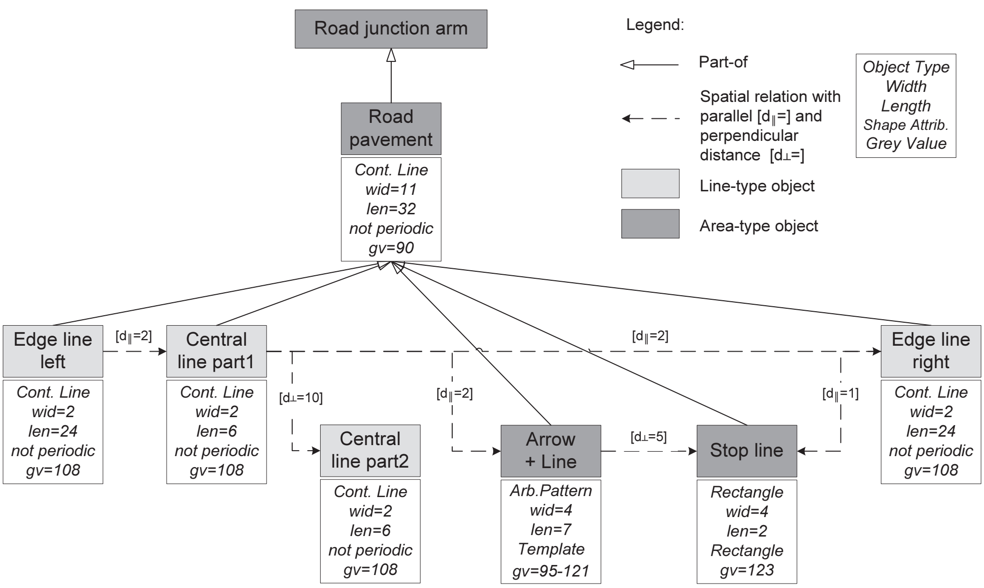

Fig. 6: Adapted example object model in target resolution $R_t \approx$ 0.8 m.

Rectangle (*Stop Line*) and one *Arbitrary Pattern* (*Arrow* + *Line Part*) for the merged part of the central line and the direction arrow; their extents are given by the width and length of a fitted rectangle of their blob support regions $Supp_{Rt}$; the grey values are determined from the blob brightness inside its predicted extent (mean value for area-type object parts, maximum value in cross-section for line-type object parts). The distances being attributes of the spatial relations (edges) are derived from the shortest distance of the blob support regions for area-type object parts.

The adapted object model of the road junction arm for the target resolution $R_t \approx 0.8$ m is illustrated in Fig. 6. Most line-type object parts changed only their attributes (width and contrast); whereas one part of the previous dashed central line was subject to a scale event and was merged with the adjacent area-type arrow symbol during scale change. The resulting object is another arbitrary pattern, which is to be extracted by pattern matching. The operator for this new object part can use a template that is derived from the support region $Supp_{Rt}$ of the merged blob in the target resolution image L_{Rt} for cross-correlation matching.

4 Conclusions and Outlook

In this paper a new methodology was presented for an automatic adaptation of image analysis object models, created for a specific high resolution, to a lower resolution image. The modelled landscape objects can consist of both arbitrarily oriented line-type and area-type object parts. In order to adapt the representation of the objects, the scale behaviour of the object parts is analysed taking into account 2D scale events and changes in the object's appearance. Using an object model for a road junction area, the adaptation method is exemplarily described.

A general constraint of the described method is that interaction with other objects can always influence the objects' appearance in the target resolution; also other non-modelled objects in the vicinity of the modelled objects can influence the appearance. Therefore, strictly speaking the described method is only valid for a modelled object, if the neighbouring object is a homogeneous area and no other objects influence the adaptation. This means that the spatial distance to neighbouring object must be larger than the computed threshold for interaction (which depends on the amount of scale change). This is also true for the case that a modelled object can influence itself, because it is strongly curved (e. g., serpentine roads may cause adaptation problems). This condition forms a current limitation with regard to automatically adaptable object models using our methodology.

Our future work will therefore focus on the incorporation of relevant local context objects such as trees or buildings into the adaptation process in order to be able to deal with more realistic scenes. This will allow us to account for occlusions and shadows in the images. Due to the high complexity of the scale behaviour simulation for local context objects with unknown position, however, we will not process the road objects simultaneously with the local context objects, as the number of possibly resulting low resolution object models can easily become very high. Instead, we intend to consider the local context object as a separate object model, for which a scale change is derived independently. In cases where in the low resolution the road extraction fails, we will then try to explain this failure through the introduction of a building, a tree or their shadows.

The 2D concept presented in this paper is until now essentially limited to theoretical work. However, once extended this approach to automatic object model generation could prove useful in a number of applications: e. g., for multi-sensor image interpretation without the need to create more than one object model manually, as the models for sensors with lower resolution can be automatically derived; generally, the developed method for blob linking can also support many-to-many matching of spatial entities in different representations.

Acknowledgements

This study has been funded by the Deutsche Forschungsgemeinschaft under grant HE 1822/13. The project is part of the bundle "Abstraction of Geoinformation in Multi-Scale Data Acquisition, Administration, Analysis, and Visualisation".

References

Florack, L., Haar Romeny, B., Koenderink, J. & Viergever, M., 1994: Linear Scale-Space. – Journal of Mathematical Imaging and Vision **4** (4): 325–351.

Forberg, A. & Mayer, H., 2002: Generalization of 3D Building Data Based on Scale-Spaces. – The International Archives of the Photogrammetry, Remote Sensing and Spatial Information Sciences **34** (4): 225–230.

Hay, G., Dubé, P., Bouchard, A. & Marceau, D., 2002: A scale-space primer for exploring and quantifying complex landscapes. – Ecological Modelling **153** (1–2): 27–49.

Heuwold, J., 2006: Verification of a methodology for the automatic scale-dependent adaptation of object models. – The International Archives of the Photogrammetry, Remote Sensing and Spatial Information Sciences **36** (3): 173–178.

Heuwold, J., Pakzad, K. & Heipke, C., 2007: Scale Behaviour Prediction of image analysis models for 2D landscape objects. – The International Archives of the Photogrammetry, Remote Sensing and Spatial Information Sciences **36** (3/W49A): 43–49.

Koenderink, J., 1984: The Structure of Images. – Biological Cybernetics **50** (5): 363–370.

Lindeberg, T., 1993: Detecting Salient Blob-Like Image Structures and Their Scales with a Scale-Space Primal Sketch: A Method for Focus-of-Attention. – International Journal of Computer Vision **11** (3): 283–319.

Lindeberg, T., 1994. Scale-Space Theory in Computer Vision. – Kluwer Academic Publishers, Dordrecht, The Netherlands, 423 p.

Pakzad, K. & Heller, J., 2004: Automatic Scale Adaptation of Semantic Nets. – The International Archives of the Photogrammetry, Remote Sensing and Spatial Information Sciences, **35** (B3): 23–28.

Tönjes, R., Growe, S., Bückner, J. & Liedtke, C.-E., 1999: Knowledge Based Interpretation of Remote Sensing Images Using Semantic Nets. – Photogrammetric Engineering & Remote Sensing **65** (7): 811–821.

Witkin, A., 1983: Scale Space Filtering. – 8th Int. Joint Conference on Artificial Intelligence: 1019–1022.

Address of the Authors:

Dipl.-Ing. Janet Heuwold, Dr.-Ing. Kian Pakzad, Prof. Dr.-Ing. Christian Heipke, Leibniz Universität Hannover, Institut für Photogrammetrie und GeoInformation, D-30167 Hannover, Tel.: +49-511-762-19953 (Heuwold) 3893 (Pakzad), 2482 (Heipke), Fax: +49-511-762-2483, e-mail: heuwold | pakzad | heipke@ipi.uni-hannover.de

Manuskript eingereicht: Dezember 2007
Angenommen: März 2008

Photogrammetrie • Fernerkundung • Geoinformation 3/2008, S. 207–215, 2 figs.

From Detailed Digital Surface Models to City Models Using Constrained Simplification

ROLAND WAHL, RUWEN SCHNABEL & REINHARD KLEIN, Bonn

Keywords: DSM, City Model, Geometry Simplification, Abstraction, Visualization.

Summary: We present a method to simplify high-detail full-featured digital surface models (DSM) of cities (i. e., containing the heights of trees, cars, buildings, etc.) geometrically in such a way that all relevant features are preserved, whereas noise and superfluous details collapse. The relevance of features is automatically evaluated using a semantically motivated shape detection and serves as constraint during the simplification. Our results show that we are able to preserve fine details of complex roof structures while all irrelevant features are effectively removed. Thus, we achieve an excellent abstraction of the city data without any interaction of the user, which is not only beneficial for visualization, but could also be used for GIS related applications.

Zusammenfassung: *Von digitalen Oberflächenmodellen zu Stadtmodellen mittels eingeschränkter Simplifizierung*. Wir stellen ein geometrisches Simplifizierungsverfahren für hoch detaillierte ungefilterte digitale Oberflächenmodelle (DOM) von Städten (inkl. Abtastwerten von Bäumen, Autos, Gebäuden, etc.) vor, welches alle relevanten Merkmale erhält, aber Rauschen und überflüssige Details verwirft. Die Relevanz der Merkmale wird automatisch mittels semantisch motivierter Formerkennung bewertet und dient als Einschränkung der Simplifizierung. Unsere Resultate zeigen, dass wir in der Lage sind, feine Details komplexer Dachstrukturen zu erhalten, während irrelevante Merkmale effektiv eliminiert werden. Auf diese Weise erreichen wir ohne jegliche Benutzerinteraktion eine ausgezeichnete Abstraktion der Stadtdaten, die sich nicht nur für Visualisierungszwecke eignet, sondern auch in GIS-Applikationen benutzt werden könnte.

1 Introduction

Conventionally, the sole aim of geometry simplification in the context of real-time visualization of landscape or urban environments is to enable smooth, real-time navigation through the scene without disturbing interruptions for data loading or decoding. To this end, the simplification generates a suitable set of geometric levels of detail (LOD) of the terrain data. To sustain a satisfactory user experience, the blending in of additional detail without notable flickering or jumps while the user zooms in on objects should be supported by the underlying LOD structure. Hence, the LODs are usually generated with respect to a geometric error measure, e. g., Hausdorff error that guarantees pixel correct images at given viewing distances. However, often additional requirements arise when dealing with city-data:

- In the context of city visualization, a photorealistic visualization is not always desired, e. g., on a small PDA or cell phone display, the overwhelming amount of detail is difficult to grasp for the user and an abstracted view is usually preferred. The abstraction however should be semantically motivated and cannot be based on geometric error alone.
- A lot of existing GIS related software, e. g., for city-planning, operate on abstracted data in the form of CityGML or similar formats. To this day no automatic

1432-8364/08/2008/207 $ 2.25

conversion of height-field data into this representation is available.

- For city visualization in a client-server setting over the internet, as it is available in a primitive form in Google Earth today, it is usually not possible to transmit all the necessary detail of geometry and texture in the short time available while the user navigates through the scene because of limited bandwidth. Therefore it is unavoidable that the user will frequently see coarser LODs from a distance where the simplifications therein become clearly visible (i. e., larger than a couple of pixels). Current simplification methods for high resolution height-field data however are only based on geometric error considerations, so that often façades of houses are askew or roofs have unnatural looking shapes, which results in views that are irritating to the user.

All of these requirements are not vital as long as we deal with city models derived from cadastral data or semi-automatic reconstruction, given that these models are generally reasonably abstract. However, considering the ongoing advances in camera and reconstruction techniques and the consequently increasing detail and extent of full-featured digital surface models (DSM), automatic abstraction methods capable of handling out-of-core data are necessary.

In order to address this situation, in this work, we propose a novel form of constrained simplification that incorporates additional shape information together with geometric error considerations to generate LODs from highly detailed DSMs that respect both geometric as well as semantically motivated criteria. The incorporated shape information is low-level and very general. It is used to find edges and corners in the geometry that make up the important features of building geometry without resorting to more involved and specialized building models. The simplification is constrained to preserve these features even in coarse LOD. Due to the continuous nature of the LOD and the consideration of geometric error, this representation is still suitable for real-time pixel correct photorealistic terrain and city renderers. Moreover, due to the preservation of important edges and corners, it is applicable in client-server settings on the internet or visualization on mobile devices as well – all from the same data representation and generated fully automatically.

2 Previous Work

In Computer Graphics, LOD representations of objects and scenes have been extensively researched during the last 15 years. In combination with methods for efficient occlusion calculations, image based rendering as well as prediction and caching mechanisms they are employed for efficient visualization of large scenes.

2.1 *Topology-Preserving Simplification*

Even for triangulated height fields it is challenging to find an optimal approximating mesh with a given small number of faces in the sense of the L1-norm. Indeed Agarwal & Suri (1994) have proven this problem to be NP-complete. Therefore, iterative greedy algorithms have prevailed which in each simplification step either eliminate a vertex (vertex contraction) or an edge (edge collapse) from the triangulation (Schroeder et al. 1992 and Hoppe et al. 1993). Several different error measures have been proposed and evaluated in the literature. Compared to other distance measures, the Hausdorff metric has the advantage that the projection of the 3D approximation tolerance onto screen space can be used to select a corresponding LOD automatically for pixel correct rendering (Klein et al. 1996). The quadric error metric introduced later by Garland & Heckbert (1997) has the advantage of a simpler and more efficient computation. Therefore, it has become very widespread, although it does not guarantee any bounds on the screen space error. Since then, there were also improvements in computing fast Hausdorff distance approximations (Cignoni et al. 1998 and Guthe et al. 2005).

2.2 *Topology-Changing Simplification*

The family of *vertex clustering* methods has been introduced by (Rossignac & Borrel 1993) and has been refined in numerous more recent works (Kok-Lim & Tiow Seng 1997). The algorithms of this family essentially apply a 3D grid to the object and for each cell contract all the vertices inside the cell. This way holes in objects are closed or objects in close proximity are merged. Although the degenerate faces are subsequently removed, it is difficult to influence the fidelity of the result due to lack of control over the induced topological changes. The already mentioned *vertex contraction* operator (Garland & Heckbert 1997 and Popovic & Hoppe 1997) offers more control over the topological modifications. However, without further processing it possibly generates non-manifold meshes.

2.3 *Out-of-Core Simplification*

To simplify models of ever increasing size, a number of out-of-core simplification algorithms have been developed. El-Sana & Yi-Jen (2000) sort all edges according to their lengths and use this ordering as decimation sequence. Lindstrom (2000) uses vertex clustering to reduce the number of vertices. As the representing position of each vertex cluster is computed from an accumulated quadric error metric, the memory requirement of the algorithm is proportional to the size of the output model. For cases where neither input nor output model fit into main memory, an out-of-core vertex clustering (Lindstrom & Silva 2001) was developed. The multiphase algorithm (Garland & Shaffer 2003) uses vertex clustering to reduce the complexity of the input model followed by a greedy simplification approach and achieves high quality results. Another way for out-of-core simplification is to split the model into smaller blocks, simplify these blocks and stitch them together for further simplification. In (Hoppe 1998) this approach is applied to terrain and in (Cignoni et al. 2003) to arbitrary meshes. The approach has the problem that special care has to be taken at patch boundaries. Recently, stream decimation algorithms (Wu & Kobbelt 2003; Isenburg et al. 2003) for out-of-core simplification have been developed, but the resulting model is not optimal with respect to mesh size and Hausdorff distance of the simplified model to the original.

2.4 *Remeshing*

Another area related to our approach is remeshing of triangulated geometry. Remeshing algorithms take a triangle mesh and resample it such that some quality requirements are satisfied but the original geometric shape is retained. In this sense, mesh simplification can be seen as a special case of remeshing. Other remeshing techniques include surface fairing (Taubin 1995 and Desbrun et al. 1999), where connectivity is preserved but vertex positions are optimized in order to remove noise or to evenly distribute vertex positions. Hildebrandt & Polthier (2004) presented a bilateral mesh smoothing algorithm that is able to preserve edges and corners in the geometry. A similar approach is given by Vorsatz et al. (2001) who describe a remeshing algorithm that is feature sensitive. Both approaches however are not combined with simplification and are not robust to outliers.

3 Overview

Given a high-resolution height-field model, it is converted into a 3D point-cloud and decomposed by our recently proposed efficient RANSAC shape detection (Schnabel et al. 2007) into areas that correspond to primitive shapes such as planes, spheres, cylinders etc. and a set of remaining points. The points of the original DSM are then tagged with the indices of shapes detected in their proximity. These index sets then implicitly define the shape, edge or corner property of the points, which is subsequently used to constrain the geometric simplification. Only those simplification operations are allowed that respect the detected primitives on the corresponding LOD. This way it is asserted that coarse building models are generated which obey the abstract structure defined by the segmentation into primitives. Depending on the chosen size and approximation fidelity of the detected primitives, the resulting coarse polygonal models adhere to different semantically motivated levels of detail. In areas where no primitives could be detected (e. g., areas of natural cover such as in parks), the simplification is guided by geometric error alone, which has been proven to give good results for terrain in general.

4 Geometric Simplification

We build our simplification framework around the edge-collapse operation with tight upper bounds on the Hausdorff distance against the original mesh. Each edge of the original mesh generates three collapse candidates, which are either of the two corresponding halfedge-collapses or an edge-collapse with vertex placement. As optimizing the new vertex position with regard to the Hausdorff distance, which includes evaluating the maximum, does not make sense, we use the quadric error metric (Garland & Heckbert 1997) for candidate generation. This metric is fast and easy to compute, and directly yields the optimal vertex for the edge collapse operation in general cases. For degenerate cases the distance to the original edge is used as an additional criterion. Each collapse candidate is then checked for validity, that is whether it introduces flipping of orientations or degeneration of neighboring triangles, and scheduled in a priority queue keyed to its approximation error. For the sake of speed we again use the quadric error metric for computing priorities.

After these preparational steps, iteratively the best collapse candidate is evaluated, this time using the actual distance metric and if it does not surpass the current error threshold, it will be applied to the mesh. As it changes the appearance of its 1-ring, all conflicting candidates are rescheduled or deleted from the priority queue. This process comes to an end when each remaining valid collapse operation surpasses the threshold and therefore the bottom-up simplification scheme is in a local optimum. Although this approach is greedy, it is able to collapse a mesh completely, if the distance threshold allows it (i. e., it does not get stuck in a local minimum).

4.1 *Distance Metric*

For pixel-true rendering, the Hausdorff distance is almost the perfect choice, since it guarantees two crucial properties, directly linked to its definition:

Firstly, for every feature of the original mesh, there exists a part of the proxy mesh which represents that feature within a distance of at most the predefined threshold. And secondly, as also the inverse Hausdorff hemimetric is accounted for, the resulting approximation does not introduce artifacts which have no justification from the original mesh.

The arguments against using Hausdorff distance are that it is very difficult to compute and that in many cases, simpler approximations well serve their purpose.

Especially, in the domain of terrain rendering, measuring only along the z-axis is a popular alternative. Its main advantage is that opposed to strict Hausdorff distance, the counterpart on the other mesh is implicitly given and therefore, we get two piecewise linear distance functions parameterized over the plane. It has been observed that evaluating this metric only at the vertices of the two corresponding meshes does not yield tight bounds on the Hausdorff distance, but also the edges need to be considered, as otherwise the error can become arbitrary large. It can be shown that for small maximum steepness angles α the overestimation of the distance is bounded by $\cos^{-1}\alpha$. So this does not lead significant overheads for coarsely sampled terrain datasets.

However, in the presence of high-frequency signal, which is very common in high-resolution digital surface models, this approximation is no longer effective. Therefore, we only use the implicit correspondence between the meshes as given by the z-projection and evaluate the Hausdorff distance locally between the corresponding parts. That way, the distance computations remain local (i. e., in the 1-ring of the edge in question) and still we get tighter bounds and effective simplification of steep geometry.

5 Semantic Constraints

As mentioned in the introduction, LOD generation based on purely geometric simplification often leads to unwanted results, since it does not consider the overall shape, but only local geometric features. For terrain datasets, the resulting approximation is generally good enough, but especially for manmade objects as buildings, where the shape is often dominated by recurring patterns, geometric simplification fails to maintain symmetries and structures and is therefore not well suited as an abstraction method. Nevertheless, it has the big advantage that it always yields a complete representation of the underlying scene automatically, irrespective of whether it can interpret the scene or not. Therefore, it is desirable to combine its strengths with global semantic analysis which is able to identify important feature edges and corners in order to get the best of both worlds.

One way to have simplification respect the overall shape is via accordingly designed constraints. For this approach care must be taken that the constraints achieve the desired feature preservation and that they do not limit the effectiveness of the simplification.

In the following we will first discuss a very general method to automatically add semantically motivated metainformation to the input data. Then, we deal with how these data are used as constraints during simplification.

5.1 *Edges & Corners*

In this work, we propose to use primitive shapes to detect important edges in the height data. The reason a shape-based detection is preferred over more traditional methods such as Laplace edge detection is that the shape detection can handle outliers and noise in a robust fashion and has a more global notion of structure (i. e., based on connected components of parts with equal curvature), which enables it to detect edges reliably comprising a wide angle between two primitives, e. g., on top of a shallow roof.

As a first step, we employ the shape detection described in (Schnabel et al. 2007). As it operates on 3D point-clouds, the input height-field is first converted to 3D by insertion of additional points at discontinuities in the 2.5D data (e. g., for facades). We use the same sampling density for this vertical upsampling as in the planar domain, in order to maintain a close relation between the number of samples and surface area. The resulting point-cloud $P = \{p_1, \ldots, p_N\}$ is partitioned into subsets S_i associated to shape primitives Φ_i (i. e., planes, spheres, cylinders, cones and tori) as well as a single subset R containing any remaining points that could not be assigned to a shape for the given parameters. In order to ensure heuristically that only parameterizable patches are created, a point is considered compatible if its Euclidean distance to the shape is within a given distance threshold and its normal does not deviate from the respective shape normal by more than a given angle threshold. After removing the compatible points, the algorithm is restarted on the remaining points until no more shapes can be found for the given set of parameters.

For details on the efficient probabilistic RANSAC-based algorithm we refer to the original work, we only want to emphasize here that there are parameters which allow us to select what kind of shapes are considered valid and therefore define a low-level interface to the interpretation of the data (e. g., surface area). If wanted also more complex parameters (e. g., neighboring shapes, shape orientation) can be used to decide whether the shape is important or not (cf. Schnabel et al. 2008) or the results can be cross-validated against cadastral data. But as we aim at a high level of automatism and generality we will work with the inherent data and few parameters if possible.

In our setting, we define vertices of the DSM to be edge points if they are close to

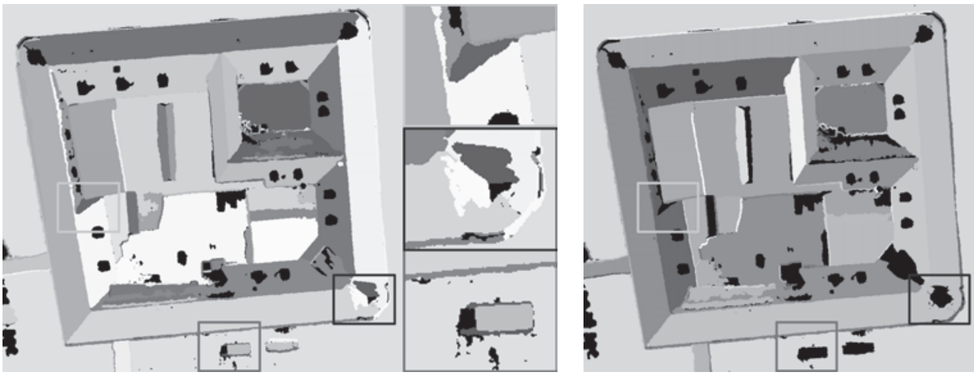

Fig. 1: Shape detection results with 4 m² (left) or 16 m² (right) size thresholds. Intensities are random, black means no shape detected. The middle column shows close-ups of a small part of the roof, a large dormer and a truck, which are no longer present in the 16 m² detection result.

two different shape primitives. Points that are close to even more primitives are classified as corner points. For closeness again we use a distance threshold ε, but this time we do not measure to the ideal shape but its points. That is, a point is close to Shape j if it is within ε distance of any of the points from S_j. In order to identify all edge and corner points efficiently, the point-cloud P is sorted into an axis aligned 3D grid. Then for all grid cells that contain points belonging to different shapes, the contained points' distances are compared to ε and a counter is increased for each potentially different assignment. In order to avoid discretization dependencies due to the location of the grid cells, we use eight translated versions of the grid, corresponding to the eight corners of a cube. Given the distance threshold ε, the width of the cells is set to ε and shifted versions of the grid are created with an offset of ε/2 along the respective axes. Cells are stored in a hash table, so that memory is only allocated for occupied cells. However, in order to get most out of the semantic constraints it is valuable not only to classify edges and corners, but to keep the whole information to which shape each point corresponds. This additional information will be used to not restrict simplification in the presence of features blindly, but to guide which of the possible combinations of features are allowed. This information is stored in an additional raster of shape-IDs, which is read along with the height field during simplification.

5.2 *Constrained Simplification*

In order to respect and maintain the shape information of the vertices, we pose an additional constraint to each collapse candidate during validity check (see sec. 4): The vertex which is about to collapse must ensure that its set of shape-IDs is a subset of the shape-IDs of its collapse partner.

That this simple rule maintains the vertex' shape-IDs is obvious, but how does it help in maintaining features? The principle is that a vertex, once it collapsed to a corner or edge, cannot move away from there, as it can only move along the feature. So, as the IDs are globally unique and each two planes share only one line (cf. Section 6 for discussion of non-planar shape primitives), this approach guarantees that every corner and every edge as defined by the shape-map is maintained.

But whenever a feature edge is not detected along its whole extent, or is not enclosed by two corner features, it might collapse to a single point, which is of course not the desired representation. This case occurs very often due to the presence of noise and occlusions and because of the incomplete shape segmentation. In digital surface models, this is probably the default case. In order to cope with that situation, we suggest the use of additional topological constraints. We define border vertices of a shape as those vertices which have one incident edge pointing to a vertex that is not in the same shape. Such vertices are not allowed to move inside the shape, but may only collapse to neighboring border vertices. This constraint can be checked by looking at the shape-IDs of the two tip vertices of the incident triangles. One of these must be outside of the shape if the collapse takes place at the border. As opposed to labeled edge vertices, this criterion does not allow finding a low-error approximation within a defined small range in the proximity of the hypothetical intersection, but the purpose of maintaining the border is served and still effective complexity reduction along the border is possible.

Now there remains one situation in which detected features still might degenerate, namely if two edges of the same shape do not meet in a common corner but are connected via a series of border vertices. As the collapses along each of the two edges are legitimate, they may again collapse to their next corners respectively introducing an unwanted shortcut edge. We deal with this problem by detecting the implicit corners defined as those edge vertices which only have one neighboring border vertex with respect to one of their shapes. Implicit corners are then treated as corners and may not be collapsed to other vertices unless they are of the same corner type.

6 Results

We tested the proposed methods on a 256 m × 256 m part of a highly detailed digital surface model of downtown Berlin, featuring complex buildings at an input resolution of 12.5 cm (resampled from the 7 cm resolution dataset courtesy of DLR). The original heightmap therefore contained 4.2 million vertices. After adding the façade points, the point-cloud had more than 11 million points. The shape detection took 197 sec. and resulted in 1,658 planes larger than 4 m^2 and 695 planes larger than 16 m^2.

The resulting segmentations are depicted in Fig. 1. The small borders around the buildings are no artifacts but belong to the façades which are not represented in 2.5D. Now we performed geometric simplification

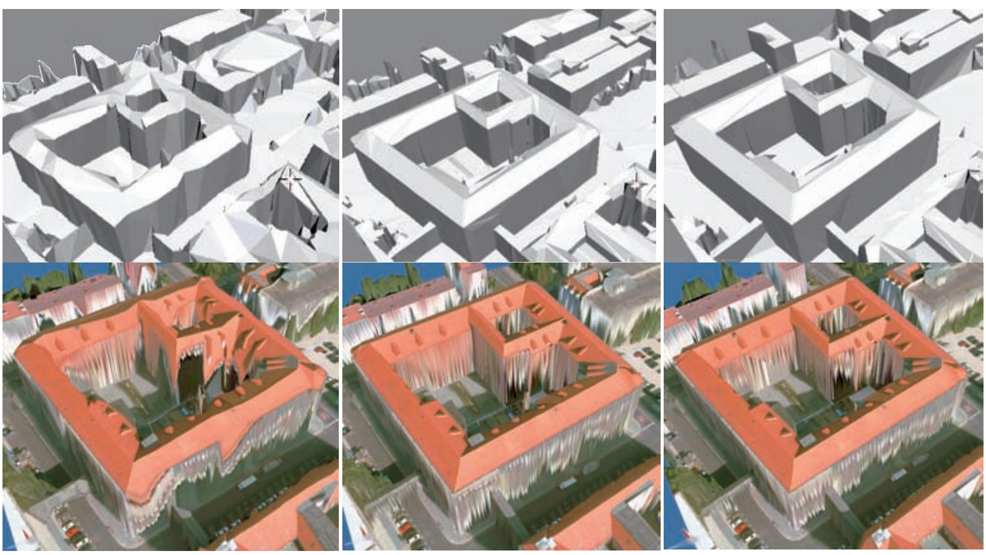

Fig. 2: Simplification results. Left column: unconstrained, 4 m threshold. Middle column: constrained, 4 m threshold. Right column: constrained, 32 m threshold. The upper row shows the shaded TIN whereas the lower row shows a rendering textured with full 12.5 cm resolution.

with exactly the same algorithm but either using a map of shape-IDs or not. Without shape-IDs the simplification of the 4.2 million vertices took 266 sec. and resulted in 2172 vertices, with the constraints it took 291 sec. and resulted in 7493 vertices. Fig. 2 shows the resulting models. The leftmost column of Fig. 2 shows the results at an error threshold of 4 m without additional constraints. Even the huge gable roofs look already scrambled, the small chimney in front turned into a strange looking peak and also on the flat roofs in the background we see some disadvantageous collapse artifacts. Texturing this model (lower row) reveals the spatial inaccuracy of the feature edges. That is definitely not what we would expect from an abstracted model, even though from a distance where a pixel projects to about 4 m it will be almost indistinguishable from the original.

In the middle column we see which difference the constraints make here. Geometric error is the same, but all collapses trying to demolish feature edges were inhibited. A lot of features, which are significantly smaller than 4 m and hence missing in the leftmost mesh are still present in the data, e. g., the glass roof in the courtyard or the chimney are reasonably represented. The textured rendering reveals the high positional accuracy of the feature edges which is due to the small ε threshold used during point classification. This effect becomes even clearer when we look at the rightmost column of Fig. 2. As the whole patch is only little more than 30 m high, distance threshold 32 m means collapse everything you can. So, every feature which is still there is there due to the shape-IDs it has.

7 Conclusions

We proposed a robust way to derive feature edges and corners from highly detailed digital surface models. Such constraints can be easily integrated into a Hausdorff distance simplification framework. Adding topological shape constraints and inhibiting collapse-vertex placement makes the resulting mesh strictly following the prescribed edge features, while still simplifying along these edges. Since the features are defined using a low-level shape detection, we are able to preserve the shape of very complex roof structures and buildings without having a specialized model of them. If a semantic annotation was added, the resulting geometry could be directly exported into a high-level format as CityGML.

Directions of future work will include a better support for curved features, such that there also the positional accuracy is independent of the global error threshold and also refining the definition of shapes, such that they approximately match existing concepts of semantic LODs. As the results in Figure 2 revealed that, the resulting triangulation is in some places even less complex than the pure geometric simplification, we will also try to improve the concept of shape such that vegetation and point-cloud artifacts do not lead to additional constraints.

Acknowledgements

We thank DLR – Institute of Robotics and Mechatronics for providing us the high-detailed Berlin dataset. This work was funded by the German Research Foundation DFG as a part of the bundle project "Abstraction of Geographic Information within the Multi-Scale Acquisition, Administration, Analysis and Visualization".

References

Agarwal, P.K. & Suri, S., 1994: Surface approximation and geometric partitions. – Proceedings of the SCCG (5th ACM-SIAM Sympos. On Discrete Algorithms): 24–33.

Cignoni, P., Rocchini, C., Montani, C. & Scopigno, R., 2003: External memory management and simplification of huge meshes. – IEEE Trans. on Vis. and Comput. Graph. **9** (4): 525–537.

Cignoni, P., Rocchini, C. & Scopigno, R., 1998: Metro: Measuring error on simplified surfaces. – Computer Graphics Forum **17** (2): 167–174.

Desbrun, M., Meyer, M., Schröder, P. & Barr, A. H., 1999: Implicit fairing of irregular meshes using diffusion and curvature flow. – In Computer Graphics (SIGGRAPH) **33:** 317–324.

El-Sana, J. & Yi-Jen, C., 2000: External memory view-dependent simplification and rendering. – Computer Graphics Forum **19** (3): 139–150.

Garland, M. & Heckbert, P., 1997: Surface simplification using quadric error metrics. – Computer Graphics (SIGGRAPH) **31:** 209–216.

Garland, M. & Shaffer, E., 2003: A multiphase approach to efficient surface simplification. – In IEEE Visualization: 117–124.

Guthe, M., Borodin, P. & Klein, R., 2005: Fast and accurate Hausdorff distance calculation between meshes. – Journal of WSCG **13** (2): 41–48.

Hildebrandt, K. & Polthier, K., 2004: Anisotropic Filtering of Non-Linear Surface Features. – Computer Graphics Forum **23** (3): 391–400.

Hoppe, H., DeRose, T., Duchamp, T., McDonald, J. & Stuetzle, W., 1993: Mesh Optimization. – SIGGRAPH: 19–26.

Hoppe, H., 1996: Progressive meshes. – Computer Graphics (SIGGRAPH) **30:** 99–108.

Hoppe, H., 1998: Smooth view-dependent level-of-detail control and its application to terrain rendering. – IEEE Visualization: 35–52.

Isenburg, M., Lindstrom, P., Gumhold, S. & Snoeyink, J., 2003: Large mesh simplification using processing sequences. – IEEE Visualization: 465–472.

Klein, R., Liebich, G. & Straßer, W., 1996: Mesh Reduction with Error Control. – IEEE Visualization: 311–318.

Kok-Lim, L. & Tiow Seng, T., 1997: Model simplification using vertex-clustering. – Symposium on Interactive 3D Graphics: 75–82.

Lindstrom, P., 2000: Out-of-core simplification of large polygonal models. – SIGGRAPH: 259–262.

Lindstrom, P. & Silva, C., 2001: A memory insensitive technique for large model simplification. – IEEE Visualization '01: 121–126.

Popovic, J. & Hoppe, H., 1997: Progressive simplicial complexes. – SIGGRAPH '97: 217–224.

Rossignac, J. & Borrel, P., 1993: Multi-resolution 3D approximations for rendering. – Modeling in Computer Graphics: Methods and Applications. Springer: 455–465.

Schnabel, R., Wahl, R. & Klein, R., 2007: Shape Detection in Point Clouds. – Computer Graphics Forum **26** (2): 214–226.

Schnabel, R., Wessel, R., Wahl, R. & Klein, R., 2008: Shape Recognition in 3D Point Clouds. – WSCG '2008 Full Papers: 65–72.

Schroeder, W., Zarge, J. & Lorensen, W., 1992: Decimation of triangle meshes. – Computer Graphics (SIGGRAPH '92) **26:** 65–70.

Taubin, G., 1995: A signal processing approach to fair surface design. – SIGGRAPH '95: 351–358.

Vorsatz, J., Rössl, C. & Kobbelt, L. & Seidel, H.-P., 2001: Feature Sensitive Remeshing. – Computer Graphics Forum **20** (3): 393–401.

Wu, J. & Kobbelt, L., 2003: A stream algorithm for the decimation of massive meshes. – In Graphics Interface: 185–192.

Address of the Authors:

Dipl.-Inform. Roland Wahl, Dipl.-Inform. Ruwen Schnabel, Prof. Dr. Reinhard Klein, Universität Bonn, Institut für Informatik II, AG Computergrafik, D-53117 Bonn, Tel.: +49-228-73-4146 (Wahl), 4122 (Schnabel), 4201 (Klein), Fax.: +49-228-73-4212, e-mail: wahl | schnabel | rk@cs.uni-bonn.de

Manuskript eingereicht: Dezember 2007
Angenommen: März 2008

Photogrammetrie • Fernerkundung • Geoinformation 3/2008, S. 217–225, 5 figs.

Integration of Language in GIS: Models in Ownership Cadastre and Disaster Management

Christian Lucas, Marina Mueller & Hans-Peter Bähr, Karlsruhe

Keywords: Disaster Management, Data Modeling, Abstraction, Knowledge Representation

Summary: This paper discusses relevant aspects of interrelationships between graphically and verbally represented information. The research is focused on both ways of transformation – from textual to graphical information and from graphical to textual information – with respect to automation. Analyses based on examples of *Boundary Descriptions of the Brazilian Ownership Cadastre* as well as *Communication Systems in Disaster Management* are presented. Due to the various levels of detail of given attributes, the textual representation contains various abstraction levels. Such experiences are implemented in terms of data modeling and processing.

Zusammenfassung: *Integration von Sprache in GIS*: Modelle im *Eigentumskataster und Katastrophenmanagement*. Dieser Beitrag präsentiert theoretische Untersuchungen zur Verarbeitung graphischer und sprachlicher Zusammenhänge. Den praktischen Hintergrund dieser theoretischen Ansätze lieferten zum einen die verbalen *Grenzbeschreibungen des brasilianischen Katasters* und zum anderen die verbal ausgerichteten *Kommunikationssysteme im Katastrophenmanagement*. Dabei zeigte sich, dass die textuell repräsentierte Information auf Grund der verschiedenen Detaillierungsgrade der Beschreibung verschiedene Abstraktionslevel bedingt. Dies wurde speziell bei der Modellierung der Wissensbasis berücksichtigt.

1 Background

1.1 *The Necessary Step from ''Real World'' to a Symbolic Level*

Language in written or spoken form is certainly the most important medium for human communication. Therefore, language represents a very important factor in GIS, too. The formal neighborhood of language to the GIS domain and to image analysis is proven by many metaphors taken from linguistics and transformed to geospatial descriptions. These are for instance *context, understanding, redundancy, completeness*, or *abstraction*. The listed examples, which may be completed, reveal a semantic neighborhood of verbal and graphical descriptions of our environment. The presented paper does not give a contribution for automatic language recognition but aims to show how to integrate verbal or written language into formal spatial models. This task is basically of the same nature as data fusion. Textual processing together with images or maps requires as a necessary first step the transformation of data from the iconic (or *verbal*) level to a symbolic level.

This scenario is formally presented in Fig. 1. Images, maps and text to be fused are taken from a ''real world'' which cannot be captured directly by human cognition. However, its transformation yields images, maps or texts, according to specific tools applied. On the iconic or verbal level which is directly accessible by humans, numeric processing or fusion is impossible. In order to do so, a second transformation to the so-called symbolic level is necessary which ends up with a formal representation of the three

1432-8364/08/2008/217 $ 2.25

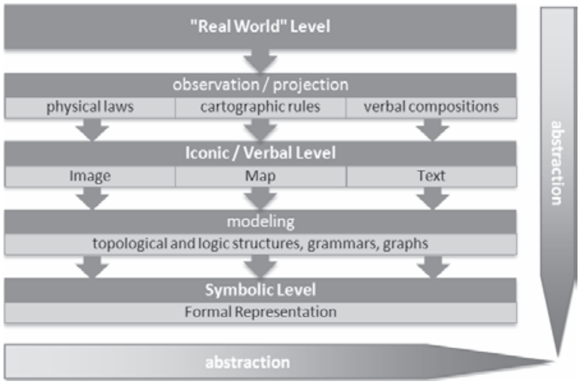

Fig. 1: Levels of knowledge representation from the ''real world'' to a formal representation.

mentioned components image, map and text. The step from iconic to symbolic is called *modeling* and may be performed by very different tools like topological and logical structures, grammar and graphs. The result is a closed formal knowledge representation at a high level of abstraction, an ontology[1], respectively.

Both steps, from real world to formal representation as well as from image to text increase the level of abstraction. In consequence images are closer to reality than texts and pictorial, cartographic or textual representations are closer to human perception than e. g., a semantic network used for modeling. Therefore, integration of text into geospatial data sets necessarily includes components of data abstraction.

1.2 *Introduction of two Applications*

A straightforward application where the intimate interrelation of language and maps can be observed is way finding or navigation. This has already been widely recognized (Tversky 2003). Another topic related to this application is the description of borders used in ownership cadastres, where borders of parcels may be considered as a navigational task, i. e., a path to be followed. Thus the research is focused on the *Brazilian ownership cadastre*. Legal validation of the ownership in Brazil is primarily verbal and not based on coordinates or a similar graphic representation, however the available data consisted of descriptions and accompanying maps. The verification of consistency between both levels, graphic and verbal, gives a sound example for combining graphs (maps) and language (text) together in the context of practice.

The research topic *Communication Systems in Disaster Management* focuses on transformations of verbal descriptions in German language concerning the status and location of disaster events. Aim is to represent such information automatically and up to date by a GIS. During disaster events, the emergency operations center (EOC) receives hundreds of textual reports from damage sites, given by several on-site units and passer-by. The information of all reports needs to be evaluated as soon as possible by an operator of the EOC and added into a situation map that serves for information sharing as well as a basis for decision making.

2 The Abstraction Levels

2.1 *Abstraction Levels of Textual Descriptions in the Brazilian Ownership Cadastre*

Current texts in the Brazilian rural ownership cadastre are formulated very precisely in general. Such accurate texts are generated

[1] The term ontology is defined as an explicit specification of a conceptualization (Gruber 1993).

by surveys where coordinates of a starting point and the complete polygon of the boundary with length and angle of direction for each line are measured as exactly as possible. Due to missing standards for texts of the Brazilian land register up to the year 2001, levels of detail and styles of older descriptions vary strongly depending on the author of the cadastral text. These texts cannot be assigned to a single level of abstraction, as assumed at the beginning of the research. Various geometrical attributes (e. g., distance *and* direction) of *one* boundary as well as a single attribute (e. g., distance *or* direction) of *some* boundaries correspond to different levels of detail as well as different levels of abstraction. Within the explicit knowledge representation (here an ontology) the abstraction hierarchies are integrated so that all occurring combinations of geometric attributes are considered. Due to the intended transformation from textual to graphical representations, the abstraction hierarchy is based on transformation aspects of necessity and uncertainty. Thus the transferable information always corresponds to one of the four derived hierarchical levels of geometric attributes:

- none/general knowledge: All necessary information for interpreting a single boundary attribute is readily available by the text passage. Example: *It begins at point 01 with the geographical coordinates N = 7.734.679,703 and E = 248.328,107.*
- context dependent knowledge: Information which is given for a single attribute cannot be reconstructed independently because of included references to already given information within the textual description. Example: the direction of the previous edge is essential to handle phrases like *from here it turns left for 30°.*
- external sources: Information include references to objects or spatial attributes which has to be acquired from external sources. Example: the course of the river is essential to handle phrases like *it runs along the river for a length of 162 m.*
- all/new acquisition: Usable information is completely missing and has to be acquired on site. Example: *the area extends in depth as far as the cows graze.*

More detailed explanations for the Brazilian land register as well as the abstraction levels appearing in texts are in (Mueller 2008).

2.2 *Abstraction Levels of Reports in the Domain of Disaster Management*

The format of reports in the domain of disaster management is different to the descriptions of the Brazilian land register. Disaster reports, given by on-site units and passer-by, consist of fixed entries, e. g., for time stamps, sender and receiver, as well as a free-form text element where current information can be given in natural language. The report templates usually contain for a representation in a situation map both, information about relevant facts like the damage sites including its spatial references and also information about irrelevant facts for visualization like the resources, which has to be separated. This is in contrast to the cadastral descriptions were all the given information are relevant. The level of detail of information and thus the level of abstraction vary as well because of the different reporting persons. Consequently the subdivisions of the main abstraction levels for a disaster management application were adopted from the Brazilian cadastre application. However the characteristic of the levels of abstraction is adjusted as follows:

- none/general knowledge: All necessary information for interpretation of a single fact is given by the report. This case is possible but implausible because practically no-one uses coordinates for reporting a disaster event.
- context dependent knowledge: The given fact cannot be interpreted independently because it refers to previous reports. Example: to handle the reported fact *at the accident are 3 injured people*, information about the existent accident is essential.
- external sources: The reported fact include references to objects or attributes which

have to be required from external sources. Example: to handle the reported fact *midland school is burning*, the location and function of buildings, here the midland school, are essential.

- all/new acquisition: The reported fact is not processible. Example: *a few minutes ago, I have heard something anywhere*. Acquisition on-site is usually difficult because of missing references.

A basic difference to the cadastral application is the "segmentation" of facts from a report as well as the autonomous processing of facts. This is already a result of the separation of relevant facts, but also a simplification. In consequence of this approach a single fact occupies only a single abstraction level. The successive arriving reports usually deal with different facts from different disaster sites. Nevertheless there are necessary references to already given reports, which have to be considered.

3 Semantic Augmentation and Knowledge Representation

3.1 *Common Symbolic Representation*

There are a number of tools supporting an explicit modeling of domain knowledge such as rule based systems or semantic networks. Different systems are often equivalent concerning their abilities to model different types of information and to draw conclusions from it. Therefore, the decision for one or the other tool depends on e. g., the form of explicit knowledge representation that is preferred (rules, networks) and the kind of tools that the knowledge engineer is familiar with (Sowa 2000). In the current application, a semantic network is chosen. Fig. 2 shows an example excerpt of a possible semantic network for the cadastre and disaster scenario that can be realized e. g., by tools such as Protégé (Protégé 2007).

Since both data sources, texts and maps, are supposed to include similar spatial and attribute information, they can be modeled with similar structures on the level that is displayed in Fig. 2. However, explicit geometric information is more relevant in a map representation than in a textual description. First differences become already visible at the displayed level of detail on closer examination of the data model. Each object node is modeled according to the frame-model by Minsky (1975) using a frame with different slots, i. e., characteristic attributes for each object. Fig. 3 shows cadastral examples for the frames boundary-part-in-text and boundary-part-in-map. Besides information that is identical for both frames (neighbor), other attributes such as the length of a boundary include different semantics for each source of information. The text refers to the length value of boundary parts which can be measured in a field survey. In the case of the map, this length value is included in written

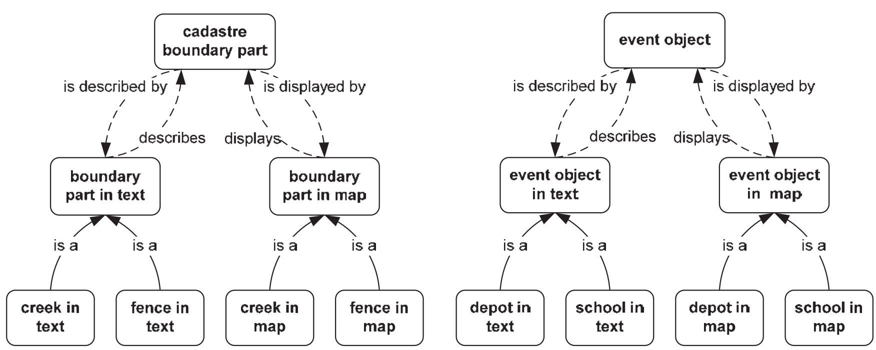

Fig. 2: Excerpt of a semantic network for the cadastre example (left) and a similar disaster example (right).

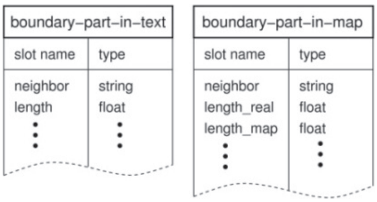

Fig. 3: Boundary-part-in-text and boundary-part-in-map of the semantic network.

numbers close to the drawn line. Additionally, this drawn line has its own length resulting from the scale of the map and from the precision in drawing.

3.2 *Knowledge Representation for an Application of the Brazilian Ownership Cadastre*

Basis for a transformation from texts into maps is the knowledge how textual phrases about geometrical information have to be interpreted in terms of discrete values in the context of the Brazilian ownership cadastre. While e. g., directional information like *an azimuth of 328.2°* can be directly used for map drawing, phrases like *turn slightly left* will give an interval of possible degree values. The ontology that describes how geometrical information is represented in texts of the Brazilian cadastre naturally contains the basic geometrical elements (points, lines with direction and length) and their typical relations such as *a line consists of two end points*. However in order to capture also the uncertainty that is connected with the texts, indicators of uncertainty – e. g., the use of quantifiers such as *slightly* – needed to be identified in the text corpus and integrated (including a quantification of the qualitative expression) at the associated level of abstraction of the affected geometrical attribute.

3.3 *Knowledge Representation for Communication Systems of the Disaster Management*

For the specific representation of knowledge existing data models offer a good starting point for developing ontologies. Such standardizations for the disaster management domain are given by the Emergency Data Exchange Language (EDXL) and the Common Alerting Protocol (CAP). Unfortunately, these data models are primarily oriented on the management of disaster resources. A detailed comparison of the diverse data models are given by Werder et al. (2006). It turned out that the NATO standard for military interoperability, the *Command and Control Information Exchange Data Model* (*C2IEDM*), satisfies in most instances the requirements of disaster management and provides a good basis for the development of the *Disaster Management Data Model* (*DM^2*). Because of focusing on information storage, retrieval and processing, there are a couple of differences between DM^2 and C2IEDM. Therefore, one of the most obvious changes is the philosophy of object representation. The focus of the domain specific ontology is on modeling the spatial aspects of objects. In this manner the common spatial attributes of objects are the location as well as geometric attributes of form, size and feature alignment. These elementary attributes, traditionally supported by spatial ontologies and geographical information systems (GIS), describe discrete objects unambiguously by their dimension and location in space. In order to support a spatial reasoning process for disaster events based on textual descriptions, a more comprehensive level of spatial information is necessary. The method of object modeling within the ontology has to be similar to the mental model of the reporting person (Frank 1998). This mental model contains, besides discrete objects, spatial scenes with interactions of two or more spatial objects in the meaning of neighborhoods or part-of-relations like include, overlaps or tangent. Such detailed information level is essential for analyzing e. g., coherences of cities, districts, damage sites and operation areas. Furthermore, time is modeled explicitly in the DM^2 as well as the mutable attributes of the objects. Mutable attributes in terms of object modeling are state and location. Such dynamic aspects are modeled by asso-

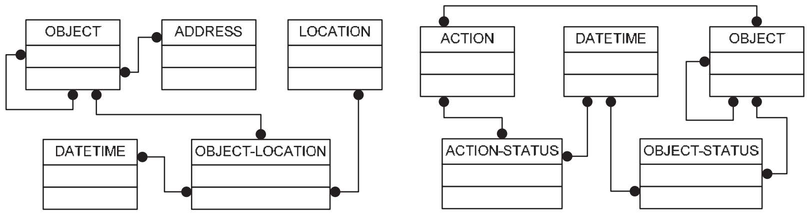

Fig. 4: Associations of Object, Location and DateTime (left) as well as the associations of Action, DateTime and Object (right) – in IDEF1X notation.

ciations of the relevant classes (cf. Fig. 4). In the DM^2 this was done by creating tuple of *object-state-time* and *object-location-time*. The concept as shown in Fig. 4 is explained in more detail in (Lucas et al. 2007).

4 Results

4.1 *Results of the Application of the Brazilian Ownership Cadastre*

Generating Maps from Texts: Assuming a precise text that contains (a) a starting point with precise coordinates and (b) boundaries as straight lines with precise direction and length, a transformation to a map representation is simple. Necessary additional definitions for such a transformation are the desired *scale of the map, orientation of the map and local map coordinates of the starting point*.

Conversion of coordinates and length information of the text into map coordinates can be done by using straightforward mathematical computations. Saving the generated map information in widely used standards such as XML (Extensible Markup Language) allows its graphical visualization with different tools (e. g., ArcGIS from ESRI). Fig. 5 shows an example of an automatically generated map and its corresponding original map. Although the general outline of the boundaries is identical, the generation of the new map reveals that the north arrow of this otherwise very precise original map deviates about 15 degrees from the true northward direction. Such variations of the north arrow within maps of the Brazilian land register are not unusual because of inaccuracies of observation.

If the text is vague, with unknown references and missing essential boundary information, the generation of maps usually requires additional sources of information (maps of neighboring real estates, topographical maps, or remote sensing data such

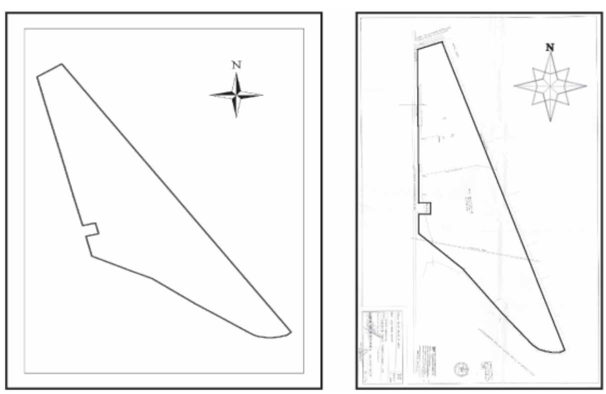

Fig. 5: Automatically generated map from a precise text (left) and the cadastral map (right).

as aerial images). However, vague sketch maps are often useful to give a first overview of the actual information provided in texts and even vague texts include constraints, such as

- length of each boundary part or
- end point of the description = starting point of the description.

Additional to such constraints, a reasonable quantification of qualitative expressions (e. g., left / right) and further heuristics (such as typical errors in descriptions) can be used to generate maps even from texts with incomplete information (MUELLER 2008).

Generating Texts from Maps: Besides geometrical information given as drawn lines, boundary parts in maps of real estates include further attributes. Such attributes are the type of the boundary part displayed by the special type of line drawing as well as directly given information like length and direction of the real boundary part as written text in the map.

Given a precise map with detailed attribute values, the generation of a text only requires the definition of (a) a starting point and (b) the direction of description (clockwise/ counterclockwise). Topological information such as connectivity between boundary parts can be modeled in the semantic network. This information can be directly used to deduce the succession of boundary parts in the description.

In case a map is only a sketch of the real situation, such a vague map can nevertheless be transferred to a vague text where relative relations between boundary parts are expressed by relative textual information. In order to generate a text from a vague map, a starting point has to be chosen and to be described as meeting point between neighboring real estates. Similar to the generation of a precise map, the direction of the description (clockwise / counterclockwise) has to be decided.

4.2 *Results of the Application of the Disaster Management Domain*

For processing, a computational representation of the reported information is needed. A standard formalism of computational linguistics for representing extracted information is the *typed feature structure*. These typed feature structure is an XML-representation (Extensible Markup Language) of the relevant information. Here, the extraction was done by an operator, who has to register the relevant information into the graphical user interface (GUI, an input mask for the domain requirements) and the application generates the XML.

Reports of the disaster management domain in general include temporal uncertainties as well as semantic and spatial ambiguities. By explicit modeling of temporal aspects in the DM^2 (cf. Section 3.3), a basis for both, historiography and temporal reasoning are given. Temporal reasoning provides a possibility for solving ambiguities by using interval algebra[2] and allows building up a temporal context. This temporal context is focused on searching for events which take place in the same frame in time. Detailed considerations of domain specific temporal logic are given by WERDER et al. (2007). Semantic ambiguities are amongst others a result of alternative (*Fußballplatz* vs. *Bolzplatz*), multiple (*Bahnhofstraße*, exists 3 times) and abstract (*church* without specific name) object denotations and can be limited or solved by a-priori knowledge, given by the DM^2. In consequence of the diversity of this task, collecting as well as modeling of such background knowledge is very comprehensive and complex. Spatial ambiguities are an effect of using adverbial phrases and spatial identifiers. Such terms like *behind* or *north* of are already given by descriptions of spatial scenes within the reports. Because of the diverse types of ambiguities different approaches for reducing and solving are necessary.

[2] Here the interval algebra of (ALLEN & FERGUSON 1994) is used.

One method for solving is using context knowledge based on the reports. Initial situation for processing is a range of reports describing one or maybe more events[3]. First indicator of dependence between diverse reports and their facts is the time frame of receiving. Thus the first context is a temporal one. Next point of interest for processing and basis for creating a further level of context is the location. If compatible events like a *cloud of gas* and an *explosion* are at the same frame in time and close to each other, coherence is probable. Proximity for creating a local context is possible by the introduction of the so-called event horizon, which defines the sphere of influence of a specific event. This sphere of influence depends in shape and size on the reported fact. According to that approach, the reported facts are related whenever their event horizons overlap. This location context now offers possibilities to analyze and evaluate the reported facts. In this knowledge based reasoning process the reported facts are first evidences for a respective event, a so-called hypothesis. The reasoning is made possible by defining conditions and relations between them. These basic relations are $A \wedge B$, $A \vee B$ and $A \rightarrow B$ which are quite simple relations but adequate for representing the important dependences. Such dependences are for example, *gas* $\wedge$ *explosion* $\rightarrow$ *fire*. Furthermore the relations are complemented by a certainty factor which represents a weighting for evaluation. That way the credibility of a fact respectively the credibility of the reporter can also be considered. Result of this reasoning is an array of possible events including an evaluation. For the above-mentioned example of the gas and the explosion, the possible hypotheses are the events *fire*, *toxic cloud* and *building damage*. Detailed explanations of this procedure are given by (LUCAS et al. 2007).

[3] According to definition, an event relates to just one object.

5 Conclusions and Outlook

Due to the various levels of detail for spatial attributes within descriptions of spatial scenes, four levels of abstraction were defined for an application of the Brazilian ownership cadastre. These levels allow processing of spatial phrases under considerations of the inherent uncertainty. For processing, an adequate representation of knowledge is also necessary, especially for including context dependent as well as external knowledge. For a disaster management application, the levels of abstraction were adapted from the cadastral application and adjusted to the domain requirements. The verbal representation of the facts demands the use of complex structures of knowledge modeling and representation, as given by ontologies. For a more robust spatial reasoning process the linguistic vagueness and the mental model have also to be taken into account. Furthermore the area of validity for the spatial identifiers has to be represented exactly by a weighting function e. g., by fuzzy logic.

Acknowledgements

The research was sponsored by the Deutsche Forschungsgemeinschaft (DFG), project no. BA 686/16. Moreover, this work was supported by Stefan Werder (Collaborative Research Center 461).

References

ALLEN, JF. & FERGUSON, G., 1994: Actions and Events in Interval Temporal Logic. Journal of Logic and Computation. Special Issue on Actions and Processes **4** (5): 531–579.

FRANK, A., 1998: Formal models for cognition – taxonomy of spatial location description and frames of reference. – Spatial Cognition: An Interdisciplinary Approach to Representing and Processing Spatial Knowledge, LNAI 1404, Springer: 293–312.

GRUBER, T-R., 1993: A Translation Approach to Portable Ontology Specifications. Knowledge Acquisition, Volume **5** (2): 199–220.

LUCAS, C., WERDER, S. & BÄHR, H.-P., 2007: Information Mining for Disaster Management.

– International Archives of Photogrammetry, Remote Sensing and Spatial Information Science **36** (3): 75–80.

MINSKY, M., 1975: A framework for representing knowledge. – The Psychology of Computer Vision, McGraw-Hill, New York: 211–277.

MUELLER, M., 2008: Transformations of Cadastral Descriptions with Incomplete Information into Maps. – Transactions in GIS **12** (1): 83–101.

PROTÉGÉ, 2007: Homepage, protege.stanford.edu (last visited: December 2007).

SOWA, J.-F., 2000: Knowledge Representation: Logical, Philosophical and Computational Foundations. – Pacific Grove, Brooks/Cole, CA.

TVERSKY, B., 2003: Navigating by mind and by body. – Spatial Cognition III: Routes and Navigation, Human Memory and Learning, Spatial Representation and Spatial Reasoning, Springer: 1–10.

WERDER, S., MUELLER, M., MUELLER, M. & KÄMPF, C., 2006: Integrating Message Information into Disaster Management Maps: Transferability of a System of the Military Domain. – ISPRS Symposium on Geospatial Databases for Sustainable Development, Goa, India, on CD.

WERDER, S., LUCAS, C. & BÄHR, H.-P., 2007: Information Extraction from Messages in Disaster Management. ISPRS Symposium on Geoinformation for Disaster Management, Toronto, Canada, on CD.

Addresses of the Authors:

Dipl.-Ing. CHRISTIAN LUCAS, Prof. Dr.-Ing. habil. Dr. h.c. HANS-PETER BÄHR, Universität Karlsruhe, Institut für Photogrammetrie und Fernerkundung, Kaiserstrasse 12, 76128 Karlsruhe, Tel.: +49-721-608-2315, Fax.: +49-721-6088450, e-mail: christian.lucas | hans-peter.baehr@ipf.uni-karlsruhe.de

Dr.-Ing. Marina Mueller, COMSOFT GmbH, Wachhausstrasse 5a, 76227 Karlsruhe, Tel.: +49-721-79076-84, Fax.: +49-721-79076-89, e-mail: marina.mueller@comsoft.de

Manuskript eingereicht: Dezember 2007
Angenommen: März 2008

Berichtigung

Photogrammetric Measurements in Oblique Aerial Images

von Joachim Höhle im Heft 1/2008

Die Formeln auf Seite 8 müssen richtig heißen:

$\beta_{back} = t + \alpha(back)$ and $\beta_{front} = t - \alpha(front)$

Berichte von Veranstaltungen

7. Oldenburger 3D-Tage

vom 30.–31. Januar 2008

Die siebte Konferenz für „Optische 3D-Messtechnik – Photogrammetrie – Laser-Scanning“ (Oldenburger 3D-Tage) wurde vom 30. bis 31. Januar 2008 an der Fachhochschule Oldenburg veranstaltet. Zu der Veranstaltung hatten Prof. Dr. THOMAS LUHMANN vom Institut für Angewandte Photogrammetrie und Geoinformatik (IAPG) und Prof. Dr. HEINZ-JÜRGEN PRZYBILLA vom Arbeitskreis Nahbereichsphotogrammetrie der Deutschen Gesellschaft für Photogrammetrie, Fernerkundung und Geoinformation (DGPF) eingeladen. Zudem wurde die Konferenz von dem Institut für Mess- und Auswertetechnik und dem Institut für Innovations-Transfer Emden, FH Oldenburg unterstützt. Auch die siebte dieser jährlich ausgetragenen Konferenz wurde wie ihre Vorgängerveranstaltungen durch eine Fachausstellung begleitet.

Die Einleitung übernahm Prof. LUHMANN mit einem Abriss über die vorangegangenen sechs Veranstaltungen. In ihren anschließenden Grußworten betonte die Präsidentin der Fachhochschule Oldenburg/Ostfriesland/Wilhelmshaven, Frau VERA DOMINKE, den hohen Stellenwert der dreidimensionalen Mess- und Auswertetechnik nicht nur an der Hochschule sondern auch für die Region. Sie wies darauf hin, dass dadurch auch ein erheblicher Anteil an der Bewerbung der Stadt Oldenburg für den Titel „Stadt der Wissenschaft“ geleistet wird. Die Konferenz gliederte sich in insgesamt 11 Sitzungen, von denen 10 jeweils parallel zu den Themenschwerpunkten *Dynamische Prozesse, Laserscanning, Mikroskopie, Genauigkeitsprüfung von Laserscannern, Optische Messverfahren, Sensoren, Algorithmen, Anwendungen* und *Bildverarbeitung* abgehalten wurden. Die Vortragsreihe wurde mit dem Beitrag von Prof. NORBERT PFEIFER, TU Wien, zum Thema „*Range-cameras: Kalibrierung und Modellierung in 5D*“ eröffnet. Er zeigte darin auf, dass die aktuellen Entwicklungen in der dreidimensionalen Datenerfassung noch ein hohes Innovationspotenzial besitzen und sich neue Anwendungsperspektiven ergeben.

In zwei weiteren Sitzungen verwiesen die Hersteller auf aktuelle Entwicklungen zu den genannten Themenschwerpunkten und zeigten damit die Ausgewogenheit der Veranstaltung zwischen Forschung und Anwendung auf. Der Veranstaltung wohnten 239 Teilnehmer aus sechs Nationen bei, was auf die Aktualität der Konferenzinhalte und den hohen Praxisbezug der Veranstaltung zurückzuführen ist. Den sozialen Höhepunkt der Veranstaltung bildete das traditionelle Grünkohlessen in der Weser-Ems Halle.

Aus den Sitzungen, die der Nahbereichsphotogrammetrie zugeordnet werden können, ist Folgendes zu berichten:

In der Sitzung *Dynamische Prozesse* wurde die besondere Problematik bei der Vermessung dynamischer Prozesse zur Diskussion gestellt. Die Anwendungen reichten dabei von der Erfassung orthopädischer Laufparameter zur Ganganalyse, über das wasserbauliche Versuchswesen und die Bestimmung von Flugzeuggeschwindigkeiten auf Rollbahnen, bis hin zur Vermessung von Baumpositionen.

Durch den Vortrag über die *Physiologie und Funktion der Retina – Moderne Methoden der Mikroskopie* wurde die Sitzung *Mikroskopie* eingeleitet. Dem Auditorium wurde ein Überblick über das Auflösungsvermögen von konventionellen und kofokalen Mikroskopen gegeben. Mit einem Beitrag zur bildbasierten 3D-Oberflächenrekonstruktion sowie Oberflächencharakterisierung wurde die Sitzung abgerundet.

In der Sitzung *Optische Messverfahren* wurde in dem ersten Vortrag über die Anwendung von 3D-Messtechnik in der dentalen Implantologie berichtet. In dem zweiten Beitrag stand die Verwendung eines Mehrkamerasystems in einer parallelkinematischen Werkzeugmaschine zur Diskussion. Weiter wurde über die flächenhafte 3D-Merkmalsbestimmung an Werkzeugoberflächen sowie von der photogrammetrischen Freiformerfassung aus Bildsequenzen berichtet.

Hinsichtlich aktueller Beiträge im Bereich *Sensoren* wurde über die Evaluierung der Leica „Image Assisted Total Station“ für die konkrete Aufgabenstellung der Oberflächenrekonstruktion, über kabellos handgeführter 3D-Scanner mit WLAN sowie einen Beitrag zur Stabilität digitaler Kameras und zur schnellen, optischen 3D-Untersuchung biologischer Objekte mit Mikrospiegelarrays berichtet.

In den letzten beiden Sitzungen wurden aktuelle Arbeiten zu *Algorithmen* und der *Bildverarbeitung* diskutiert. Die Beträge im Bereich Algorithmen reichen von erweiterten Verfahren zur Mehrmedienphotogrammetrie, automatische Orientierung von zwei Stereokamerasystemen, der 3D-Kartierung mittels Punktwolken bis hin zum Funktionsprinzip der Ensemble-Korrelation. Im Bereich der Bildverarbeitung wurde über aktuelle Forschungsarbeiten zur Risserkennung mittels Neuronaler Netze, der digitalen Echtzeit-Stereobildverarbeitung mit dem DMSoC sowie von Verfahren zur automatischen Auswertung von terrestrischen Laserscannerdaten und einem Mehrkamerasystem zur räumlichen Vermessung von Objektkonturen berichtet.

Die zweite Vortragschiene war überwiegend durch Vorträge zur Prüfung und Anwendung von terrestrischen Laserscannern (TLS) sowie zur Modellierung von TLS-Daten geprägt. Dabei standen zunächst Fragestellungen zur Modellierung, der Sensorentwicklung und dem dynamischen Laserscanning im Vordergrund. Unter dem Thema „*Segmentierung und Datenapproximation von Laserscanneraufnahmen mittels statistischer Methoden*“ wurden vielversprechende Forschungsansätze präsentiert, mit denen zukünftig automatisierte Auswerteprozesse für TLS-Punktwolken ermöglicht werden sollen. In einem Vortrag zum Thema „*Echosignaldigitalisierung und Full-Waveform Processing für terrestrisches Laser Scanning*“ wurde aufgezeigt, dass analog zum airborne Laserscanning auch mit TLS die Erfassung von DGM, DTM und DOM möglich sein wird. Die Verknüpfung von GPS und TLS wurden im Vortrag „*Ein Verfahren zur schnellen statischen Georeferenzierung von 3D-Laserscans*“ und dynamisches Laserscanning unter dem Titel „*Validierung eines TLS-basierten Mobile-Mapping-Systems*“ vorgestellt.

Im Vortragsblock „*Genauigkeitsprüfung von Laserscannern*“ stellten Vertreter einzelner Hochschulen ihre aktuellen Arbeiten auf diesem Gebiet vor. Dabei wurden neben den unterschiedlichen Ansätzen zur Prüfung terrestrischer Laserscanner auch ein Beispiel handgeführter Scanner am Messarm vorgestellt. Die sich dem Vortragsblock anschließende Diskussion zeigte, dass die sehr heterogenen Genauigkeitsdefinitionen seitens der Hersteller eine Vergleichbarkeit der Sensoren für den Anwender stark beeinträchtigt. Des Weiteren wurde der Mangel an einheitlichen Prüfverfahren für TLS herausgestellt, die eindeutige Aussagen sowohl über die Leistungsfähigkeit als auch temporale Veränderungen der Sensoren ermöglichen.

Aus der Diskussion entwickelte sich eine Initiative zur Gründung eines runden Tisches „*Prüfung und Genauigkeit des terrestrischen Laserscanning*“. Die Zielsetzung dieser Initiative ist es, im Konsens zwischen Anwendern, Herstellern und Forschungsinstitutionen eine Vereinheitlichung von Genauigkeitsangaben und aussagekräftigen Prüfverfahren herzustellen. Dazu soll zunächst eine Bestandsaufnahme der aktuellen Aktivitäten erfolgen, um darauf aufbauend eine Harmonisierung und Weiterentwicklung der Verfahren, vergleichbar mit den VDI/VDE Richtlinien 2634, durchzuführen. Die Federführung dieser Initiative wurde den Professoren STAIGER, Leiter des DVW Arbeitskreises 3 „*Messmethoden und Systeme*“ und PRZYBILLA, Leiter des Arbeitskreises Nahbereichsphotogrammetrie der DGPF, übertragen. Weitere Beratungen sind für den Zeitraum Mai bis Juni 2008 sowie eine gemeinsame Zusammenkunft mit Herstellern von TLS-Systemen parallel zur INTERGEO 2008 in Bremen vorgesehen.

Unter dem schlichten Titel „*Anwendungen*“ wurde in einem Vortragsblock das breite Anwendungsspektrum dreidimensionaler Messtechnik zusammengefasst. Darin wurden Anwendungen des TLS in Archäologie und Denkmalpflege vorgestellt, aus der Industrievermessung die Anwendung photogrammetrischer Verfahren zur Inspektion von Drehgestellen bei der Deutschen Bundesbahn gezeigt sowie dynamische Messungen von Flügeldeformationen bei Flugzeugen während des Fluges demonstriert.

In den beiden Vortragsblöcken des Herstellerforums stellten Firmen aktuelle Entwicklungen und Highlights ihres Produktportfolios vor. Darin wurden sowohl neue Sensoren zur 3D-Objekterfassung gezeigt, als auch Einblicke in die Leistungsfähigkeit der Auswertetechnik gewährt, über die sich die Kongressteilnehmer auch vertiefend in der begleitenden Fachausstellung ausgiebig informieren konnten.

Die Veranstaltung bot zusammenfassend einen interessanten Mix aus Forschung, Entwicklung und Anwendungen in der optischen 3D-Messtechnik und einen Einblick in ihr breites, interdisziplinäres Anwendungsspektrum. Durch eine gelungene Zeitplanung wurde den Teilnehmern ausreichend Gelegenheit zum Gedankenaustausch geboten. Da sich die 3D-Messtechnik dynamisch weiterentwickelt, bleibt die Hoffnung, dass auch im nächsten Jahr die Tradition der Oldenburger 3D-Tage fortgesetzt wird.

AXEL WENDT, Hildesheim
HEINZ RUNNE, Dessau-Roßlau

EARSeL SIG Workshop
vom 5.-7. März 2008 in Bochum

Vom 5.–7. März 2008 wurde ein internationaler Workshop der EARSeL Vereinigung (European Association of Remote Sensing Laboratories) an der Ruhr-Universität Bochum veranstaltet. Unter dem Arbeitsthema „*Remote Sensing – New Challenges of High Resolution*“ trafen sich mehr als 70 internationale Wissenschaftler. Eine Neuerung stellte die Tatsache dar, dass gleich vier sog. Special Interest Groups (SIG) an einem Ort zusammenkamen: 3D Remote Sensing, Developing Countries, Radar Remote Sensing und Urban Remote Sensing.

Der Eröffnungsvortrag wurde von RICHARD SLIUZAS vom International Institute for Geo-Information Science and Earth Observation (ITC) in Holland gehalten. Er gab einen fundierten Überblick über das weit gefächerte Spektrum der vier SIGs vor dem Hintergrund der urbanen Planung, speziell der Erfassung von ungeplanten Siedlungen in Entwicklungsländern.

Die ersten parallelen Sitzungen der SIGs 3D und Developing Countries handelten von neuen Möglichkeiten, die der Stereosatellit Cartosat bietet und von der Anwendung hochauflösender Bilddaten zum Monitoring von Prozessen in Entwicklungsländern. Eine Landnutzungsanalyse von Peking auf Basis von ASTER und SPOT Daten und von München mit hyperspektralen Bilddaten folgte in der SIG Urban Remote Sensing. Parallel dazu wurde in der SIG Developing Countries über generelle Kartiermethoden auf Basis hochauflösender Bilddaten referiert und das Monitoring zur Erstellung einer BIO-GEO-Datenbank für den Himalaya vorgestellt. Hyperspektrale Bilddaten sind insbesondere für das urbane Monitoring geeignet, weil sich die vielfältigen Oberflächenmaterialien aufgrund ihrer individuellen Spektren gut differenzieren lassen (SIG Urban RS). Ein multi-sensorales Monitoring von Bangladesh und die Ableitung eines speziellen Armutsindexes aus Fernerkundungsdaten waren Themen der SIG Developing Countries. Die anschließende Sitzung der SIG Radar befasste sich in zwei Vorträgen mit der Analyse von Brücken (insbesondere von Schäden an Brücken), ein weiterer Vortrag stellte den Nutzen von Radardaten zur Abschätzung von Gebäudehöhen vor. Im letzten Vortrag wurde der Test einer Methode zur Verknüpfung von Höhenmodellen aus LIDAR und InSAR dargestellt. Die Genauigkeit liegt derzeit bei etwa 40 % und hat noch Potential zur Verbesserung. Die folgende Sitzung der SIG 3D hatte zwei Vorträge zur 3D-Stadtmodellierung und zum Einsatz von Quickbird Daten in der Verwaltung der Stadt Istanbul, um neu errichtete Gebäude zu detektieren. In der anschließenden Sitzung der Radar SIG wurden erste TerraSAR-X Daten und Ergebnisse der Auswertung auch mit objektorientierten Bildanalysemethoden vorgestellt. Mit der Kombination von TerraSAR-X und optischen Bilddaten durch „Ehlers Bildfusion" eröffnen sich zukünftig neue Möglichkeiten der Visualisierung. Parallel dazu wurde eine SIG Sitzung mit dem Thema Urban Remote Sensing abgehalten und hier Ergebnisse des Langzeitmonitorings der Stadt Graz mit hochauflösenden Bilddaten präsentiert. Die Kombination von multi- und hyperspektralen Bilddaten für eine städtische Veränderungsanalyse wurde gezeigt und abschließend eine neue Methode der Segmentierung und objekt-orientierten Bildauswertung eingeführt. Die Bilddaten der Corona Missionen aus den 1960er Jahren sind heute sehr wertvoll für die Rekonstruktion des damaligen Zustandes (SIG 3D). Im Vergleich mit aktuellen Bilddaten wurde beispielhaft an Corona Daten in mehreren Regionen im Südwesten Deutschlands die Landnutzungsänderung aufgezeigt. Luftbildserien werden in Portugal verwendet, um die Erosion der Atlantikküste zu kartieren. In einer parallelen Sitzung der SIG Developing Countries wurde eine Methode vorgestellt, mit der Bodenerosion in der Ukraine analysiert wird, und abschließend eine Möglichkeit der Erfassung von Malaria Erkrankungen in Kamerun mit dem populären Programm Google Earth vorgestellt. Neben den Vortragsreihen wurden in einer Postersession weitere wissenschaftliche Arbeiten präsentiert.

Das Konzept der parallelen Tagung von vier EARSeL SIGs kann als sehr positiv gewertet werden. So gelang es vielen Teilnehmern, über den Rand der eigenen SIG hinaus auch Einblicke in aktuelle Forschungen von Teilnehmern anderer SIGs zu erhalten. Da die Schnittmenge der vier Themenbereiche naturgemäß groß ist, kann das Konzept der gemeinsamen Tagung den eigenen Horizont nur positiv erweitern und sollte unbedingt in Zukunft fortgesetzt werden.

Der Workshop wurde von einem sehr ansprechenden Rahmenprogramm begleitet, das genug Raum und Zeit für den persönlichen Erfahrungsaustausch bot. An dieser Stelle sei dem Gastgeber der Ruhr-Universität Bochum, CARSTEN JUERGENS und seinem engagierten Team ein großes Lob für die professionelle Gestaltung und für die Rundum-Versorgung gesagt. Für die technische Organisation durch EARSeL muss insbesondere GESINE BÖTTCHER (Leibniz Universität Hannover) herzlich gedankt werden, die einen reibungslosen Ablauf sicherstellte.

MATTHIAS MÖLLER, Bamberg

3D-Forum Lindau – Ansichten, Einsichten, Aussichten

vom 11.–12. März 2008 in Lindau

In der Inselhalle Lindau fand das siebte „*Internationale 3D-Forum Lindau*" statt. Schnell entwickelte sich diese Veranstaltung, seit der Premiere im Februar 2002, zu einem Muss für die Kenner und Könner der dreidimensionalen (3D) Stadt- und Landschaftsmodelle. Auch in diesem Jahr ist es wieder geglückt, das Fachpublikum aus Wirtschaft, Wissenschaft und Verwaltung mit aktuellen Themen und interessanten Referenten zu begeistern.

Unter der bewährten Leitung von Dipl.-Ing. Claus Bihl (Vermessung, Stadt Lindau) und Dr.-Ing. Achim Hellmeier (Real.IT, Schwäbisch Gmünd) gelang es erneut, ein Programm zusammenzustellen, das mit den Schwerpunkten „*Virtuelle Globen und Luftbild-Schrägaufnahmen*", „*Das Thema 3D im Tief- und Wasserbau*" und „*Virtuelle Stadtmodelle für Stadt- und Standortmarketing*" genau die Themen zusammenfasst, welche die Fachwelt zur Zeit bewegen.

Stadtbaudirektor Georg Speth eröffnete mit einer herzlichen Begrüßungsrede den ersten Tag. Er konnte einen neuen Teilnehmerrekord von erstmals knapp über 100 Gästen aus sechs Nationen vermelden, über den sich auch die Mitveranstalter, die Stadtwerke Lindau GmbH & Co. KG und der DVW (Deutscher Verein für Vermessungswesen) sehr freuten.

Bevor Dr. Josef Kauer (Microsoft Deutschland GmbH, München) ein Schwerpunktthema aufgriff und über neue Ansätze bei virtuellen Globen, in diesem Fall das Produkt „Virtual Earth" referierte, lies Prof. Dr. Armin Grün (ETH Zürich) tief und intensiv in die theoretischen Grundlagen und die zu bewältigenden Problematiken des 3D-Mappings aus hochauflösenden Satellitendaten blicken. Sehr interessant, vor allem für die anwesenden Fachleute aus der Lindauer Stadtverwaltung, war der Vortrag von Dipl.-Ing. Karl-Heinz Schramm über „*Sechs Jahre Stadtmodell Bamberg – Von der Bebauungsplanung bis zum Standortmarketing*". Mit ansteckender Begeisterung berichtete er über eine Vielzahl überzeugender, in Bamberg praktizierter Einsatzmöglichkeiten virtueller Stadtmodelle. Neben Brand-, Hochwasser- und Schallausbreitungssimulation bietet ein 3D-Stadtmodell auch unvergleichliche Möglichkeiten in der Stadtplanung. Vom Architekturwettbewerb bis zur Präsentation beim Bürger sind die 3D-Modelle in den Entscheidungsprozessen der Stadt Bamberg nicht mehr wegzudenken.

Nach der Mittagspause informierte Jürgen Ohneberg (IT-Leiter, Stadtwerke Lindau) über den aktuellen Stand und die verschiedenen Möglichkeiten des in das Internetportal der Stadt Lindau (www.lindau.de) eingebundenen Standortinformationssystems VisitCity. Auf der geografischen Grundlage eines interaktiven Stadtplans kann sich der Besucher auf ein breites Informationsangebot, vom aktuellen Luftbild über die Anzeige gewünschter Anbieter (Hotels, Apotheken, Gaststätten, Kindergärten, Bäckereien, usw.) bis zu touristischen Highlights oder dem Stadtbusnetz mit seinen Haltestellen samt Abfahrtszeiten freuen. Weiter aufgewertet werden wird dieses System in nächster Zeit durch die Einbindung von 3D-Modellen Lindauer Sehenswürdigkeiten oder gar eines kompletten 3D-Stadtmodells.

Von der gelebten Praxis in Bamberg und Lindau zurück in die vorausblickende Wissenschaft führte anschließend Prof. Dr. Jürgen Döllner vom Hasso-Plattner-Institut an der Universität Potsdam mit dem aktuellen Stand der automatisierten Herstellung komplexer 3D-Stadtmodelle. Ganz neue Möglichkeiten, von vielen Besuchern mit Spannung erwartet, beleuchtete Carsten von Rymon-Lipinski (Blom Deutschland GmbH) mit seinem Vortrag „*Pictometry – Eine innovative Lösung für 3D-Stadtmodelle*". Hierbei werden neben den klassischen Reihen-Senkrechtaufnahmen bewusst, durch spezielle Kameraanordnung, die Betrachtung sehr bereichernde, geodätisch brauchbare Schrägbilder geliefert.

Abgerundet wurde das Vortragsprogramm am Nachmittag durch zwei Berichte praktischer Anwendungen von 3D-Modellen im Tiefbau. Zuerst stellte Dipl.-Ing. Bernd Zimmermann vom Ingenieurbüro Zimmermann & Meixner in Amtzell seine Arbeit mit 3D-Geländemodellen als notwendige Grundlage für Regenrückhaltemaßnahmen vor. Am brandaktuellen Beispiel der Hochwassergefährdung Lindaus, vor allem durch die Oberreitnauer Ach, erklärte er die Verwendungsmöglichkeiten der durch eigene tachymetrische Aufnahmen ergänzten Lindauer Laserbefliegungsdaten von 2001. Die 3D-Geländemodelle, auf der einen Seite der örtliche, ursprüngliche Bestand, auf der anderen Seite die geplanten, und zum Teil inzwischen auch fertig gestellten Regenrückhaltebecken und geänderten Achufer, kamen in der Berechnung der Beckenvolumen, der geplanten, theoretischen Hochwasserlinien und der Ermittlung von zu bewegenden Erdmassen zum Einsatz. Zum Schluss erklärte Dipl.-Ing. Werner Rieger, vom Landratsamt Neckar-Odenwaldkreis, wie er erfolgreich virtuelle Modelle als Entscheidungshilfe für Straßenbauprojekte zur Anwendung brachte. Nach jahrzehntelanger Planung verschiedener Trassenvarianten und deren Anbindungsmöglichkeiten ans bestehende Straßennetz konnten die Entscheidungsträger, wie auch die äußerst kritischen Vertreter verschiedener Bürgerinitiativen erst mit dem Einsatz der 3D-Modelle von der Richtigkeit und auch Verträglichkeit der von den Planern vorgeschlagenen Variante überzeugt werden.

Die Qualität und der hohe Stellenwert des Lindauer 3D-Forums liegen nicht allein in den fein ausgewählten Vorträgen und der Kompetenz ihrer Referenten, sondern auch in der regen Diskussion der einzelnen Beiträge auf hohem fachlichen Niveau. Auch der traditionelle Ausklang des ersten Tages in einer gutbürgerlichen Inselwirtschaft, bei dem sich zu deftiger Brotzeit und vielleicht dem einen oder anderen Starkbier die Vortragenden und Gäste noch einmal ganz entspannt austauschen können, trägt zum guten Ruf der Veranstaltung bei.

Angenehm überrascht zeigten sich die Veranstalter über die hohe Teilnehmerzahl am zweiten Veranstaltungstag. Prof. Dr.-Ing. Volker Coors (Hochschule für Technik, Stuttgart, Fachbereich Geoinformation) leitete durch den ersten Teil des Workshops und stellte die Themen „*Integration von 3D-Stadtmodellen in eine GIS-Umgebung*“ und „*Fortführung von 3D-Stadmodellen*“ vor. Prof. Dr.-Ing. Günter Pomaska (Fachbereich Architektur und Bauingenieurwesen, Fachhochschule Bielefeld), seit Jahren Dreh- und Angelpunkt des Workshops, führte anschließend sehr praxisbezogen durch die Bereiche „*3D-Bauwerksmodellierung*“, „*Einführung in KML*“ und „*Mobile GPS-Navigation*“.

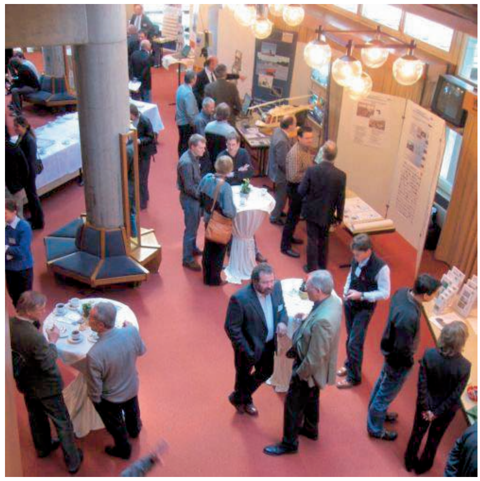

Neben den steigenden Besucherzahlen, sowohl des Vortragsprogramms als auch des Workshops, wächst auch die kleine Fachmesse im Foyer der Inselhalle. Acht Aussteller aus den Bereichen Software, Dienstleistung und Ausrüstung nutzten dieses Jahr diese gute Gelegenheit und bereicherten die Veranstaltung nicht nur mit ihren aktuellen Produkten, sondern auch mit freundlichem, diskussionsbereitem Personal. Der Aufwärtstrend bestätigt die Linie der Veranstalter und so freut sich die Fachwelt auf ein Wiedersehen in Lindau 2009.

Andreas Lindenmüller, Lindau

Mitteilungen

DeSecure
Satellitengestützte Kriseninformation für Deutschland

DeSecure ist ein Verbundprojekt mit dem Ziel der Verbesserung der satellitengestützter Kriseninformation in Deutschland. Das Projekt wird über das DLR Raumfahrtmanagement gefördert. Die Koordination von DeSecure obliegt der Abteilung Umwelt & Sicherheit im Deutschen Fernerkundungsdatenzentrum des DLR.

Schnellere Krisenlageinformationen mit Hilfe von Satellitendaten

Mit der weltweiten Zunahme von Naturkatastrophen, humanitären Notsituationen und zivilen Gefahrenlagen steigt auch der Bedarf an zeitnaher, präziser und flächendeckender Lageinformation. Diese aktuellen und umfassenden Informationen können inzwischen zu einem großen Teil durch Analyse von satellitengestützten Fernerkundungsdaten bereit gestellt werden. Voraussetzung hierfür ist die Sensor- und Systementwicklung. Innerhalb der letzten 10 Jahre haben Satellitenbilder eine Qualität im Bezug auf Verfügbarkeit und Genauigkeit erreicht, die es ermöglicht, sie routinemäßig für die Gewinnung von zeitnaher Kriseninformation einzusetzen. Ferner sind Strukturen und Kapazitäten notwendig, die eine schnelle Aufnahme und Aufbereitung der Satellitendaten ermöglichen.

Übergeordnete Ziele & Verbundpartner

Die Bereitstellung von Krisenlageinformation mit Hilfe von Satellitendaten ist eine hoch-komplexe Aufgabe, bei der vor allem Schnelligkeit sowie geometrische und thematische Genauigkeit der gewonnenen Information von übergeordneter Bedeutung sind. Die Gewinnung von satellitengestützter Kriseninformation erfolgt heute noch zu einem überwiegenden Teil durch visuelle Interpretation der unterschiedlichen Bilddaten, da das semantische und synoptische Bildverständnis von geschulten Bildinterpreten bis heute kaum oder nur sehr schwer in standardisierten und automatisierten Algorithmen, allgemeingültig und für die verschiedensten Bildquellen gleichsam geltend, gefasst werden kann. Folglich gibt es hier ein bedeutendes Entwicklungspotential und verschiedene Forschungsfragen für die Optimierung der Notfallkartierungen. Ferner gibt es auch im Bereich des Datenempfangs und der Vorverarbeitung der Satellitenbilddaten Potential zur Verbesserung, vor allem in Bezug auf Geschwindigkeit und Genauigkeit. Daher ist das übergeordnete Ziel des Verbundprojektes die Verbesserung der operativen Bereitstellung von Krisenlageinformationen, u. a. um die Arbeiten am Zentrum für satellitengestützte Kriseninformation (‚ZKI'- Service des DFD) zu unterstützten.

Hierfür wird der gesamte Produktionszyklus von satellitengestützter Kriseninformation (Satellitendatenempfang, Prozessierung, Informationsextraktion, Kartenerstellung und -bereitstellung) bis Ende 2010 analysiert und verbessert.

Insbesondere soll durch das Projekt DeSecure eine Stärkung der in Deutschland verfügbaren methodisch-technischen Not-

Arbeitsablauf im Notfallkartierungskontext fallkartierungskapazitäten erzielt werden, u. a. durch die Optimierung der Schnittstellen zwischen den Partnern aus Forschung und Industrie und die Entwicklung neuer, nach Möglichkeit standardisierter Methoden der Informationsgewinnung aus Satellitenbilddaten. Neben dem Deutschen Fernerkundungsdatenzentrum sind das Institut für Methodik der Fernerkundung des DLR sowie die Industriepartner Definiens, GAF, Infoterra, PRO DV und RapidEye sowie die technischen Universitäten Berlin und München beteiligt.

Enge Kontakte zu deutschen und europäischen Lagezentren sowie weiteren Nutzern

Für das Projekt DESECURE sind vor allem Zivilschutz- und Hilfsorganisationen (z. B. THW, DRK) sowie besonders die deutschen und europäischen Lagezentren von Bedeutung. Dazu zählen das Gemeinsame Melde- und Lagezentrum des Bundes und der Länder (GMLZ), das Lagezentrum des Auswärtigen Amtes (AA) und das ‚Monitoring and Information Centre‘ der Europäischen Kommission (MIC).

Daher werden in DESECURE Nutzerbedarf und Informationsanforderungen auf verschiedenen Ebenen (international, national und regional) gesammelt und in einer Nutzerdatenbank zusammengeführt. Ziel ist es unter anderem dabei, die Nutzer für den Einsatz von satellitengestützter Kriseninformation zu sensibilisieren.

Deutsche Satelliten TerraSAR-X und RapidEye liefern Daten für Notfallkartierungen

Mit dem Projekt DESECURE werden die deutschen Sensoren TerraSar-X und RapidEye in die Krisenkartierung eingebunden und damit neben den deutschen auch den europäischen Nutzern bekannt gemacht. Ferner werden durch Universitäten und Industriepartner technisch operative Analysemethoden geschaffen, die die Anwendungsentwicklung und Vermarktung der Daten und Informationsprodukte auch über den Krisensektor hinaus stärken.

DESECURE im europäischen Kontext

Der Aufbau von Krisenkartierungskapazitäten auf deutscher Seite geht einher mit dem Ausbau der GMES Aktivitäten auf europäischer Ebene. GMES (Global Monitoring for Environment and Security) ist eine gemeinsame Initiative der Europäischen Kommission und der europäischen Raumfahrtagentur ESA für Globale Umwelt- und Sicherheitsüberwachung. Ziel ist es, eine eigenständige, dauerhaft verfügbare, kosteneffiziente und nutzerfreundliche Beobachtungskapazität für politische Entscheidungsträger und Behörden zu schaffen.

Durch DESECURE wird gewährleistet, dass die deutsche Position im Bereich der Notfall- und Krisenkartierung besser vernetzt und im europäischen Kontext verankert wird.

Weitere Informationen und Kontakt

e-mail: Monika.Gaehler@dlr.de
Info: www.desecure.info

MONIKA GÄHLER

Hochschulnachrichten

Universität Zürich

Dipl.-Ozeanograph Felix Morsdorf promovierte am 05. 02. 2007 am Geographischen Institut (Fernerkundung / RSL) der Universität Zürich mit der Arbeit „*LIDAR Remote Sensing for Estimation of Biophysical Vegetation Parameters*“ zum Dr. sc. nat.

Promotionskomitee: Prof. Dr. Klaus Itten, Dr. Britta Allgöwer, Dr. Erich Meier, Prof. Dr. Robert Weibel, Dr. Emmanuel Baltsavias

Kurzfassung:
Waldbrände stellen eine enorme Bedrohung für Menschenleben und ökonomische Werte in vielen Ländern dar. Diese Feuer sind ökologische Prozesse, welche räumlich und zeitlich variierenden Randbedingungen unterworfen sind. Airborne (flugzeugbasiertes) laser scanning (ALS) ist eine aktive Fernerkundungsmethode, welche die direkte Messung der Position von zurückstreuenden Elementen auf der Erdoberfläche ermöglicht. Durch die Abtastung der Erdoberfläche mit einem Laserstrahl erzeugen ALS Systeme eine dreidimensionale Punktwolke, welche die strukturellen Eigenschaften der Vegetation enthalten sollte. Deswegen wurde vermutet, dass man aus dieser Punktwolke Information über die räumliche Verteilung von Brandgut extrahieren kann, welche hilfreich zum Einschätzen des Risikos oder der Auswirkungen von Waldbränden sein könnte.

Die vorgelegte Dissertation beschäftigt sich mit der Ableitung von struktureller Information aus ALS Daten in ihrer rohen, unverarbeiteten Form (3D-Punktwolke) und versucht robuste Methoden zur Bestimmung von biophysikalischen Vegetationparametern zu entwickeln, zu implementieren und zu validieren. Eine Methode zur Erfassung der Geometrie von Einzelbäumen wurde entwickelt und mit Hilfe von Feldmessungen validiert. Es wurde gezeigt, dass Eigenschaften wie Baumposition, Baumhöhe und Kronendurchmesser in einem automatischen Verfahren aus der Punktwolke abgeleitet werden können, und dieses mit einer Genauigkeit, welche der von Feldmessungen entspricht. Ebenfalls wurde eine Methodik entwickelt, die es erlaubt Größen, die die Dichte der Vegetation beschreiben, aus ALS Daten abzuleiten. Hierzu wurden der Blattflächenindex (leaf area index, LAI) und der Bedeckungsgrad (fractional cover, fCover) mit Hilfe von physikalisch basierten Statistiken der einzelnen ALS Echotypen (erstes und letztes Echo, first/last echo) und Regressionsmodellen bestimmt. Die Validierung dieser Methode erfolgte mittels Feldmessungen, welche mit differentiellen GPS auf einige Zentimeter genau lokalisiert waren. Dadurch war es möglich, Feldmessungen und die aus den ALS Daten abgeleiteten Parameter auf kleinen Skalen von wenigen Metern zu korrelieren, im Gegensatz zu bisherigen Methoden, welche meist auf der Fläche eines Bestandes implementiert wurden.

Die entwickelten Methoden verfügen über einen hohen Grad der Automation, sobald sie mit Feldmessungen kalibriert werden, und sind unempfindlich gegenüber Änderungen des Abtastwinkels, zumindest für den kleinen Bereich in dem der Winkel des in dieser Arbeit verwendeten Systems variiert. Hingegen beeinflusst eine größere Änderung der Flughöhe die Methoden zur Ableitung der Vegetationsdichte erheblich, während die Methode zur Einzelbaumextraktion weniger beeinflusst wird. In beiden Fällen ist allerdings eine Rekalibrierung der Algorithmen mit Felddaten für unterschiedliche Flughöhen erforderlich, es sei denn, man kann die Auswirkungen der veränderten Flughöhe für jeden Parameter direkt quantifizieren.

Die im Rahmen dieser Arbeit entwickelten Methoden und Algorithmen zur Ableitung von Struktur und Dichte der Vegetation unterstreichen das große Potential von ALS Daten für die Extraktion von biophy-

sikalischen Parametern der Vegetation. Aus den gewonnenen Erkenntnissen lässt sich weiterhin die Schlussfolgerung ziehen, dass man die Interaktion des Laserpulses mit den streuenden Objekten besser verstehen muss, um dieses Potential weitergehend ausnutzen zu können.

Universität Zürich

Dipl. El.-Ing. ETH Maurice Rüegg promovierte am 31. 07. 2007 am Geographischen Institut (Fernerkundung / RSL) der Universität Zürich mit der Arbeit „*Ground Moving Target Indication with Millimeter Wave Synthetic Aperture Radar*“ zum Dr. sc. nat.

Promotionskomitee: Prof. Dr. Klaus Itten, Prof. Dr. Daniel Nüesch, Dr. Erich Meier, Dr. Konrad Schmid

Kurzfassung:
Die Bewegtzielerkennung (ground moving target indication – GMTI) bei Radar mit synthetischer Apertur (synthetic aperture radar – SAR) liefert Informationen zu bewegten Objekten in Radarbildern der unbewegten Erdoberfläche. Während allgemeine Anwendungen so unterschiedliche Themen wie Messungen von Meeresströmungen und Gletschereisfluss beinhalten können, ist Millimeterwellen (mmW) SAR gut geeignet für Aufgaben in der Verkehrsüberwachung, Aufklärung und der Identifikation von speziellen Bewegungen wie Objektvibrationen und -rotationen. Mittels einer ausführlichen Analyse von Bewegungen in einem SAR Systemmodell zeigt diese Dissertation die Effekte von konstanten und beschleunigten Zielbewegungen wie auch von Vibrationen und Rotationen in mmW SAR auf.

Ein effizienter Ansatz der Bewegtzielerkennung ist der Einsatz von mehrkanaligen SAR-Systemen und einer räumlich und zeitlich variierenden Analyse von bewegten Radarzielen. Dadurch wird sowohl eine Indikation als auch eine Korrektur von Positionsverschiebungen im SAR Bild und eine Schätzung der radialen Geschwindigkeitskomponente solcher Ziele möglich. Die kleine Wellenlänge des Radars bei mmW SAR bietet eine hochempfindliche Bewegungsdetektion und Messung der Objektgeschwindigkeit. Die vorliegende Arbeit bespricht theoretische Überlegungen, die spezifisch für mmW SAR GMTI sind, einen adaptiven Algorithmus, um Geschwindigkeits- und Positionsinformationen von Bewegtzielen mit Amplituden-vergleichendem Monopuls Radar zu erhalten und eine Diskussion zur Beseitigung von GMTI Blindgeschwindigkeiten und Mehrdeutigkeiten der Objektgeschwindigkeit mittels Zweifrequenz-SAR. Vier großangelegte Experimente mit dem FGAN MEMPHIS mmW System in unterschiedlichen Umgebungen werden vorgestellt.

Freie Universität Berlin

Universitätsprofessor Dr. Joachim Hill, Inhaber einer C4-Professur für Fernerkundung im Fachbereich VI der Universität Trier, hat vom Senator für Bildung, Wissenschaft und Forschung in Berlin, einen Ruf auf die Professur „Fernerkundung und Geoinformatik“ im Fachbereich Geowissenschaften an der Freien Universität Berlin erhalten.

Veranstaltungskalender

2008

2.–7. Juni: 28th **EARSeL Symposium & Workshops “Remote Sensing for a Changing Europe”** in **Istanbul**, Turkey. Info: www.earsel28.itu.edu.tr

6. Juni: **Forum Geoinformation “Airborne Laserscanning”**, Hochschule München. Info: www.hm.edu/geo

10.–12. Juni: **GIS/SIT 2008 – Schweizer Forum für Geoinformation**, Universität Zürich-

Irchel, Schweiz. Info: www.akm.ch/gis_sit 2008

14.–19. Juni: **FIG XXXI General Assembly & Working Week** in **Stockholm**. Auskünfte durch: FIG Office, e-mail: fig@fig.net, Info: www.fig.net/events/2008/fig_2008_stockholm.pdf

20.–21. Juni: 11th **ICA Workshop on Map Generalisation and Multiple Representations**, Montpellier, France. Info: ica.ign.fr

24.–25. Juni: 5. **Hamburger Forum für Geomatik** im Bürgerhaus **Hamburg-Wilhelmsburg.** Info: www.hcu-hamburg.de/geomatik/forum2008

24.–26. Juni: **IEEE Conference on Computer Vision and Pattern Recognition** in **Anchorage,** Alaska, USA. Info: vision.eecs.ucf.edu

30. Juni – 3. Juli: **International Workshop on Computational GeoInformatics – COMPGEO'08**, University of Perugia, Italy. Info: www.gdmc.nl/compgeo

1.–4. Juli: **Geoinformatics Forum Salzburg** (GI_Forum2008). Info: www.gi-forum.org

3.–11. Juli: **XXI ISPRS Kongress** in **Beijing**, China. Auskünfte: Prof. Chen Jun (Congress Director), e-mail: congressdirector@isprs2008-beijing.org oder loc@isprs2008-beijing.org, Info: www.isprs2008-beijing.org

13.–20. Juli: 37th Scientific Assembly of the **Committee on Space Research & Associated Events – COSPAR 2008**, "50th Anniversary Assembly" in **Montreal**, Kanada. Auskünfte: COSPAR Secretariat, Tel.: +33-1-44-767510, e-mail: cospar@cosparhq.cnes.fr

4.–9. August: **GEOBIA 2008 – Pixels, Objects, Intelligence: "Geographic Object Based Image Analysis for the 21st Century"** in **Calgary**, Canada. Auskünfte: Geoffrey J. Hay, Tel.: +1-403-220-4768, e-mail: gjhay@ucalgary.ca, Info: www.ucalgary.ca/GEOBIA

8.–11. September: 10th International Symposium on **High Mountain Remote Sensing Cartography (HMRSC-X)** in **Kathmandu**, Nepal. e-mail: pmool@icimod.org, Info: menris.icimod.net/HMRSC-X

17.–18. September: **Praxisworkshop „GIS & Internet",** Universität der Bundeswehr München. Info: www.unibw.de/bauv11/geoinformatik

22.–23. September: **AgA – Arbeitsgruppe Automation in Kartographie, Photogrammetrie und GIS** in **Frankfurt am Main** beim Bundesamt für Kartographie und Geodäsie, Info: www.ikg.uni-hannover.de/aga

30. September – 2. Oktober: **INTERGEO 2008** in **Bremen**. Info: www.intergeo.de/deutsch/page/main/index.php

8.–9. Oktober: 2. **Hamburger Forum Geoinformationen für die Küstenzone** an der HafenCity Universität **Hamburg.** Info: www.gis-kueste.de

12.–18. Oktober: **ECCV 2008 – European Conference on Computer Vision** in **Marseille**. Info: eccv2008.inrialpes.fr

12.–14. November: **Digital Earth Summit on Geoinformatics: Tools for Global Change Research.** Wissenschaftspark Albert Einstein, Potsdam. Info: www.isde-summit-2008.org

8.–11. Dezember: 19th **International Conference on Pattern Recognition** in **Tampa,** Florida, USA. Tampa Convention Center, Info: www.icpr2008.org

2009

16.–19. März: **ISPRS** WG VIII/12**,** 6th **EARSeL SIG IS Workshop "IMAGING SPECTROSCOPY: Imaging Spectroscopy: Innovative tool for scientific & commercial environmental applications"** in **Tel-Aviv**, Israel. Auskünfte: Prof. Eyal Ben-Dor, e-mail: bendor@post.tau.ac.il, Info: www.earsel6th.tau.ac.il

29. September – 2. Oktober: **ICCV2009 – International Conference on Computer Vision** in **Kyoto**, Japan. Info: www.iccv2009.org

Zum Titelbild

Abstraktion von Geoinformation

Das Titelbild zeigt eine Collage von Abbildungen aus den Arbeiten des DFG-Bündelprojekts „Abstraktion von Geoinformation". Es visualisiert die vier Datentypen, die im Projekt bearbeitet wurden: Vektordaten, Bilddaten, 3D-Oberflächendaten sowie Sprache. Einen Überblick über das Bündel gibt das Editorial und Details sind in den einzelnen Artikeln in diesem Heft zu finden.

MONIKA SESTER, e-mail: Monika.Sester@ikg.uni-hannover.de

Korporative Mitglieder

Firmen

AEROWEST GmbH
AICON 3D Systems GmbH
aphos Leipzig AG
Applanix Corporation
Becker & Keller, Beratende Ingenieure
Bernhard Harzer Verlag GmbH
Blom Deutschland GmbH
Brockmann-Consult
BSF Luftbild GmbH
Büro Immekus
CGI Systems GmbH
con terra GmbH
CONPIE GmbH
Creaso GmbH
DEFINIENS AG
DELPHI IMM GmbH
Deutsches Bergbau-Museum
J. Linsinger ZT-GmbH
EFTAS Fernerkundung Technologietransfer GmbH
ESG Elektroniksystem- und Logistik-GmbH
ESRI Geoinformatik GmbH
EUROPEAN SPACE IMAGING
Eurosense GmbH
fokus GmbH
fpi Fuchs Ingenieure GmbH
FPK Ingenieurgesellschaft mbH
g.on experience gmbh
GAF GmbH
GeoCad GmbH
GeoCart Herten GmbH
GeoContent GmbH
geoplana Ingenieurgesellschaft mbH
GEOSPACE Beckel GmbH
GEOSYSTEMS GmbH
GGS – Büro für Geotechnik, Geoinformatik, Service
GIP Geoinformatics & Photogrammetric Engineering
Hansa Luftbild AG
Herbert Wichmann Verlag Hüthig GmbH
IGI – Ingenieur-Gesellschaft für Interfaces mbH
ILV Ing.-büro für Luftbildausw. und Vermessung
Imetric 3D GmbH
Dr. H. Carls Luftbilddatenbank
Inpho GmbH
Intergraph GmbH, Geschäftsbereich Z/I Imaging
INVERS – Industrievermessung & Systeme

Jena-Optronik GmbH
Johan Piedfort Photogrammétrie
KAZ Bildmess GmbH
Leica Geosystems GmbH
Luftbild Brandenburg GmbH
MAPS geosystems GmbH
Messbildstelle GmbH
Microsoft Photogrammetry
PHOENICS GmbH
PMS – Photo Mess Systeme AG
Rollei Metric GmbH
RWE Power AG, Geobasisdaten/Photogrammetrie
technet GmbH
TERRA-Bildmessflug GmbH & Co.
TerraVista Umweltdaten GmbH
TopoSys GmbH
TRIGIS Vermessung + Geoinformatik GmbH

Behörden

Amt für Geoinformationswesen der Bundeswehr
Amt für ländliche Räume Husum
Bayerische Landesanstalt für Wald und Forstwirtschaft
Bundesamt für Kartographie und Geodäsie
Bundesmin. für Ern., Landw. und Verbraucherschutz
DB Netz AG
Hess. LA für Bodenmanagement und Geoinformation
Innenministerium NRW, Gruppe Vermessungswesen
Inst. für Umwelt- und Zukunftsforschung
Landesamt für Vermessung und Geoinformation, Bayern
Landesbetrieb Geoinformation und Verm., Hamburg
Landesvermessung und Geobasisinformation Nieders.
Landesvermessungsamt Baden-Württemberg
Märkischer Kreis, Vermessungs- und Katasteramt
Regierungspräs. Stuttgart, LA für Flurneuordnung
Regierungspräs. Tübingen, Abt. 8 Forstdirektion
Regionalverband Ruhr
Staatsbetrieb Sachsenforst Pirna
Stadt Bocholt, Fachbereich 31
Stadt Düsseldorf, Vermessungs- und Katasteramt
Stadt Köln, Amt für Liegensch., Verm. und Kataster
Stadt Wuppertal, Verm., Katasteramt und Geodaten
Thüringer LA für Vermessung und Geoinformation

Hochschulen

BTU Cottbus, Lehrstuhl für Vermessungskunde
FH Bochum, FB Vermessungsw. und Geoinformatik
FH Frankfurt a.M., FB 1, Studiengang Geoinformation
FH Karlsruhe, FB Geoinformationswesen
FH Mainz, Inst. f. Raumbez. Inform.- und Messtechn.
FH Oldenburg, Inst. für Angew. Photogr. und Geoinf.
HCU HafenCity Uni Hamburg, Department Geomatik
HfT Stuttgart, Vermessung und Geoinformatik
HTW Dresden, FB Vermessungswesen/Kartographie
Ruhr-Uni Bochum, Geographisches Institut
RWTH Aachen, Geodätisches Institut
TU Berlin, Computer Vision & Remote Sensing
TU Braunschweig, Inst. für Geodäsie und Photogr.
TU Clausthal, Inst. für Geotechnik und Markscheidew.
TU Darmstadt, Inst. für Photogrammetrie und Kartogr.
TU Dresden, Inst. für Photogrammetrie und Fernerk.
TU Freiberg, Inst. für Geologie, RSG
TU München, FG Photogrammetrie und Fernerk.
TU Wien, Inst. für Photogrammetrie und Fernerk.
Uni Bonn, Inst. für Photogrammetrie
Uni Göttingen, Inst. für Waldinv. und Waldwachstum
Uni Hannover, Inst. für Kartogr. und Geoinformatik
Uni Hannover, Inst. für Photogrammetrie und GeoInf.
Uni Heidelberg, IWR Interdis. Zentr. f. Wiss. Rechnen
Uni Karlsruhe, Inst. für Photogrammetrie und Fernerk.
Uni Kiel, Geographisches Institut
Uni zu Köln, Geographisches Institut
Uni Stuttgart, Inst. für Photogrammetrie
Uni Würzburg, Geographisches Institut